United States
Environmental Protection
Agency

Industrial Environmental Research
Laboratory
Research Triangle Park NC 27711

EPA-600/7-79-017
January 1979

EPA

TRW Charged Droplet Scrubber Corrosion Studies

Interagency Energy/Environment R&D Program Report

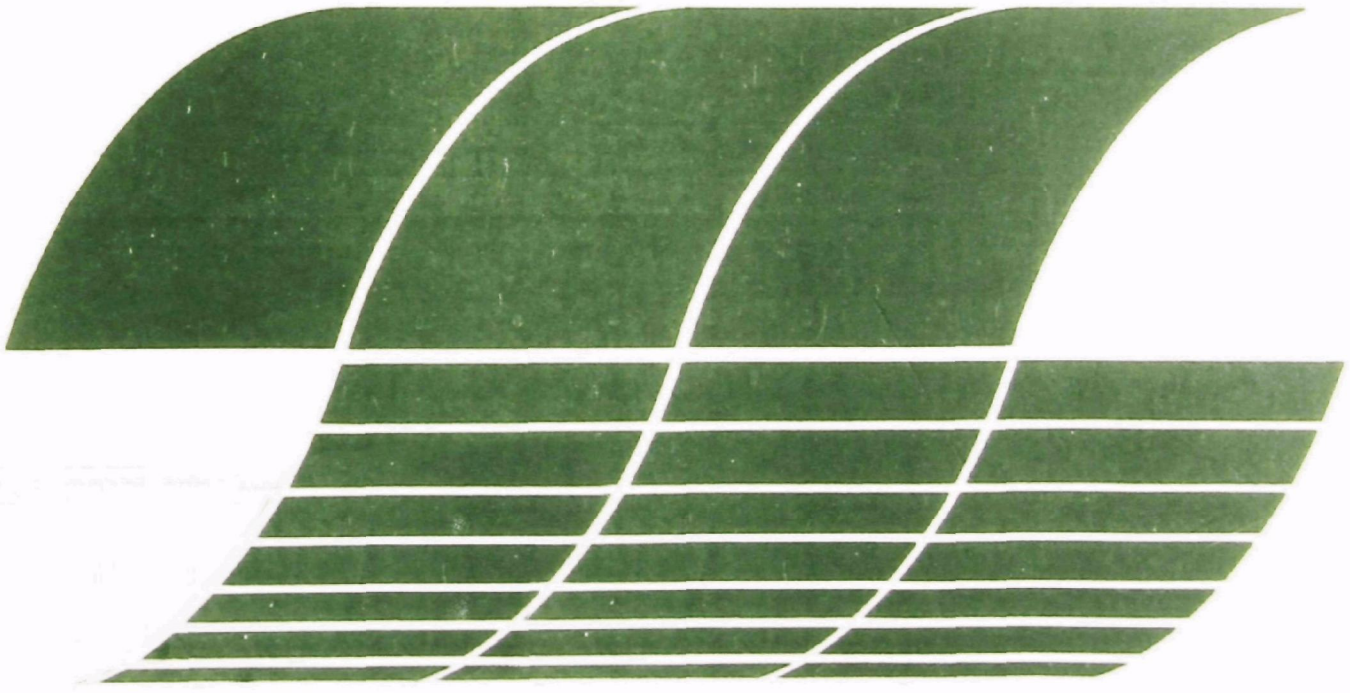

RESEARCH REPORTING SERIES

Research reports of the Office of Research and Development, U.S. Environmental Protection Agency, have been grouped into nine series. These nine broad categories were established to facilitate further development and application of environmental technology. Elimination of traditional grouping was consciously planned to foster technology transfer and a maximum interface in related fields. The nine series are:

1. Environmental Health Effects Research
2. Environmental Protection Technology
3. Ecological Research
4. Environmental Monitoring
5. Socioeconomic Environmental Studies
6. Scientific and Technical Assessment Reports (STAR)
7. Interagency Energy-Environment Research and Development
8. "Special" Reports
9. Miscellaneous Reports

This report has been assigned to the INTERAGENCY ENERGY-ENVIRONMENT RESEARCH AND DEVELOPMENT series. Reports in this series result from the effort funded under the 17-agency Federal Energy/Environment Research and Development Program. These studies relate to EPA's mission to protect the public health and welfare from adverse effects of pollutants associated with energy systems. The goal of the Program is to assure the rapid development of domestic energy supplies in an environmentally-compatible manner by providing the necessary environmental data and control technology. Investigations include analyses of the transport of energy-related pollutants and their health and ecological effects; assessments of, and development of, control technologies for energy systems; and integrated assessments of a wide range of energy-related environmental issues.

EPA REVIEW NOTICE

This report has been reviewed by the participating Federal Agencies, and approved for publication. Approval does not signify that the contents necessarily reflect the views and policies of the Government, nor does mention of trade names or commercial products constitute endorsement or recommendation for use.

This document is available to the public through the National Technical Information Service, Springfield, Virginia 22161.

EPA-600/7-79-017

January 1979

TRW Charged Droplet Scrubber Corrosion Studies

by

Frederick A. Whitson

TRW, Energy Systems Group
One Space Park
Redondo Beach, California 90278

Contract No. 68-02-2613
Task No. 7
Program Element No. EHE624

EPA Project Officer: Dale L. Harmon

Industrial Environmental Research Laboratory
Office of Energy, Minerals, and Industry
Research Triangle Park, NC 27711

Prepared for

U.S. ENVIRONMENTAL PROTECTION AGENCY
Office of Research and Development
Washington, DC 20460

ABSTRACT

The report primarily presents the results of corrosion studies undertaken by TRW Energy Management Division to provide definitive data concerning the corrosive nature of coke oven waste heat flue gas and its effect on wet type electrostatic precipitators (ESP) and specifically on the TRW/Charged Droplet Scrubber (CDS).

The task characterized the chemical composition of the waste heat flue gases; related these data to corrosion and to the effects on the electrostatic scrubbing mechanism; evaluated materials compatibility with the coking process waste heat environment; and identified candidate agents which may be introduced into the waste heat gas stream to minimize the corrosive effects. In addition, alternate designs were evaluated for high voltage isolation and electrical arc sensing and control. The results of the corrosion studies and concurrent CDS electrical control and arc sensing system improvements have measurably increased the available knowledge regarding the corrosion problems in wet ESP's and improved the potential for more reliable environmental control equipment.

CONTENTS

ILLUSTRATIONS

ILLUSTRATIONS (Continued)

ILLUSTRATIONS (Continued)

TABLES

ACKNOWLEDGEMENT

We would like to acknowledge the effective efforts of Maurice Bianchi and Lou Rosales of the Materials Division, the principal investigators for the Equipment Corrosion Study.

In a more somber vein, we would like to note the passing of Walter Krieve. With his death we lost a great human being and he will be sorely missed. Walt was involved in the birth of the CDS and his genius was the driving force behind much of the development. As principal investigator for the High Voltage Water Supply Isolation, Electrode Geometry Study and Flue Gas Stream Corrosive Control his increasing efforts in the face of personal adversity were particularly noteworthy. Without his skill, expertise and professionalism this work could not have been accomplished. The technical assistance for all of Walt's work was provided for by Andy Seaton.

We would also like to acknowledge Marshal Huberman, Ray Maddalone and Joe Sauer for their contributions.

SECTION I

SUMMARY

BACKGROUND

The Environmental Protection Agency funded a demonstration program of the TRW/Charged Droplet Scrubber (CDS) on a coke oven waste heat gas emissions control application. As a result of this, a full scale CDS was subsequently installed at the coke oven facility of Kaiser Steel Company, Fontana, California, Figure 1.

After the initial few hundred hours of operation a definite degradation in the CDS collection efficiency was noted. A preliminary inspection of the equipment revealed that the lower efficiency was due to a lower electrode operating voltage resulting from corrosion-caused mechanical failures within the CDS system. A more detailed inspection revealed that the most severe corrosion took place within a localized area of the CDS electrical collection section. This area proved to be directly downstream of a failed element of the gas distribution assembly. The resulting local overload produced excessive electrical arcing and thereby compounded the chemical corrosion with electrical erosion.

Some preliminary analysis of the CDS supply water indicated that the chloride content had increased more than tenfold (from 20 ppm to more than 200 ppm) over the high average anticipated, based on customer supplied analysis. This would account for the pit-type corrosion of the 316SS, but did not provide sufficient data to explain the generalized deterioration of the equipment internal components and outer casing.

Because the understanding of these problems is essential to the pollution control industry in general and for coke oven emission control in particular, the Environmental Protection Agency was asked and agreed to sponsor a program for an investigation of the problem.

PROGRAM SUMMARY

An investigative program was conducted during the time period of August 1977 through February 1978. The program was primarily directed at determining the types and causes of corrosion experienced in the TRW/Charged Droplet Scrubber installed on a coke oven application located at the Kaiser Steel Company plant.

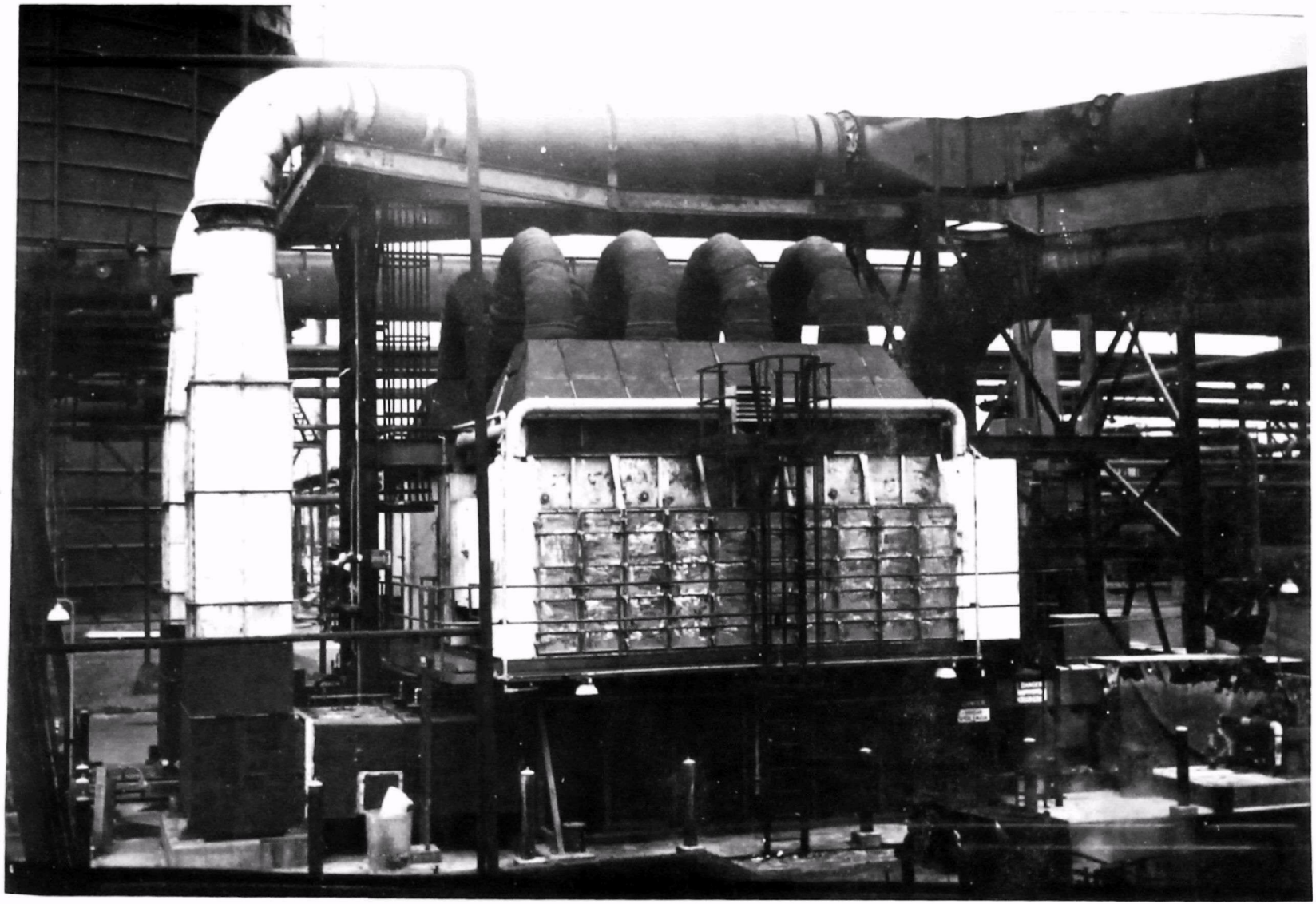

Figure 1. TRW Charged Droplet Scrubber Model 070 (140,000 acfm) Coke Oven Waste Heat Gas Kaiser Steel Company, Fontana, California

The corrosion studies program was undertaken to provide definitive data concerning the corrosive nature of coke oven waste heat flue gas and the effect of this gas on a wet type electrostatic precipitator and specifically on a wet ESP known as the Charged Droplet Scrubber.

The task was divided into the following interrelated investigations:

1) Thermochemical Mapping

2) Electrode Geometry

3) High Voltage Water Supply Isolation

4) Equipment Corrosion

5) Flue Gas Stream Corrosive Control

6) Electrical Spark Quenching

It was determined that the coke oven waste heat gases contained a wide range of compounds as expected. Those present in greatest quantity are C, SO_2, H_2S, O_2, NO_x, CH_3, H_2, HCN, S, CO, CO_2, N_2. Water reacts with these compounds in the gas stream to form sulfuric acid and, to a lesser extent, carbonic and nitric acids. Since the temperature ranges from a high of 149°C at the inlet duct to a low of 45°C within the CDS, sulfuric acid condenses on the cooler surfaces and becomes more and more concentrated as the lower vapor pressure water boils off in areas that are not frequently flushed with water. This combined with the significantly higher chloride content of the water was the primary causes of the generalized corrosion of 316-type stainless steel casing. The pit-type corrosion was primarily due to the high chloride content alone.

Material test coupons were installed throughout the gas cleaning system so as to be exposed to the complete spectrum of environmental conditions that exist within the equipment. Various coatings where also applied in the same locations. None of the coatings selected were able to withstand the hostile environment. Of the metallic sample coupons tested, commercially pure titanium and Incoloy 825 performed the best. Chemical lead samples performed satisfactorily in the lower casing. The resistance to pitting and crevice corrosion seems to roughly follow the molybdenum content. Of the fiberglass reinforced plastic panels tested, only the polybutadiene showed acceptable resistance.

As expected, those surfaces where deposits could accumulate experienced the most severe corrosion. The process was accelerated on those surfaces because the deposits would prevent the renewal of the protective oxide layer which normally protects the base metal. To minimize this occurrence, the equipment wash system was redesigned to flush all surfaces where deposits could accumulate and the frequency and duration of the wash cycle was increased.

In addition to the materials test program, an experiment was conducted to determine if additives to the gas stream could inhibit corrosion without adversely affecting the efficiency. Analysis of thermo-chemical mapping and results of the materials test performed, identified gaseous SO_2 as the compound causing the most severe corrosion problem. With this in mind, the candidate additive chosen was NH_3. The NH_3 does react with the gaseous SO_2 in such a way as to form a particulate which then can be scrubbed by the CDS. Limited testing of a single-stage test unit indicates that a four-stage CDS unit would be 99 percent efficient in removing the resultant particulate.

As a result of the corrosion which took place on the high voltage electrodes, arcing between the electrode and collector plates occurred at a lower than normal voltage because of the change in geometry. The basic electrode geometry has the desired electric field distribution characteristics but, if distorted to the degree experienced here, a significant degradation in performance can occur.

An analytical model of the electrode was generated and a parametric analysis performed. The results indicated that the collection efficiency may be increased by increasing the number of nozzles, but a basic geometry change was not indicated for increasing arc threshold (operating voltage).

One of the two CDS units which comprises the control system was isolated from the gas stream. The other was retrofitted with the design changes indicated by the analysis and included a gas distribution system design which would preclude a similar failure. The basic materials remained 316SS, but a locking gasket made of silicon rubber was replaced with Viton rubber. In addition, structural members were added to further support the gas distribution assembly. The existing wash system was expanded and additional wash assemblies were installed to ensure coverage of all areas that may be subject to deposit accumulation.

During the remaining time permitted under the program, the new wash system was proven capable of preventing deposit accumulation. The modified gas distribution assembly significantly improved the gas distribution throughout the collection system and in doing so improved the overall performance with respect to spark distribution and therefore electrode life expectancy. Since the energy as well as the frequency of the sparking influences the electrode life, it was also appropriate at this time to review the power control system design.

Standard electrostatic precipitator-type power supplies as is used in the CDS design has a high ripple characteristic. Filter capacitors are used to reduce the ripple to an acceptable level (25 percent) necessary for the Charged Droplet Scrubber applications. When an arc occurred, these capacitors discharged all the stored energy into the spark. These high energy arcs are damaging to the electrode nozzles as the result of extremely high localized temperatures. A series of tests were performed to assess the effects of removing the filter capacitors. It was demonstrated that the equipment can be operated without the filter capacitors with few minor changes to the control

system, but at the cost of reducing collective efficiency. However, an alternate method for controlling the ripple amplitude has the potential for increasing efficiency above the original level. It was also determined that the antenna-like coil used for spark sensing could not operate efficiently for extended periods of time and was subject to spurious input signals. An alternate sensing system was designed, developed and tested. It detects sparking by sensing abrupt voltage changes through a voltage divider located outside the hostile environment of the collecting section.

Another area which did not influence corrosion, but has the potential for affecting the efficient operation of the unit, is the changing conductivity of the water supplied to the electrodes and its effect on the high voltage isolation. Initially, isolation was provided by the resistance of the water along a length of non-conducting pipe. As water conductivity changed, so did the value of this resistance and caused greater leakage of current to ground. A new method of isolation was needed. A design was formulated and tested involving the use of an air gap as the isolation mechanism. The water at ground potential flows through a specially designed spray nozzle which separates the stream into discrete droplets providing discontinuity. This stream is collected in a container insulated from ground and is connected to the power supply. The container acts as a reservoir and carries the electrical charge required for atomization at the electrode as well. The design has operated with a charge as high as 50 KV and water conductivity of up 60,000 μmho/cm.

The results of the CDS corrosion studies and the concurrent CDS Redevelopment Program have measurably increased the available knowledge regarding the corrosion problems in the coke oven waste heat gas environment and demonstrated the need to fully characterize the gas constituents prior to designing a control system for any emissions problem.

SECTION 2

CONCLUSIONS AND RECOMMENDATIONS

Detailed conclusions and recommendations are presented in the sections which address specific areas of investigation. However, they are summarized here for convenience.

CONCLUSIONS

1) The tenfold increase of the CDS supply water chloride content was a major contributor to the pitting corrosion of the CDS electrodes and casing.

2) Generalized equipment corrosion in similar systems can be minimized if adequate flushing systems for the prevention of deposit accumulation are installed.

3) Greater corrosion resistance in the coke oven gas environment can be attained by the use of metals having a higher molybdenum content.

4) The corrosiveness of the coke oven waste heat gas stream can be reduced by the injection of additives such as NH_3.

5) The CDS has the potential of becoming an efficient SO_2 scrubber.

6) CDS electrode life can be significantly increased by the deletion of filter and R-C circuit capacitors with a small sacrifice in performance.

7) The basic electrode geometry utilized in the CDS has the desired electrical field distribution characteristics.

8) The CDS systems dependence on a constant water electrical conductivity can be voided by the incorporation of Air Gap electrical isolation system.

9) The CDS is capable of controlling the emissions from a coke oven waste gas system.

RECOMMENDATIONS

1) Further characterization of coke oven waste gases should be performed and the results correlated with the process equipment and coal types.

2) Long duration materials compatibility tests should be performed in the coke oven waste gas environment while simulating the conditions which might be anticipated in the various types of emission control equipment.

3) Further investigate the options of additives for corrosion control in the coke oven environment.

4) Alternate ripple control methods should be investigated for the Charged Droplet Scrubber application. The potential benefit would be an increase in collection efficiency as the result of a higher average voltage and an increase in equipment life.

5) Individual power sets should be provided for each electrode stage for the purpose of improving system performance and reliability.

6) Replace the present pickup coil-type spark detection system with a design which directly senses abrupt voltage changes (sparks) through a voltage divider.

7) Complete the development of the Air Gap high voltage isolation system.

8) Complete the overall CDS development.

SECTION 3

THERMO-CHEMICAL MAPPING

INTRODUCTION

Coking oven waste heat gas constituent measurements were conducted at the Kaiser coke plant facility during heavy and light-load conditions. These measurements consisted of a simultaneous 3-point gas/particle sampling effort. Concurrent with these gas phase samples, composite liquid samples were taken from the CDS waste water discharge and the outlet opacity was monitored.

The goal of the test program for this subtask was to provide thermo-chemical mapping based on the key locations in the CDS:

- Pre-cooler inlet (just upstream)
- CDS inlet, 24 m (3 ft) from CDS
- CDS exit, 15.2 m (50 ft) downstream

In the latter two cases significant modification of the chemical composition of the gas stream could occur due to the introduction of water, reduction of temperature, removal of particulate matter, or any combination of the three. The tests were conducted under the two different conditions experienced during normal operation: Heavy load (30 percent opacity which occurs during the oven loading cycle) and light load (after the ovens reach steady state temperature and opacity, 10 percent). During these two conditions, species such as SO_2, H_2SO_4/SO_3, HCl, and HF were measured in the gas phase. Other species such as Ni^{+2}, Cr^{+3}, Fe^{+3}, and Fe^{+2} were measured in the particulate matter collected by the sampling trains. The sampling train also had a thermocouple for the measurement of temperature.

In addition to these gas phase results, water samples from the CDS discharge were taken during the above tests. The water was analyzed for $SO_3^{=}$ $SO_4^{=}$, Cl^{-}, F^{-}, Cu^{+2}, Fe (total), Fe^{+2}, Ni, hardness, conductivity, pH and Chemical Oxygen Demand (COD). This data would be compared to gas phase data to attempt to find any sign of CDS corrosion.

CONCLUSIONS AND RECOMMENDATIONS

The Kaiser CDS facility was thermo-chemically mapped by sampling at three key locations (inlet CDS, exit pre-cooler and exit of the CDS).

The results showed that:

- Temperature profiles during heavy and light-load conditions were quite similar
- Outlet gas temperatures were at or slightly above 100°C
- Sulfur dioxide concentrations at the three locations did not vary significantly showing essentially no removal of SO_2 with the CDS operating conditions used during the tests
- Both SO_2 and SO_3 concentrations were higher during the light load tests
- Removal efficiencies for H_2SO_4 varied from 72 percent to 100 percent during the light load and heavy load tests respectively
- No significant amounts of HF was found in either test, but HCl was 23 percent by weight of the H_2SO_4 concentration during the heavy load tests

Based on these findings it is recommended that the current wash cycle be reprogrammed to prevent interruption of the cycle by upset conditions. Without this feature H_2SO_4 would tend to accumulate in the CDS and cause significant corrosion problems.

TEST PROCEDURES FOR CDS FACILITY

The equipment, the preparation, and the procedures necessary to perform a simultaneous 3 point gas/particle sampling effort at the CDS emission control system located at Kaiser Steel Company's Battery "A" coke ovens are discussed below. The location for collecting composite 1ℓ liquid samples as well as the temperature and pressure monitoring locations are also discussed.

Equipment

The particle/gas sampling train used for this test program is the Controlled Condensation System (CCS) (Reference 1). CCS is designed to measure the vapor phase concentration of SO_3 as H_2SO_4 in controlled or uncontrolled flue gas streams. This method is specifically designed to operate at temperatures up to 250°C (500°F) with up to 3000 ppm SO_2, 8-16 percent H_2O, and up to 9 g/m^3 (4 gr/cf) of particulate matter.

By using a modified Graham condenser, the gas is cooled to the acid dew point at which the SO_3 (H_2SO_4 vapor) condenses. The temperature of the gas is kept above the water dew point to prevent an interference from SO_2 removed by condensing water while a heated quartz filter system removes particulate matter. The condensed acid is then titrated with 0.02 N NaOH using Bromophenol Blue as the indicator.

The CCS, which was used for gas sampling, consists of a heated quartz probe, quartz filter holder. Tissuequartz filter, controlled condensation

coil and five impingers. For the gas sampling measurements the impingers were filled with 3 percent H_2O_2 (one) and 3 percent high purity Na_2CO_3 (two) and Drierite (one) (Figure 2). The predicted distribution of the species collected in the train is shown in Table 1. The fabrication of this equipment is described in detail in Reference 1.

TABLE 1. EQUIPMENT AND SPECIES SEPARATION IN GAS SAMPLING

SAMPLE TRAIN COMPONENT	COLLECTED SAMPLE
Probe	Particulate
Filter	Particulate
Controlled Condensation Coil	H_2SO_4
3% H_2O_2 Impinger (1)	SO_2 (HCl, HF, HCN)
3% Na_2CO_3 (high purity) (2)	H_2S, HCl, HF, HCN

The liquid sampling was conducted using a pump, Teflon tubing and a gallon gas container. During the tests a sample was taken every 5 minutes (~ 500 ml) into a 4ℓ container. These samples were either apportioned into a 1ℓ pre-cleaned polypropylene container for inorganic analysis or into a glass container with a Teflon top for organic analysis.

Preparation

The glassware and plastic containers used during this sampling test were pre-cleaned to avoid sample contamination. The procedures used for this cleaning are described in Table 2. High purity reagents (Baker Utrex or equivalent) and water (ASTM type I or better, Reference 2) were used.

Sampling Procedures

The goal of these tests was to provide a chemical map of the CDS emission control system. The three gas phase sampling trains for simultaneous sampling were located at positions which would have the greatest change in gas compositions and temperature:

- CDS inlet
- Pre-cooler exit
- CDS exit

To complement these gas sampling positions, samples of the inlet water and CDS discharge water were taken. Figure 3 and Table 3 show and describe

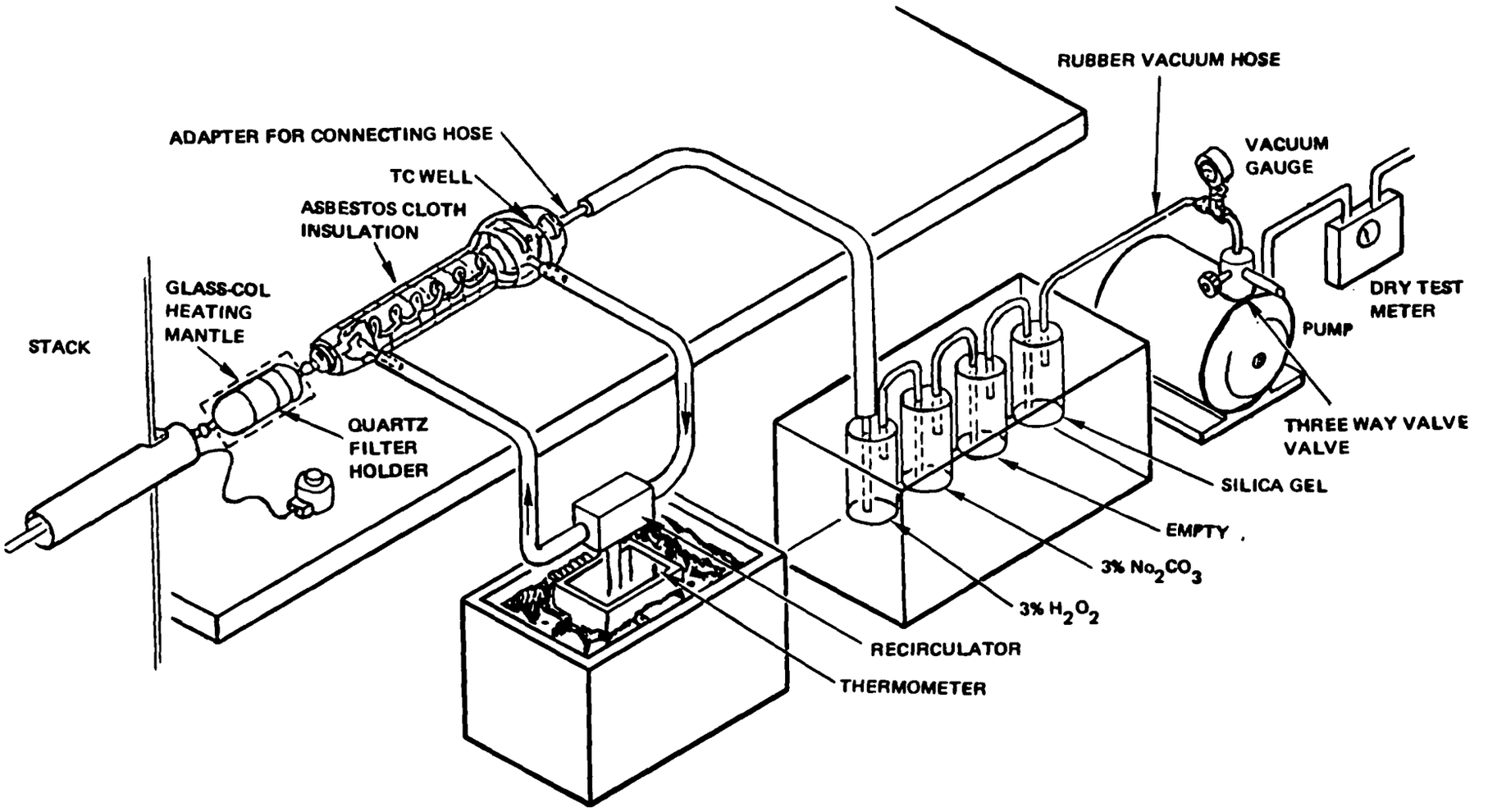

Figure 2. Controlled condensation system setup (modified).

TABLE 2. CLEANING PROCEDURES

COMPONENT	CLEANING PROCEDURES (ORDER APPLIED LEFT TO RIGHT)							
	MUFFLE (288°C)	Brush	15% HNO_3	H_2O	ACETONE	METHYLENE CHLORIDE	AIR DRY	REMARKS
Nylon Brush			3 hrs	Rinse	Rinse	Rinse	X	Inspect for corrosion, degradation and bristle shedding; discard if any found
Probe Liner		X	Rinse/Brush	Rinse	Rinse	Rinse	X	All material must be removed via brush and rinsing
Cyclone		X	Rinse/Brush	Rinse	Rinse	Rinse	X	All material must be removed via brush and rinsing
Filter Housing			Rinse	Rinse	Rinse	Rinse	X	Back flush to remove any impacted material in the front/side
Impingers		Optional	Rinse	Rinse	Rinse	Rinse	X	
Connecting Glassware		Optional	Rinse	Rinse	Rinse	Rinse	X	
Controlled Condensation Coil			3 hrs/Rinse	Rinse	Rinse	Rinse	X	HNO_3 soak not necessary if no particulate in coil - simply rinse
Filter Tissuequartz	4 hrs							Field blank samples will be analyzed in parallel with actual samples
Plastic Storage Bottles			3 hrs	Rinse			X	Linear polyethylene or polypropylene

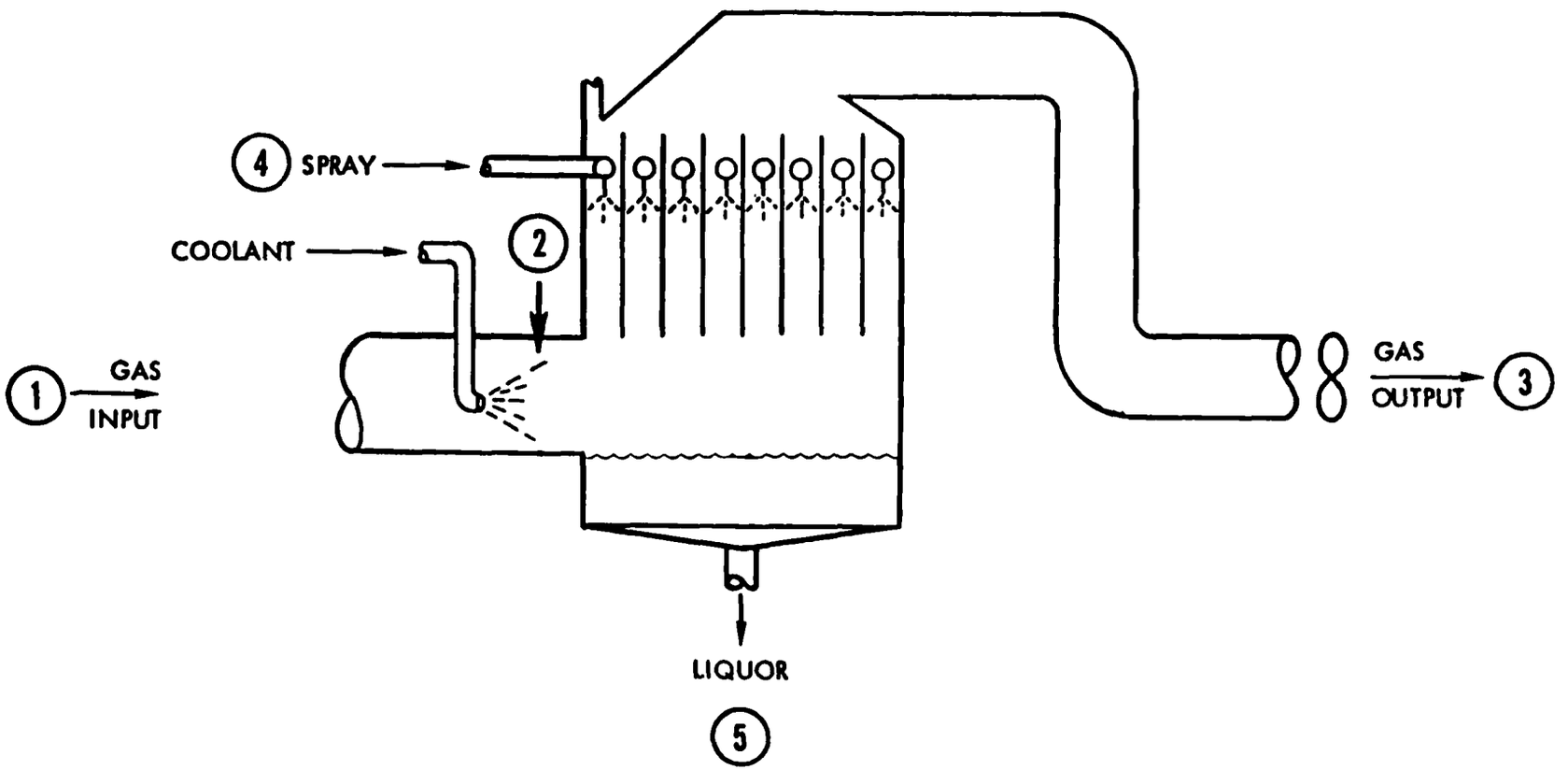

Figure 3. Gas and liquid sampling positions.

TABLE 3. GAS AND LIQUID SAMPLING POSITION

POSITION	MEASUREMENTS	CONDITIONS
1. Inlet to precooler	Gas/particulate and temperature	Just prior to precooler 230 - 260°C
2. Inlet to CDS	Gas/particulate	Just prior to CDS in transform stage 120 - 132°C
3. Exit CDS	Gas/particulate and temperature	After fan, approximately 50 ft downstream of the CDS 79 - 93°C
4. CDS spray water	Liquid	Domestic water used in the discharge line
5. CDS discharge	Liquid	Leading to the sump

the locations and lists the samples and the measurements. Engineering data such as gas flow rates, water inputs, opacity measurements and process information were also collected for later correlation with the sample analysis. The test conditions were arranged so that a sample was taken during light load and heavy load conditions. During the light load condition, a nominal run time of one hour was used. Sampling during the heavy load period continued until the opacity was below 30 percent (45 minutes). Since all of the pre-cooler water was vaporized there is no quench water sample.

All liquid sample containers were completely filled and capped to exclude air. To supplement these water samples, additional 1ℓ samples of water for COD analysis were taken. These water samples were stored in pre-cleaned (following impinger cleaning procedure) amber glass bottles with Teflon lined tops. Both water samples were returned to the laboratory for immediate analysis.

The CDS was operated as described in Reference 1 except for the following changes:

- The filter was saved
- The probe rinse was saved
- 100 ml of 3 percent H_2O_2 and 3 percent Na_2CO_3 was used
- High purity reagents were used

The list of the samples recovered is presented in Table 4.

TABLE 4. SAMPLE RECOVERY

	RECOVERY PROCEDURE	STORAGE*
Probe and Probe Rinse	Probe shaken or tapped to remove loose particles then brushed. Remaining particulate matter rinsed in container with 15% HNO_3 followed by H_2O	Plastic
Filter	Remove, fold in half and place in sealed jar	Plastic
Controlled	Remove coil from train, invert over container and rinse repeatedly with high purity H_2O	Plastic
H_2O_2 Impingers	Rinse all condensate in preceding lines into impinger with high purity H_2O. Rinse impinger with high purity H_2O and save condensate and rinses	Plastic
Na_2CO_2	Rinse all condensate in lines into next impinger. Save all impingers. Rinse with H_2O	Plastic
Blanks	Place samples of high purity H_2O, H_2O_2, Na_2CO_3, and HNO_3 in separate containers	Plastic

*Plastic refers to linear polyethylene or polypropylene precleaned containers (see preparation).

ANALYSIS OF CDS SAMPLES

The material from the individual train components was recovered and returned for analysis. Table 5 lists the train component and the analysis performed. The water samples obtained from the test were analyzed for all of the species listed in Table 5 with the addition of hardness (as $CaCO_3$), conductivity, pH, and COD.

All required samples were filtered through 0.45 micron Millipore filters. Methods used were those described in Federal Register, 41, No. 232, 1976, and are listed in Table 6.

TABLE 5. GAS SAMPLING TRAIN ANALYSIS

SPECIES	PARTICULATE		CCC*	H_2O_2 IMPINGERS	Na_2CO_3 IMPINGERS
	PROBE RINSE	FILTER			
Cr(T)	X	X			
Fe(T)	X	X			
Fe^{+2}		X			
Ni	X	X			
CL^-	X	X		X	X
F^-	X	X		X	X
SO_4^{-2}	X	X		X	X
SO_3^{-2}		X			
H^+			X		

*CCC = Control Condensation Coil

TABLE 6. ANALYSIS METHODS

SPECIES	ANALYSIS PROCEDURE
Nickel	Atomic absorption
Chromium	Atomic absorption
Copper	Atomic absorption
Iron (Total)	Atomic absorption
Chlorides	Titration with mercuric nitrate
Fluoride	Ion selective electrode (no distillation step)
Cyanide	Pyridine-Barbituric acid (no distillation step)
Sulfite	Titrimetric - iodine
Sulfate	Turbidimetric
Sulfide	Photometric - methylene blue
pH	Electrometric
Hardness	Sum of Ca, Mg and Fe by AAS
Specific Conductivity	Wheatstone Bridge conductimetry
Iron II	Photometric - 1, 10 phenanthroline

RESULTS AND DISCUSSION

The gas and liquid sampling program was conducted during heavy load and light load conditions on separate days. The CDS operating parameters are shown in Table 7. A log of electrical parameters recorded during the tests are presented in Appendix A.

The CCS trains were equipped with thermocouples to measure the waste gas temperature at the three positions sampled. The temperature profile for both cases are very similar, as seen in Table 8. This data shows that the quench water is completely evaporated and that no free liquid is available to scrub SO_2 or SO_3 in the quench area.

TABLE 7. CDS OPERATION PARAMETERS

VARIABLE	CONDITION	
	LIGHT LOAD	HEAVY LOAD
Percentage Opacity, %	9.3 ± 4	33 ± 15
Inlet Gas Flow (dsm^3/min) (dscfm)	787-827 27,800-29,200	787-827 27,800-29,200
Outlet Gas Flow (dsm^3/min) (dscfm)	932-997 32,900-35,200	932-997 32,900-35,000
Inlet % H_2O	14	9
Outlet % H_2O	14	14
Quench Water Flow (ℓ/min) (gpm)	38-57 10-15	38-57 10-15
Electrode H_2O Flow (ℓ/min) (gpm)	19 5	19 5
Average Stage Electrode Voltage (KV)	32.1 ± 2	30.7 ± 1.8

TABLE 8. TEMPERATURE PROFILES IN CDS DURING HEAVY AND LIGHT LOAD CONDITIONS

POSITION	TEMPERATURE, °C	
	LIGHT LOAD	HEAVY LOAD
Inlet to Precooler	237 ± 5	232 ± 2
Inlet to CDS	158	182 ± 5
Exit CDS	104 ± 1	97 ± 2

Acid Gas and Particulate Concentrations In the CDS

While the CCS is primarily a H_2SO_4 sampling system, the train as set up at Kaiser was capable of collecting particulate material, H_2SO_4, SO_2, HCl and HF. The results for species monitored in the gas phase are tabulated in Table 9 for the three positions monitored in the CDS.

The most striking feature of the gas phase analysis results in lack of SO_2 scrubbing by the CDS. Previous CDS tests at Kaiser indicated that a 13 percent SO_2 removal per stage was possible. However, operating conditions during the latest series of tests were different than the original SO_2 removal studies. One CDS unit was isolated from the gas stream and the total gas volume was passed through the remaining CDS unit. The resulting liquid to gas ratio was one half that of the original tests. Finally, the spark rate during the original SO_2 removal studies was approximately twice as high. The end result of these changes is to decrease the gas residence time, reduce the liquid/gas (l/g) ratio and decrease the ozone formation. The residence time and l/g ratio directly affect the SO_2 scrubbing efficiency of any scrubber system and appear in the CDS to be very important factors in SO_2 removal. The lower spark rate produces less ozone and probably reduces the SO_3 formation. Converting SO_2 to SO_3 should increase the SO_2 removal by reducing the apparent amount of SO_2 in the gas phase and actually permitting the CDS to remove SO_3 as a liquid aerosol of H_2SO_4. The latter point seems to be proven by the H_2SO_4 data obtained in the light load condition where the H_2SO_4 value steadily decreased across the CDS. The CDS system (quench water + spray nozzles) appears capable of removing 72 percent of the H_2SO_4 introduced into the system of which 60 percent is removed by the spray nozzles.

The data for the upset condition is not as clear-cut, since the $SO_4^{=}$ and H^+ titration of the coil rinse did not agree. It appears that another acidic species was condensed in the coil along with H_2SO_4. Visual observations in the field indicated that coil rinse to be discolored instead of clear as in the light load condition. The plume during the upset condition was black with coal and hydrocarbon aerosol by-products.

The filter system, which is heated to 200°C, probably allowed organic material to pass into the coil. While there was not enough solution for further confirmatory analysis, it was possible that an organic acid or phenol caused a positive interference with the H^+ analysis.

Using the $SO_4^{=}$ titration values as the true H_2SO_4 concentration, the CDS was 100 percent effective in removing H_2SO_4 during the heavy load condition. The reason for this improved efficiency was probably due to the presence of the large quantity of particles. The H_2SO_4 in the high humidity of the CDS probably condensed on the solid particles and grew in size because of the hydroscopic nature of H_2SO_4. These larger H_2SO_4 liquid aerosols were more easily removed by the CDS.

The results of these tests show that the H_2SO_4 concentrations during the light load mode are higher than the upset mode. This finding indicated that to minimize corrosion a wash cycle must be maintained during the long period of

TABLE 9. GAS PHASE SPECIES CONCENTRATION

CONDITION/ DATE	POSITION/ GAS VOLUME	SPECIES CONCENTRATION (mg/dsm^3)									Remarks
		Cr	Ni	Fe(II)	Fe(T)	Cl^-	F^-	SO_2	H_2SO_4		
									SO_4	H^+	
Heavy Load 11/8/77	Inlet	0	0	0	0	13.2	0.41	441 (154 ppm)	57 (13 ppm)	51 (12 ppm)	
	Pre-Cooler	0	0	0	9.6	1.2	0.49	466 (163 ppm)	28 (6.4 ppm)	76 (17 ppm)	
	Exit	0	0.8	0	1.1	7.5	0.50	530 (186 ppm)	0	28 (6.4 ppm)	
Light Load 11/9/77	Inlet	0	0	0	0	2.3	0.23	600 (210 ppm)	81.4 (18.5 ppm)	79.8 (18.2 ppm)	
	Pre-Cooler	0	0	0	0.2	1.6	0.34	569 (199 ppm)	57.1 (13.1 ppm)	58.4 (13.3 ppm)	2.9 mg/dsm^3 as SO_4 on filter
	Exit	0	0	0	0	1.9	0.31	620 (217 ppm)	22.6 (5.2 ppm)	21.3 (4.9 ppm)	4.3 mg/dsm^3 as SO_4 on filter

light load (i.e., non-operation of the CDS). Simply leaving the CDS in the down status will allow significant quantities (3.5 kg/hr) of H_2SO_4 to accumulate in the CDS.

The rest of the results from the gas phase test indicate no unusual amounts of HCl or HF. While there appears to be some Fe present in the particulate matter, there is no evidence of Ni or Cr which would indicate gross erosion of the 316SS in the CDS.

Liquid Sample Test Results

The analysis of the water samples taken during gas sampling are shown in Tables 10 and 11. The amount of Fe, Cr and Ni found in the discharge water roughly corresponds to the ratio of Ni and Cr found in 316SS, and might be evidence of corrosion in the CDS. It is also possible that the acidic (pH 2.5) sump water simply extracted the particulate matter collected by the CDS. Since the particulate matter collected on the filter was only water extracted, this could explain the lack of finding Fe in the inlet particulate sample.

Prior to this test series, a series of time sequenced water samples were taken from the CDS water discharge during a heavy load condition. The results

TABLE 10. INLET AND CDS DISCHARGE WATER ANALYSIS FROM HEAVY LOAD CONDITIONS

SPECIES	CDS SUPPLY WATER	CDS DISCHARGED
Chromium	<0.03 mg/l	0.50 mg/l
Iron (Total)	<0.03 mg/l	3.33 mg/l
Iron (II)	<0.05 mg/l	1.15 mg/l
Nickel	<0.03 mg/l	0.37 mg/l
Chloride	7.5 mg/l	21.7 mg/l
Fluoride	0.2 mg/l	0.5 mg/l
Sulfate (Turbidimetric)	<1 mg/l	364 mg/l
Sulfite	<1 mg/l	<1 mg/l
H^+ (as H_2SO_2)	<1 mg/l	245 mg/l
Hardness (as CaCO3)	73 mg/l	96.9 mg/l
Conductivity	210 µmhos/cm	2000 µmhos/cm
pH	8.02 units	2.46 units
COD	--	21 mg/l
Sulfate (by $BaClO_4$ Titration)	--	376.2

TABLE 11. ANALYSIS OF SEQUENTIAL CDS DISCHARGE WATER SAMPLES TAKEN DURING HEAVY LOAD CONDITION

	SAMPLE NUMBER																		
ANALYSIS	#1	#2	#3	#4	#5	#6	#7	#8	#9	#10	#11	#12	#13	#14	#15	#16	#17	#18	#19
Nickel	<0.03	0.31	0.13	0.19	0.16	0.19	0.19	0.22	0.19	0.25	0.22	0.25	<0.03	0.16	0.13	0.13	0.19	0.19	0.22
Chromium	<0.03	0.70	0.47	0.33	0.33	0.30	0.33	0.38	0.34	0.47	0.53	0.56	<0.03	0.34	0.25	0.28	0.30	0.34	0.41
Copper	<0.02	<0.02	<0.02	<0.02	<0.02	<0.02	<0.02	<0.02	<0.02	<0.02	<0.02	<0.02	<0.02	<0.02	<0.02	<0.02	<0.02	<0.02	<0.02
Iron II	<0.04	1.64	2.53	1.67	2.30	1.68	1.86	1.86	1.44	1.54	1.41	1.37	<0.04	0.99	1.86	2.17	0.67	0.61	0.72
Iron (Total)	<0.05	6.14	4.52	3.95	4.14	3.48	3.48	3.81	4.05	4.29	4.05	4.76	<0.05	3.81	3.10	3.95	3.62	4.76	4.71
Chloride	60.1	25.5	25.0	26.8	26.5	25.8	25.5	28.0	28.3	29.0	27.5	26.8	59.8	26.8	25.5	25.5	25.5	25.0	25.0
Fluoride	0.19	0.75	0.75	0.75	0.75	0.75	0.75	0.75	0.75	0.75	0.75	0.75	0.19	0.75	0.75	0.75	0.75	0.75	0.75
Cyanide	0.02	0.04	0.06	0.07	0.06	0.04	0.12	0.13	0.15	0.05	0.12	0.06	0.03	0.05	0.06	0.05	0.05	0.06	0.06
Sulfite	<0.3	<0.3	<0.3	<0.3	<0.3	<0.3	<0.3	<0.3	<0.3	<0.3	<0.3	<0.3	<0.3	<0.3	<0.3	<0.3	<0.3	<0.3	<0.3
Sulfate	11.6	286	244	236	242	240	246	280	268	256	246	240	10.0	220	216	232	250	260	265
Sulfide	<0.10	<0.10	<0.10	<0.10	<0.10	<0.10	<0.10	<0.10	<0.10	<0.10	<0.10	<0.10	<0.10	<0.10	<0.10	<0.10	<0.10	<0.10	<0.10
pH (units)	7.96	2.43	2.50	2.51	2.51	2.52	2.50	2.48	2.46	2.45	2.47	2.50	7.96	2.53	2.56	2.55	2.52	2.49	2.46
Hardness (as $CaCo_3$)	82	91	91	91	91	91	91	91	91	91	91	91	82	91	91	91	91	91	91
Specific Conductivity @ 25°C (Micromhos/cm)	290	1310	1250	1210	1230	1230	1280	1380	1440	1480	1420	1350	290	1210	1180	1220	1290	1380	1480

NOTE: All units are mg/ℓ except where noted.

of the analysis of these samples are tabulated in Table 11 and explained in Table 12. The values found are similar to the composite sample values taken on November 8 and 9, 1978. The time sequence samples show a relatively even concentration of the species measured with no large spike from any of the coke oven operational processes. The only anomaly associated with this data was the apparent loss of chloride from the discharge water compared to the inlet water. This anomaly could not be explained by re-entrainment of Cl^- in the form of liquid aerosols since there was no significant increase in the Cl^- content of the gas stream.

TABLE 12. TIME PHASED CDS WATER SAMPLE LOG

SAMPLE NO.	TIME*	LOCATION	PROCESS CONDITIONS
1	2:20	H_2O Input	Domestic water
2	3:10	CDS Disch.	Battery in steady state -- light load -- before pushing begins
3	3:15	CDS Disch.	First oven pushed -- started sample at ram retraction plus one minute
4	3:20	CDS Disch.	Oven pushed but not yet charged
5	3:23	CDS Disch.	Start of charging operation
6	3:25	CDS Disch.	Charging in process
7	3:27	CDS Disch.	Charging completed, slight stack emission - beginning of heavy load
8	3:29	CDS Disch.	Heavy load
9	3:31	CDS Disch.	Heavy load
10	3:33	CDS Disch.	Start of pushing operation on second oven
11	3:34	CDS Disch.	One minute after start of push
12	3:37	CDS Disch.	One minute after Ram retracted
13	3:57	Domestic Water	
14	3:43	CDS Disch.	Charging vent closed on second oven pushed
15	3:43	CDS Disch.	Heavy load continues -- 5 minute sample time (3:43 start, 3:48 complete)
16	3:49	CDS Disch.	High spark rate in unit - heavy load
17	3:53	CDS Disch.	One minute after ram retracted on third oven pushed
18	3:56	CDS Disch.	Heavy load continues
19	4:00	CDS Disch.	End of battery activity -- stack looks good - slight steam plume

*30 Second time period to pull one sample with vacuum pump

SECTION 4

ELECTRODE GEOMETRY

INTRODUCTION

The electric field at the tip of the spray tube influences two significant factors; 1) the charge to mass ratio of the sprayed droplets and 2) and the acceleration of the droplets away from the tip. For a given geometry the applied voltage determines not only the field at the spray tube tip but also the field strength within the remainder of the sweep volume.

In normal operation the CDS voltage is set at the highest value compatible with a permissible arc rate. Arcing frequently initiates at the tip of the spray tube since, because of the relatively small tube diameter, this is the region of highest field intensity. However, the onset of corona produces a conducting plasma around the tip which enlarges the effective tip radius and decreases the field strength at the tip. When this occurs arcing can initiate in other regions, as for example, at the wall of the electrode tube. The phenomenon is further complicated by the presence of water drops on the electrode and the influence of space charge within the scrubber.

The objective of the task described in this section was to generate analytic computer plots of the field distribution for various geometries in order to better understand the influence of geometry on the field distribution and hopefully to indicate the direction for future design improvements.

CONCLUSIONS AND RECOMMENDATIONS

The basic electrode geometry, as represented by Cases 1 and 3 of Table 13, has the desired electric field distribution characteristics. Some optimization may be afforded by further parametric investigation of needle length variation. The electric field plots also suggest that reduction in needle spacing may yield a more efficient electrode by introducing more spray tubes per unit length of electrode tube, without appreciable altering the strong potential gradient towards the collector plates.

The predicted effects are not dramatic. A parametric experimental study will be required to determine the magnitude of the improvements to be attained. Calculations for the full space charge case should also be performed. However, in view of the small effects predicted by the Laplace solutions it is anticipated no dramatic geometric dependence will be prediced by the Poisson solutions for the scale of geometric variations that have been studied.

ANALYTICAL APPROACH

Analytical models of a series of two dimensional representations of the CDS electrode geometry were programmed for parametric analysis. The geometry used is illustrated in Figure 4. The high voltage electrode is centered between two parallel, grounded collector plates at a distance 2b apart. The electrode tube has a radius of a', and holds a series of spray tubes of radius a each, spaced at distance c from one another. The spray tubes protrude a distance ℓ from the centerline of the electrode tube.

Zero space charge field distributions were calculated as functions of the various geometric parameters. This was done by obtaining computer field plots and solutions of Laplace's equation for the geometries of interest. Ultimately, it will be desirable to include space charge in the analysis, i.e. use Poisson's equation; however, the zero space charge problem is more tractable and provides an easier means of obtaining a first approximation to the total solution.

Solutions to the Laplace equation in the absence of space charge, $\nabla^2 V = 0$, were developed in the following form.

$$V(x,y) = -A \ln \frac{\cosh\left(\frac{\pi x}{2b}\right) - \cos\left(\frac{\pi y}{2b}\right)}{\cosh\left(\frac{\pi x}{2b}\right) + \cos\left(\frac{\pi y}{2b}\right)}$$

where A is defined by

$$V(0,0) = -A \ln \frac{1 - \cos\left(\frac{\pi a}{2b}\right)}{1 + \cos\left(\frac{\pi a}{2b}\right)}$$

The effects of spray tube length, ℓ, spray tube spacing, c, and electrode tube radius, a', were represented in the solutions.

Six electrode geometries were selected for parametric analysis. Table 13 lists their pertinent geometrical parameters. Equipotential plots were generated for two planes in order to analyze each of these geometries. The first plan (x-y) is normal to the collector plates and the spray tubes, and passes through the tips of the spray tubes. The second plane (y-z) is normal to the collector plates and the electrode tube, and passes through the centerline of a spray tube. Figures 5 through 15 present the equipotentials generated. The equipotentials are labelled as their ratio to electrode potential. The electrode area intercepted by the x-y or y-z plane analyzed is shown in cross-section on these figures.

TABLE 13. ELECTRODE GEOMETRY PARAMETERS

CASE	SPRAY TUBE RADIUS a (mm)	(INCH)	COLLECTOR HALF-SPACING b (mm)	(INCHES)	SPRAY TUBE SPACING c (mm)	(INCHES)	SPRAY TUBE LENGTH ℓ (mm)	(INCHES)	ELECTRODE TUBE DIAMETER a' (mm)	(INCHES)
1	0.635	0.025	63.5	2.5	43.18	1.7	38.1	1.5	9.52	0.375
2	0.635	0.025	63.5	2.5	43.18	1.7	38.1	1.5	12.7	0.50
3	0.635	0.025	63.5	2.5	43.18	1.7	15.88	0.625	9.52	0.375
4	0.533	0.021	31.75	1.25	25.4	1.0	22.03	0.8675	4.76	0.1875
5	0.533	0.021	31.75	1.25	25.4	1.0	5.33	0.21	4.76	0.1875
6	0.533	0.021	31.75	1.25	25.4	1.0	34.3	1.35	4.76	0.1875

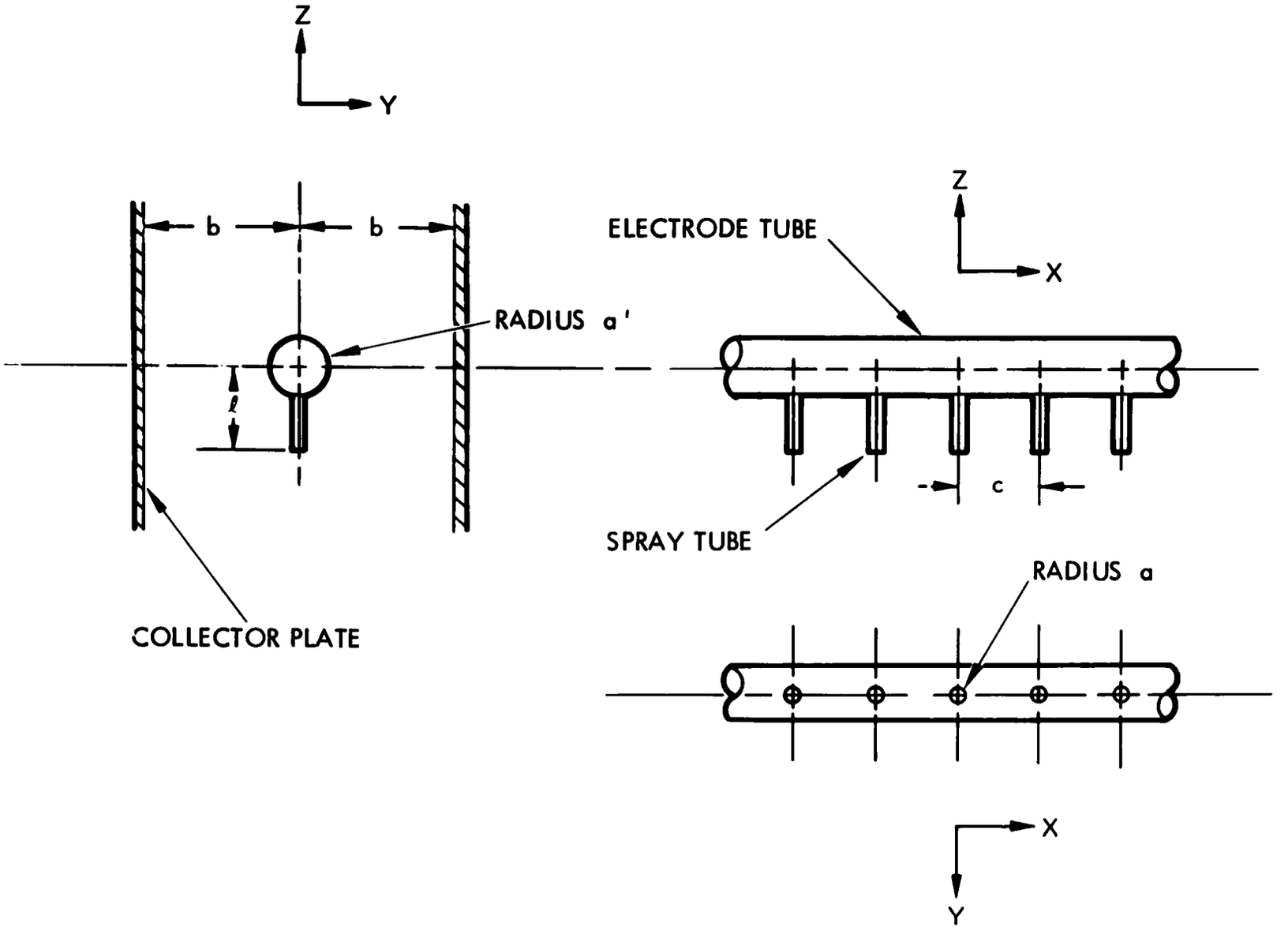

Figure 4. CDS electrode geometry.

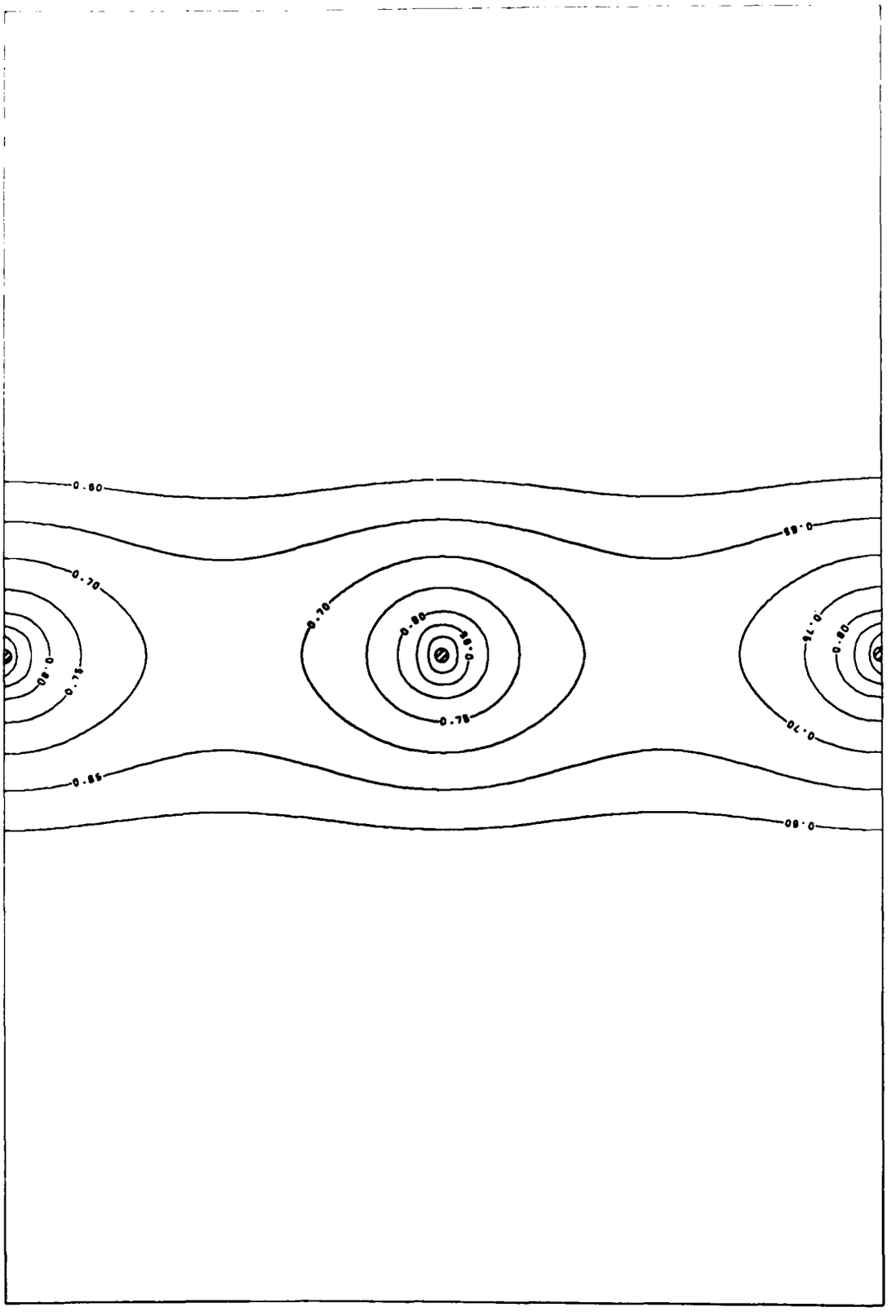

Figure 5. Case 1, electrode geometry, x-y equipotentials.

PARAMETRIC ANALYSIS

Figure 5 illustrates typical electric fields surrounding the spray needle tips. It is interesting to note that the field lines do not go to zero potential between the spray tips, that the field is most intense near the tips, and is weakest in the regions between tips and at the collector plates. Figure 6 gives further definition of the fields at the spray tip. They are more intense going towards the collector plates than they are in the flow direction (z-axis).

Figure 7 and 8 show that increasing electrode tube diameter from 19.1 to 25.4 mm (0.75 to 1.0 in.) has little effect on the electric fields near the spray tips. As would be expected, there is some distortion of the electric fields in the vicinity of the electrode tube.

Shortening the spray tubes from 38.1 to 15.88 mm (1.5 to 0.625 in.) length tends to weaken the electric field at the tips, as can be seen in Figure 9. The field distribution in the flow direction for this case is shown in Figure 10.

Figure 11 illustrates typical electric fields surrounding the spray needle tip in a more compact geometry having half the collector spacing examined above. The field distribution is very similar to Case 1 (Figure 5), but is about twice as intense because of having smaller physical dimensions. Figure 12 shows the field distribution in the y-z plane. When compared with Case 1 (Figure 6), less distortion is seen near the needle-to-electrode-tube interface.

Figure 13 shows a very short spray needle, 5.33 mm (0.21 in.) long, in the compact geometry. Shortening the needle to this length severely weakens the electric field at the needle tip, because of the dominant influence of the electrode tube.

Increasing the needle length from 22.03 to 34.3 mm (0.8675 to 1.35 in.) increases the electric field only slightly at the needle tip, as can be seen by comparing Figure 14 with Figure 11. Figure 15 shows how the axial field distribution is elongated further along the flow direction with the longer needle.

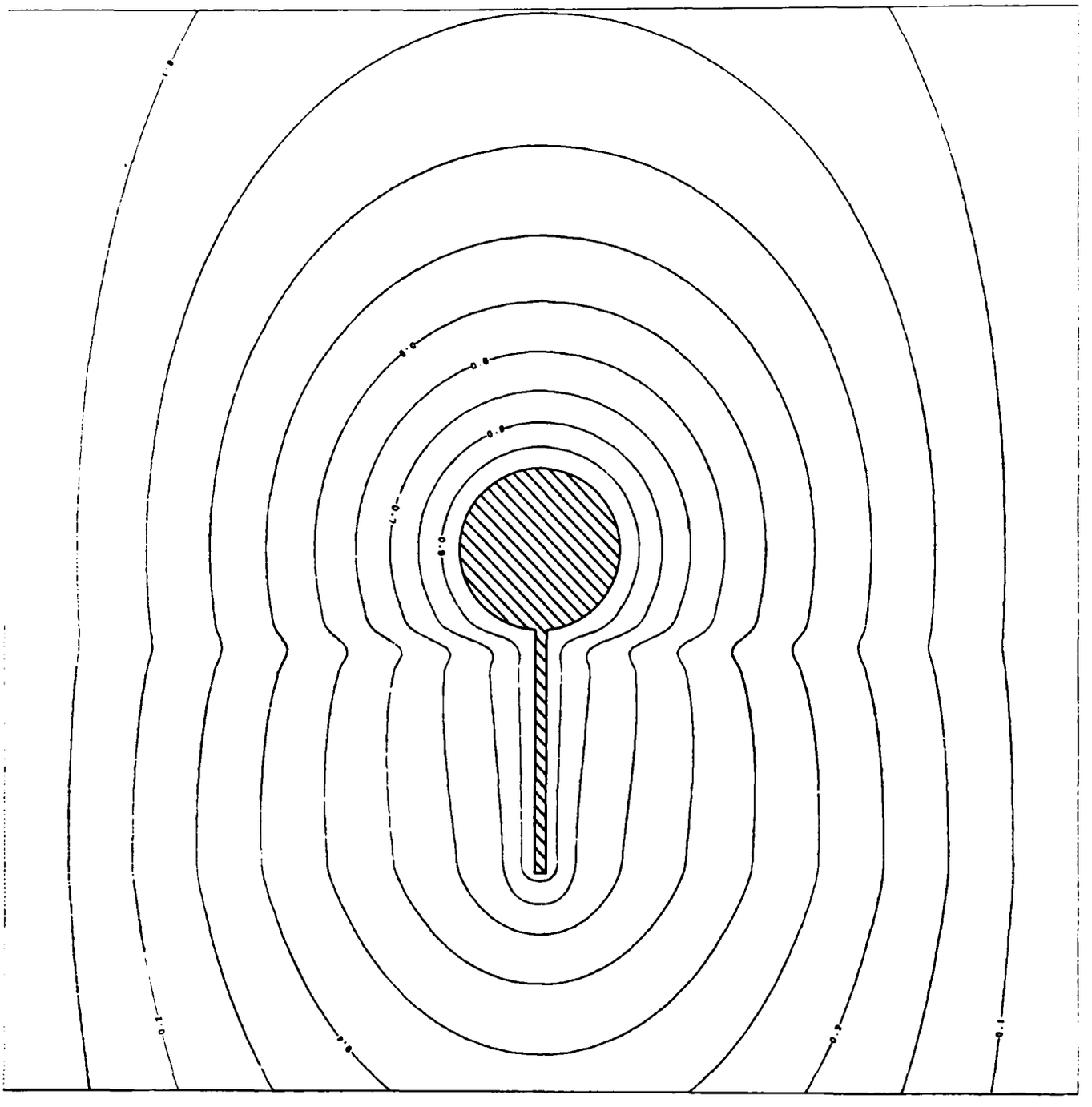

Figure 6. Case 1, electrode geometry, y-z equipotentials.

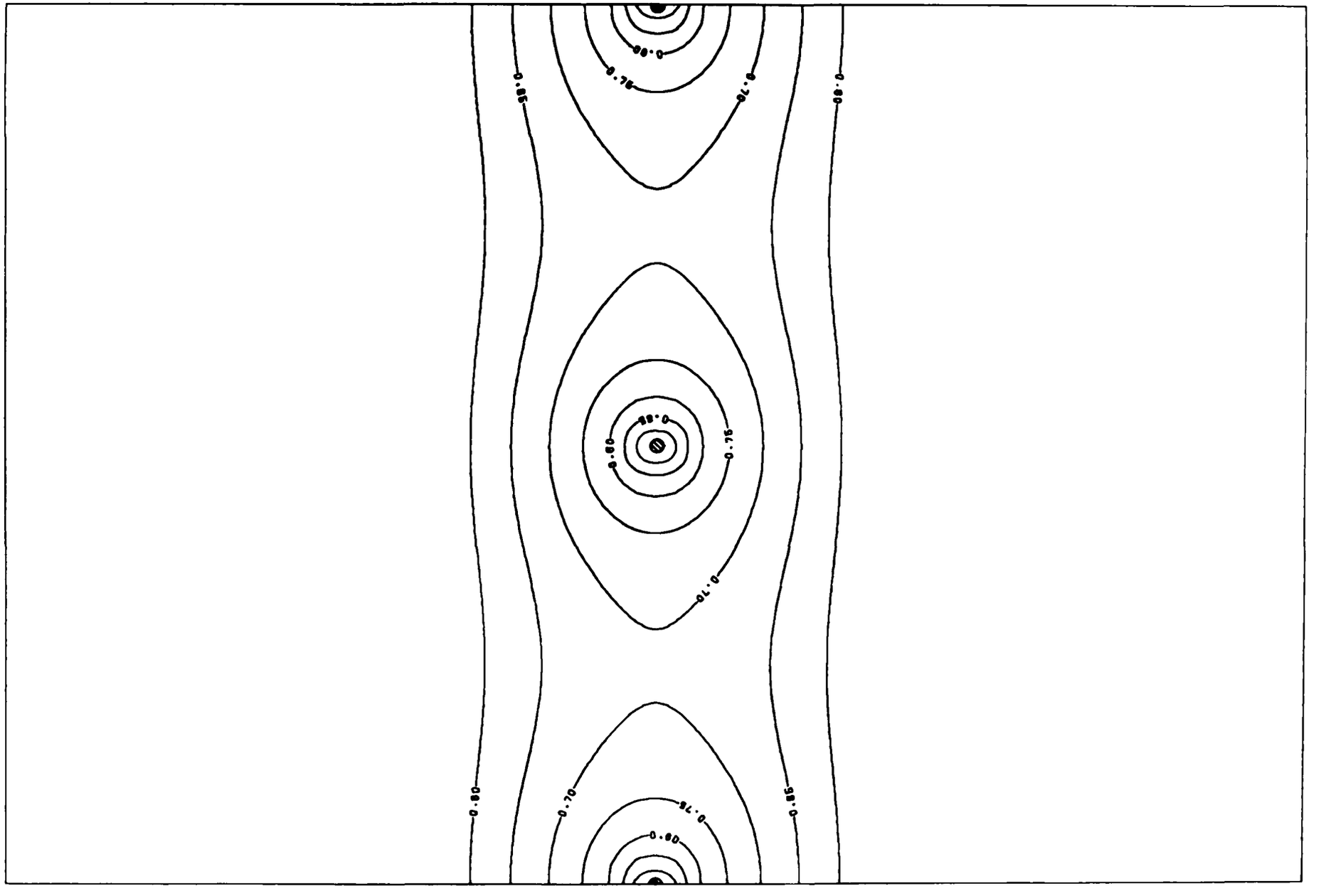

Figure 7. Case 2, electrode geometry, x-y equipotentials.

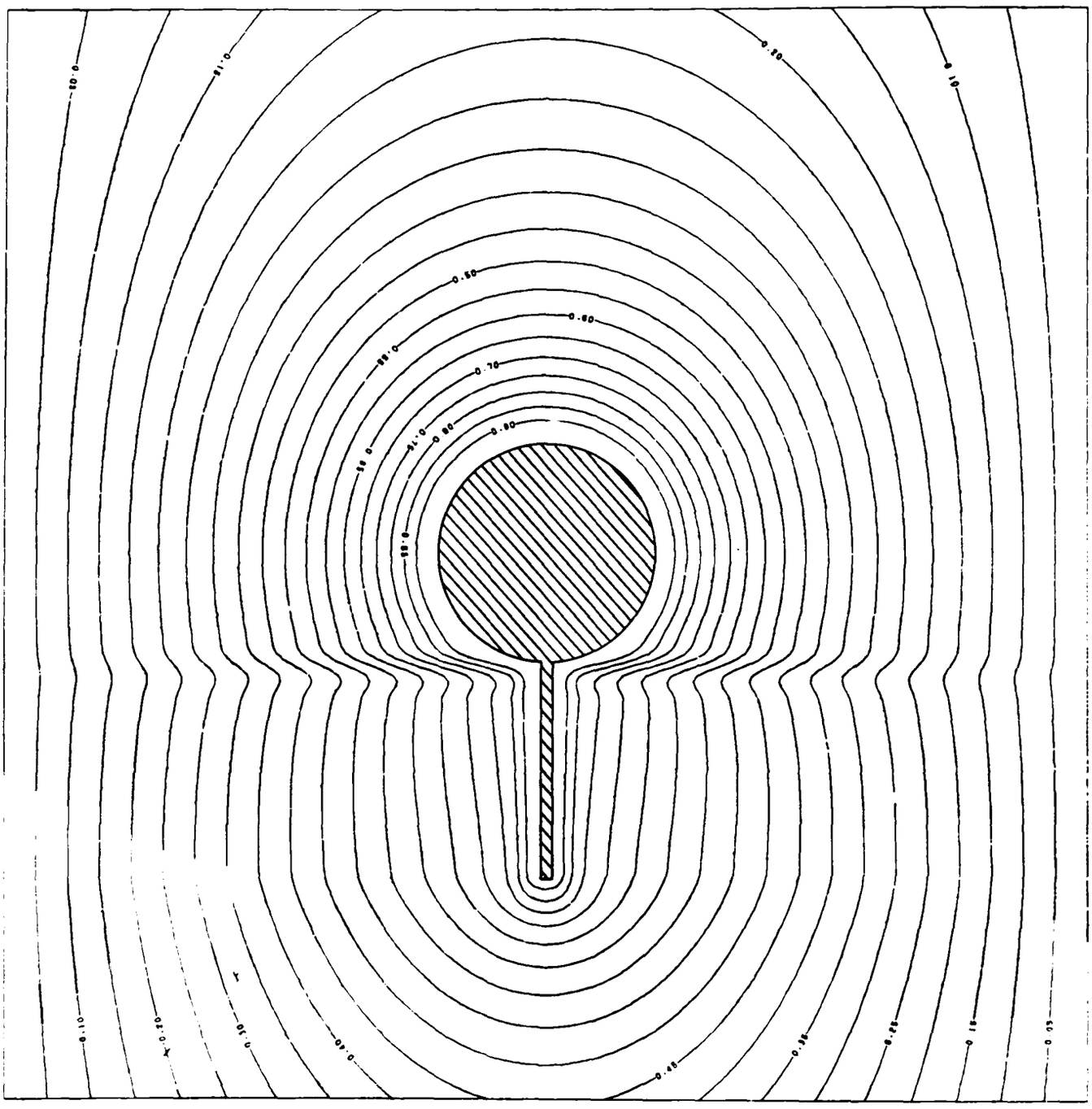

Figure 8. Case 2, electrode geometry, y-x equipotentials.

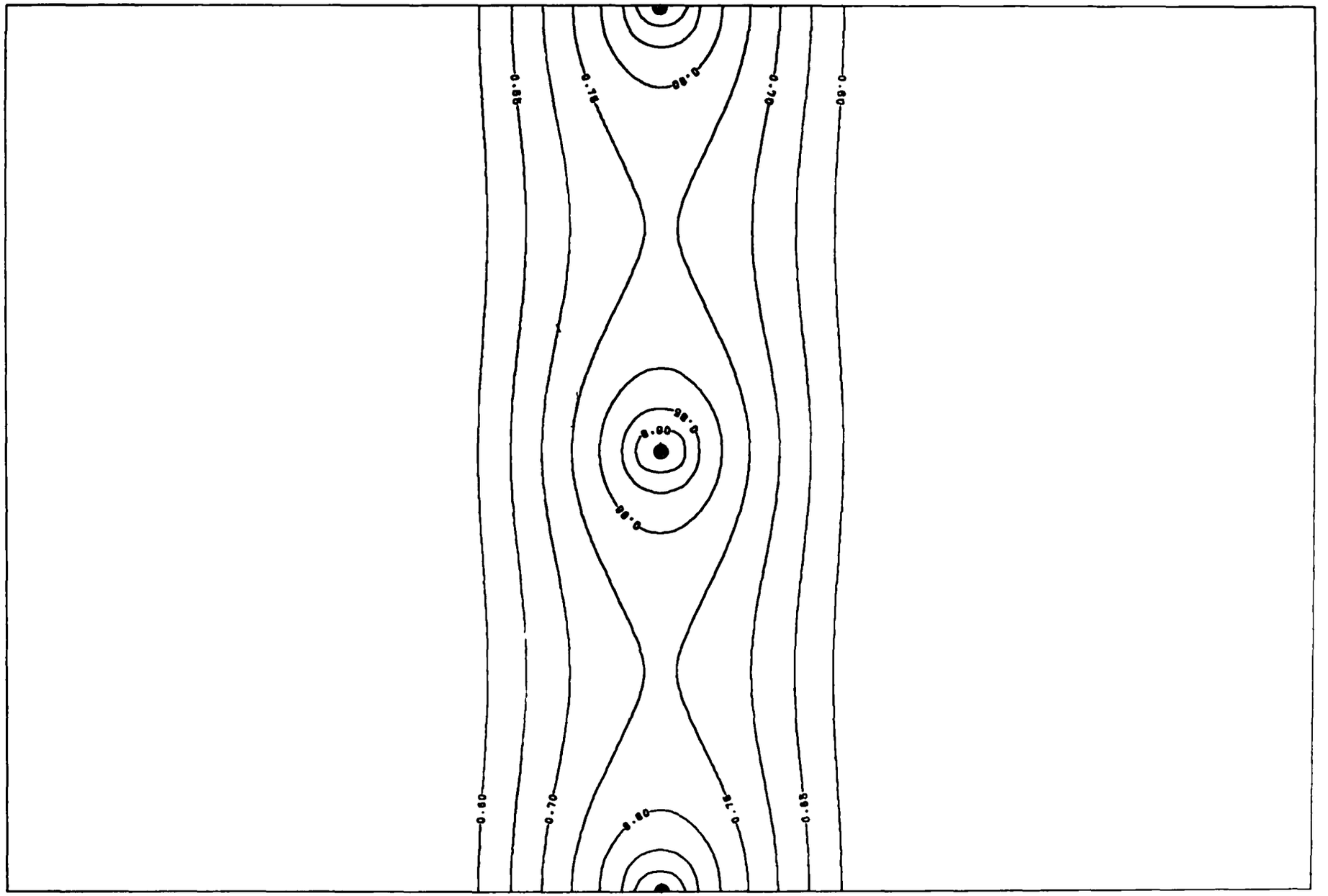

Figure 9. Case 3, electrode geometry, x-y equipotentials.

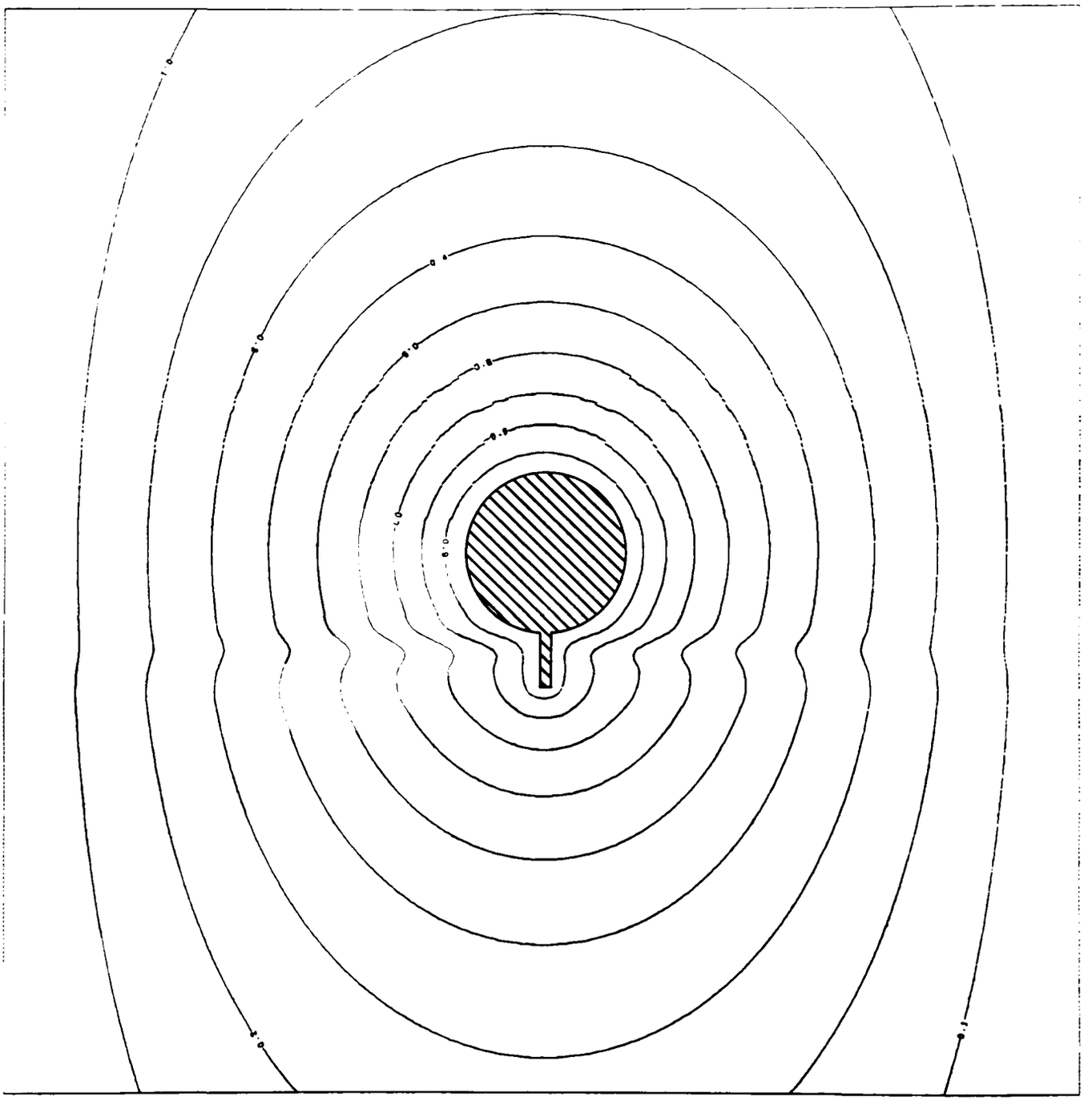

Figure 10. Case 3, electrode geometry, y-z equipotentials.

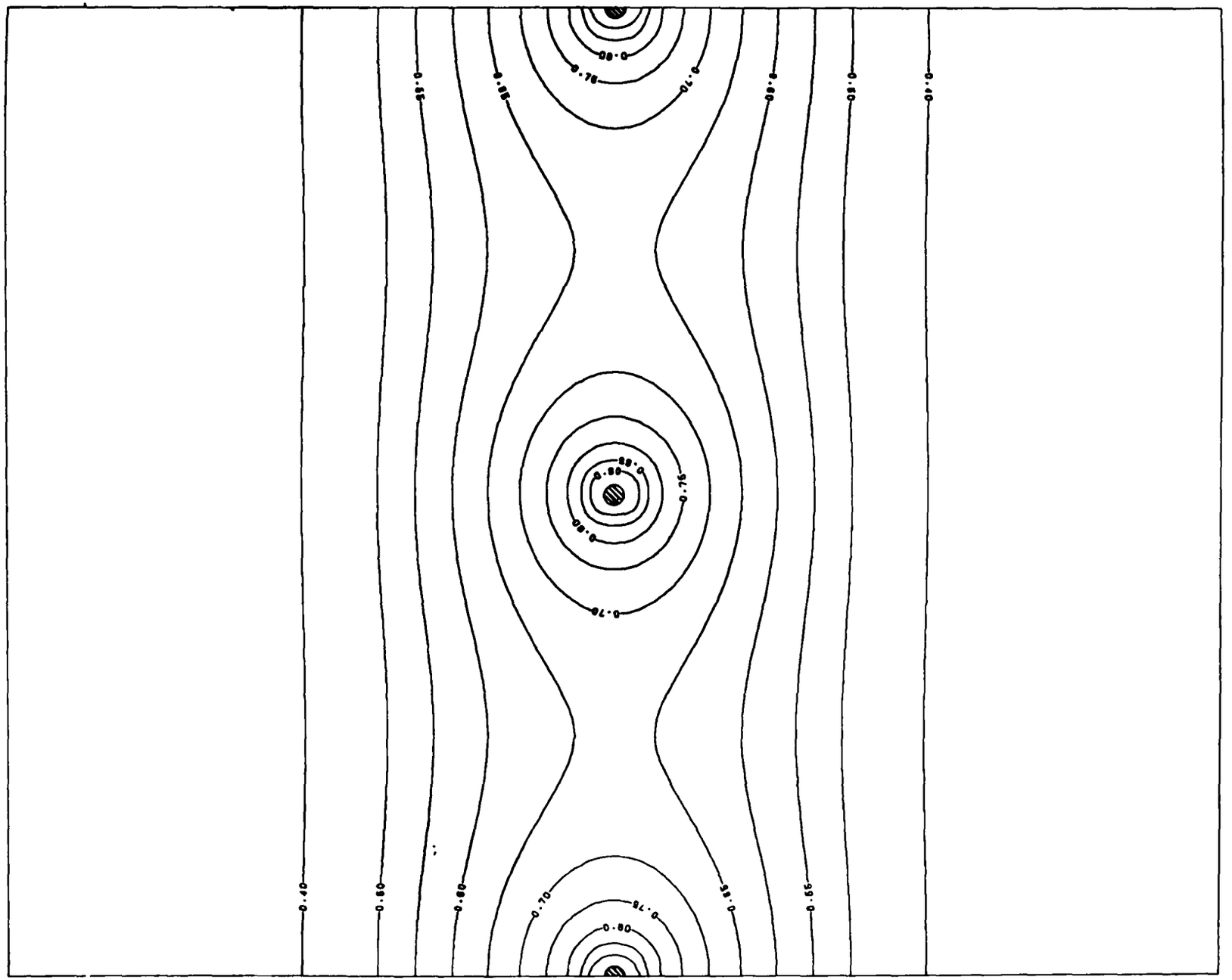

Figure 11. Case 4, electrode geometry, x-y equipotentials.

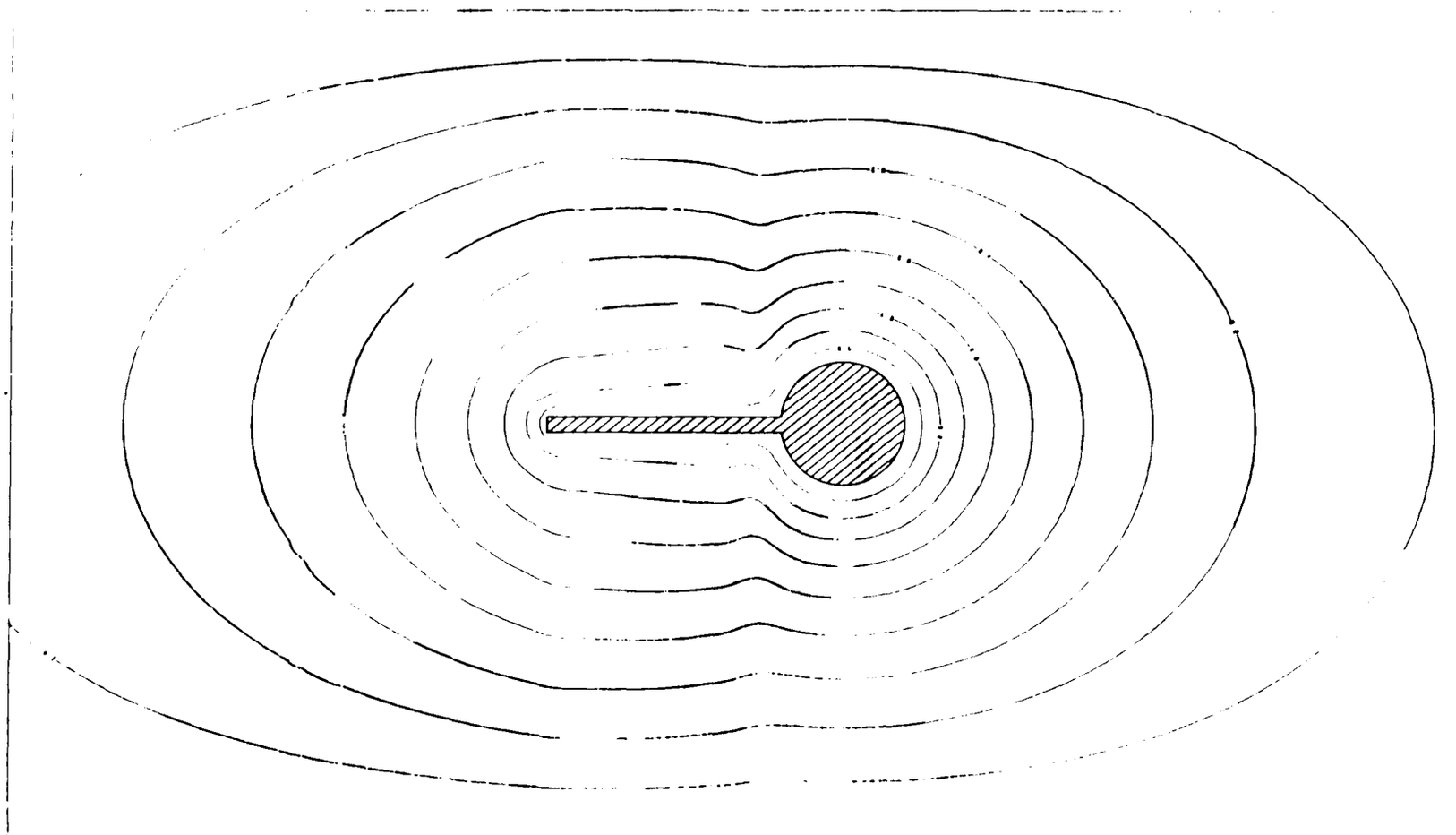

Figure 12. Case 4, electrode geometry, y-z equipotentials.

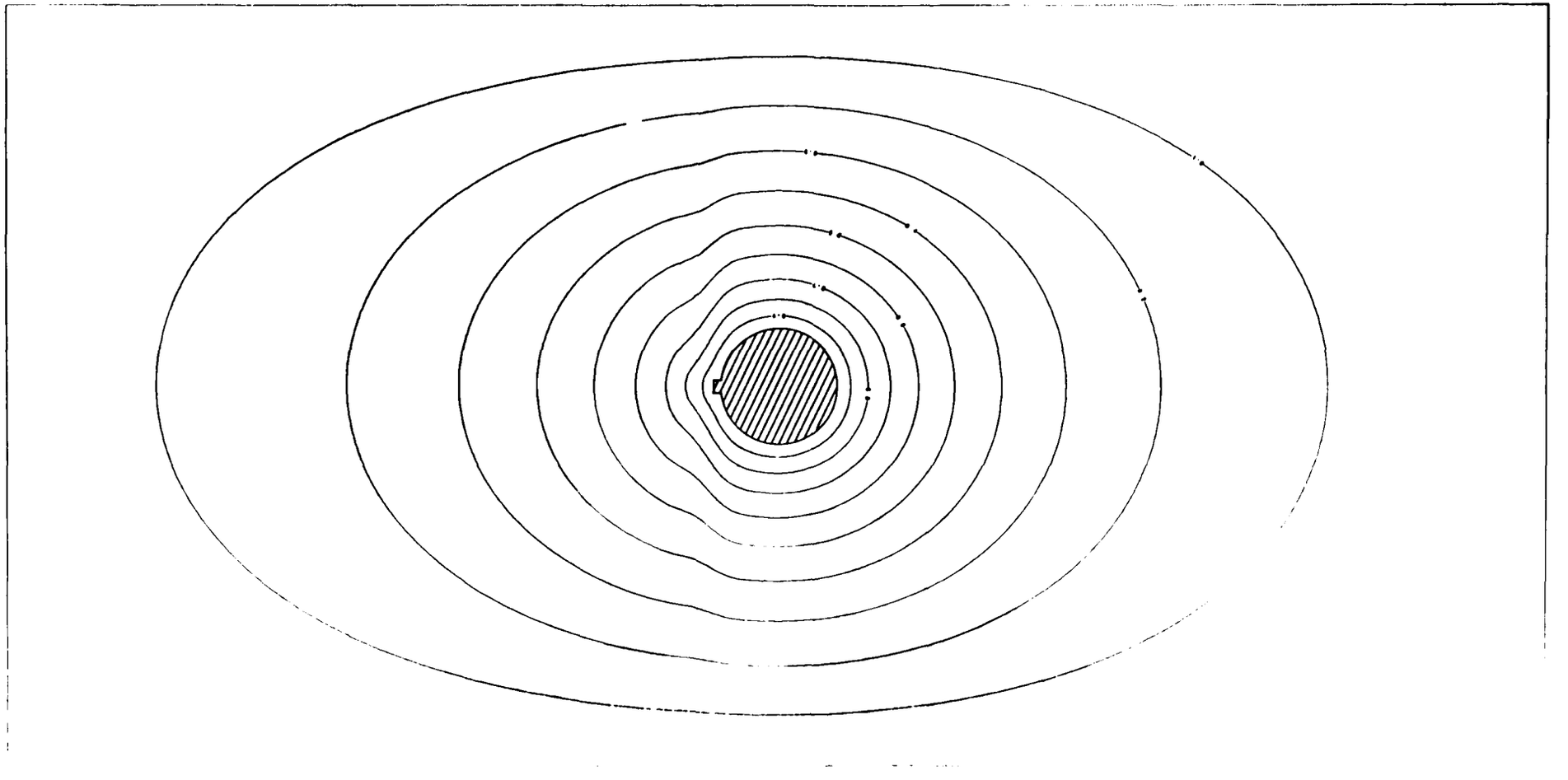

Figure 13. Case 5, electrode geometry, x-y equipotentials.

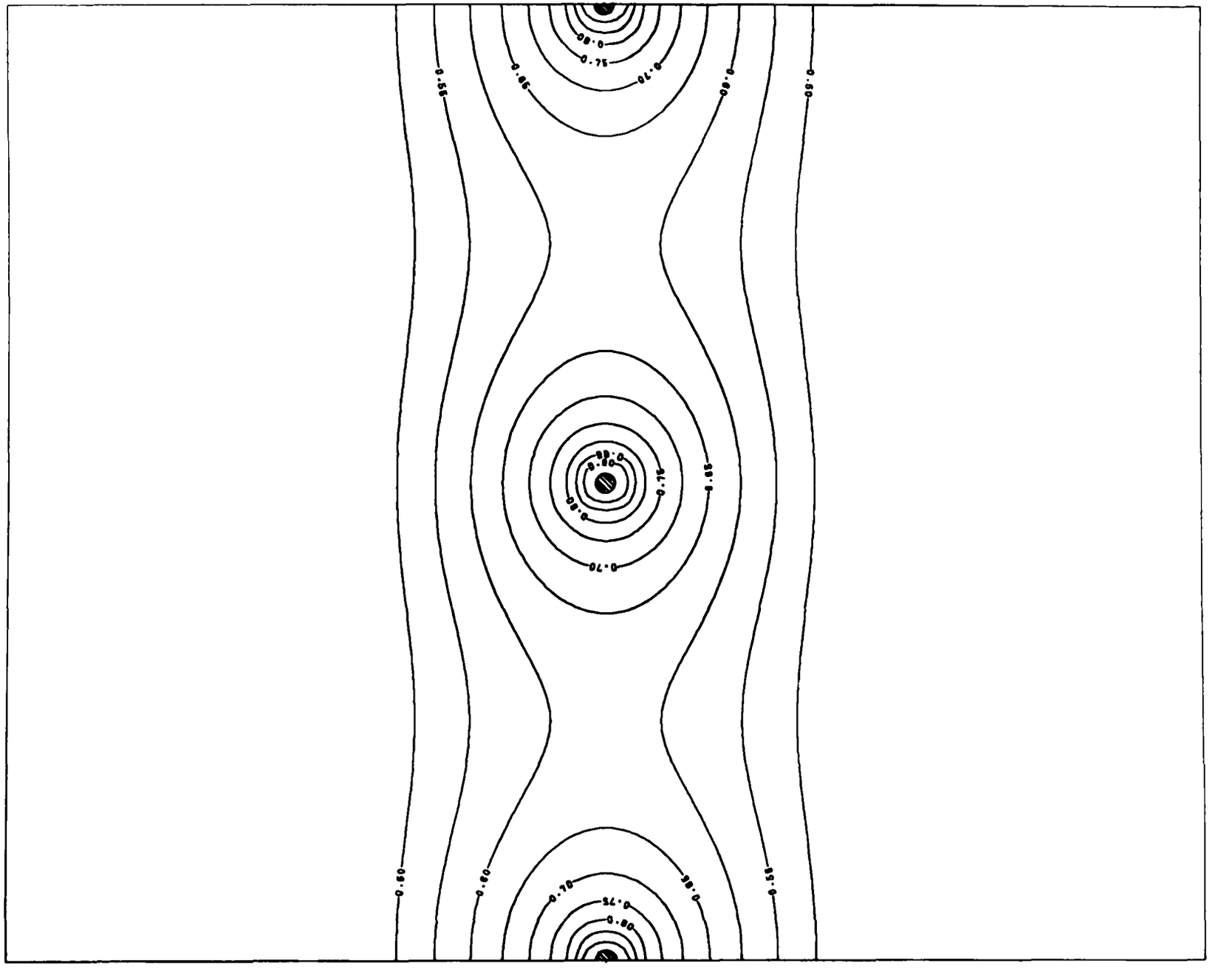

Figure 14. Case 6, electrode geometry, x-y equipotentials.

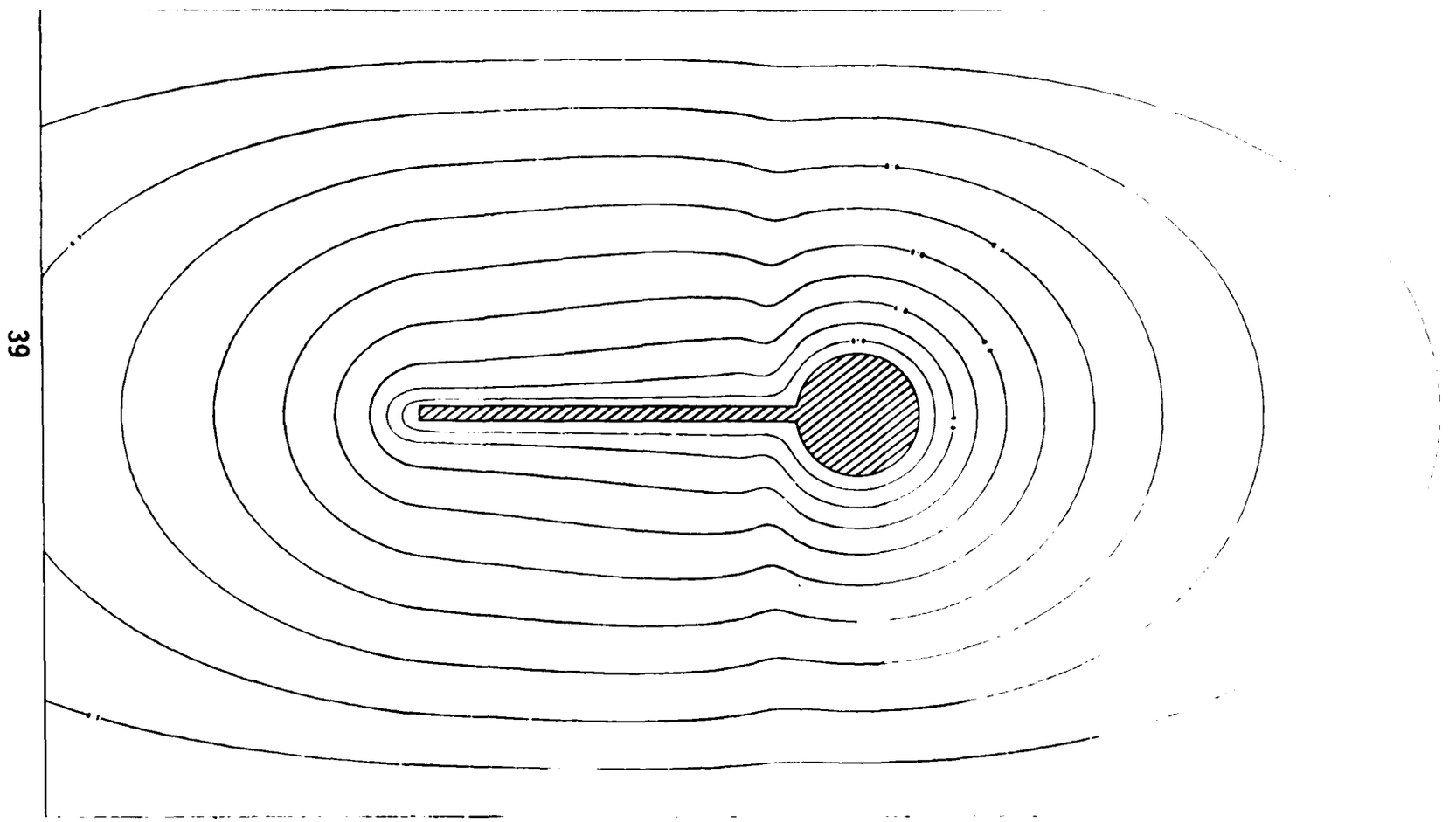

Figure 15. Case 6, electrode geometry, y-z equipotentials.

SECTION 5

HIGH VOLTAGE WATER SUPPLY ISOLATION

INTRODUCTION

The TRW Charged Droplet Scrubber (CDS) employs the principles of electrostatics to generate water droplets having an extremely high electrical charge. This is achieved by conducting the water through and ejecting it from high voltage electrodes. To accomplish this on a continuous basis, it is necessary to supply water from a source at ground potential to the electrodes at high potential without excessive power losses.

The existing design provides the necessary isolation utilizing the resistance of the supply water flowing through non-conducting plastic pipe. Although simple, the system level of isolation changes as the water conductivity varies. Since it is unlikely that a constant water conductivity can be maintained without excessive costs, an alternate water supply technique is needed. To this end, a design improvement task was initiated to develop a water supply system that is independent of water electrical property variations.

CONCLUSIONS AND RECOMMENDATIONS

The air gap isolation system design is capable of providing high voltage isolation for the Charged Droplet Scrubber where the supply water has an electrical conductivity of up to 60,000 micromho and where the potential difference across the water spray gap is as high as 50 KV.

The solid state resistor bank design will provide the necessary electrode state isolation and current limiting functions to meet the operational requirements of the Charged Droplet Scrubber.

DESCRIPTION OF EXISTING SYSTEM

Presently the isolation system consists of the electrical resistance provided by a long column of supply water contained in a plastic pipe. Normally, more than one electrode stage is operated from a single water isolation column and single power supply system. When more than one CDS stage is operated from the same power supply, it is necessary to connect each stage electrically to the power supply through a resistance. This resistance serves as a current limitor for the power supply in the event of an arc on the stage and also gives partial electrical isolation between the stages so that an arc on one stage does not significantly effect the voltage to the other stages connected to the common supply. These stage isolation resistors are also water columns of the supply water.

Using a water column of the supply water for the stage isolation and current limiting resistor has the advantage of being self cooled, but it also has the disadvantage of requiring a fairly constant water conductivity. If the water conductivity varies over any significant range, the power dissipated or lost in the current limiting resistors can be quite high if it decreases, or the stage isolation and current limiting functions can be degraded, if it increases. A schematic of a typical water column high voltage isolation system with four stages operating from a single power supply is shown in Figure 16.

APPROACH

The approach taken to achieve isolation, was a design where water could be transferred from a supply at ground potential to a reservoir at high voltage in the form of discrete droplets separated by air gaps. The air surrounding the droplets act as a current impeding dielectric. Spray nozzles generate the liquid droplets and are then collected in an electrically insulated container and fed to the stage header water distribution system by gravity through a conducting pipe. The water could be supplied from the container to the electrodes with metering pumps; however, level detectors, solenoid valves, pumps, motor and other associated controls would further complicate the system. Figure 17 presents a diagram of the Air Gap Isolation System Design.

Current limiting and stage isolating resistors are still required in the high voltage circuit. When the water column resistors were used, the flowing water provided the necessary cooling. Resistors having a fixed value however would now be necessary for current limiting and stage isolation in the spray nozzle system. As a result a cooling system to dump the heat dissipated by the resistor is now also necessary. The design of the isolation resistor bank is presented in Figure 18.

RESULTS AND DISCUSSIONS

The high voltage isolation assembly and the stage isolation/current limiting assembly would be designed to accommodate a single stage of an existing Charged Droplet Scrubber unit having forty seven electrodes per stage. This would require water to be supplied at the rate of approximately 49.2 ℓ/min (13 gpm) and have a stage isolation resistance of approximately 100 K ohms.

Since the approach with respect to the high voltage/water supply isolation is new technology, subscale testing would be performed prior to proceeding to the full-scale design. The technology utilized for the stage electrical isolation and current limiting system, however, is well established. Therefore, the subscale test phase for this assembly was not deemed necessary.

Water Isolation Tank Assembly

Two different type nozzles for supplying water to the CDS through a high voltage gradient were tested. One was a shower head nozzle composed of individual spray tubes in place of orifices. The other was a swirl nozzle type in which a tangential component is imparted to the water prior to expulsion. Figures 19 through 22 presents the two nozzle configurations. The two nozzles

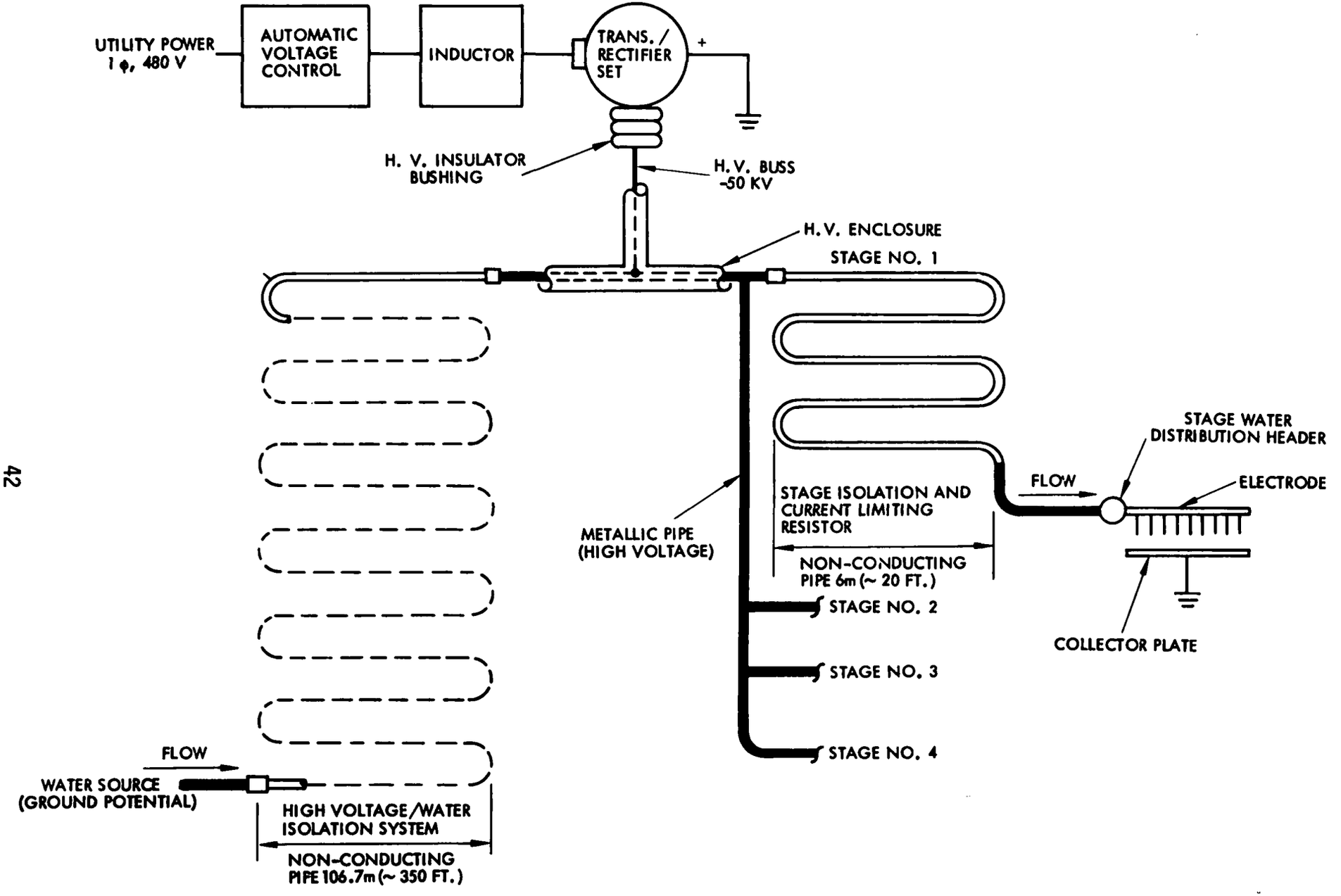

Figure 16. Water column high voltage isolation system.

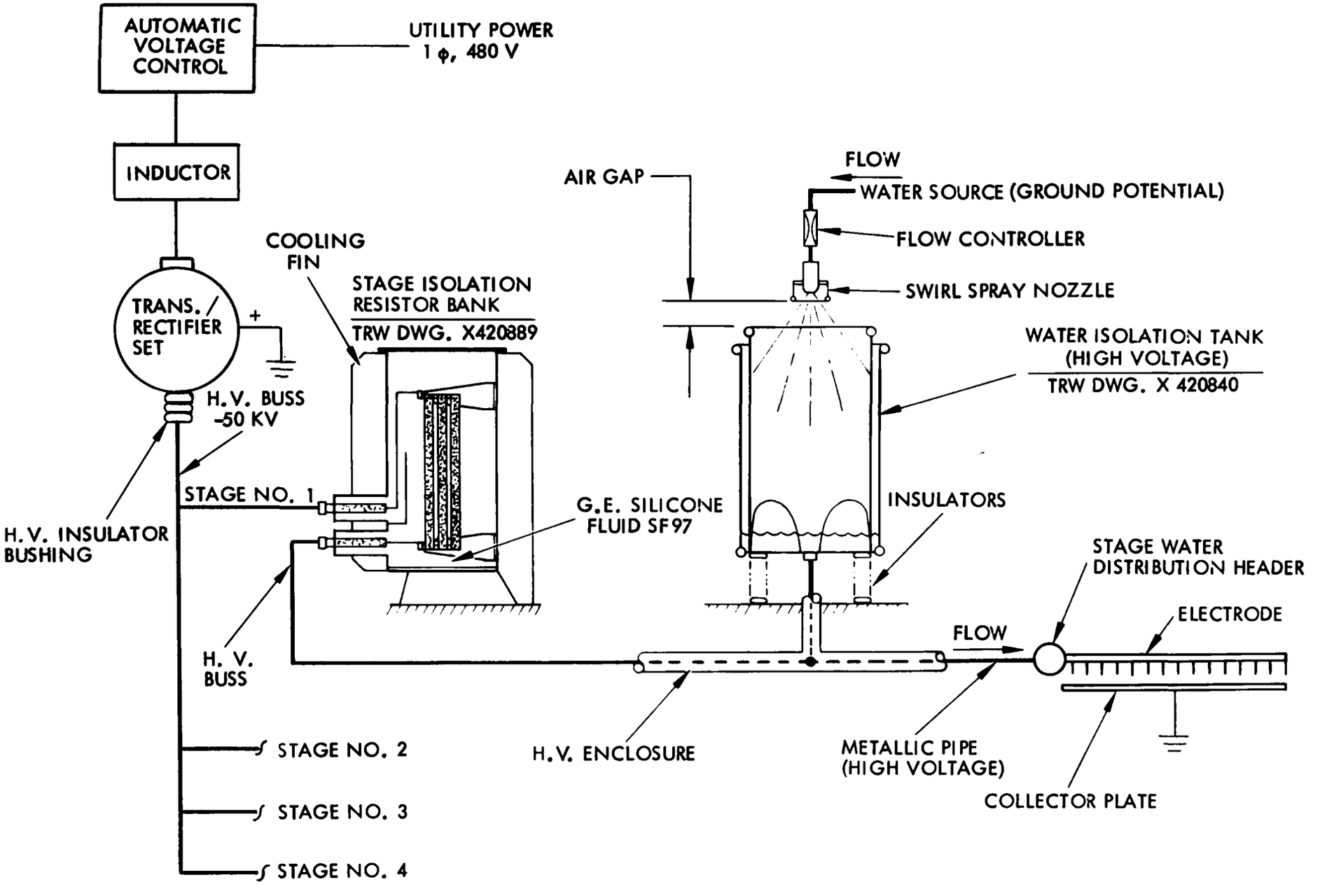

Figure 17. Air gap isolation system.

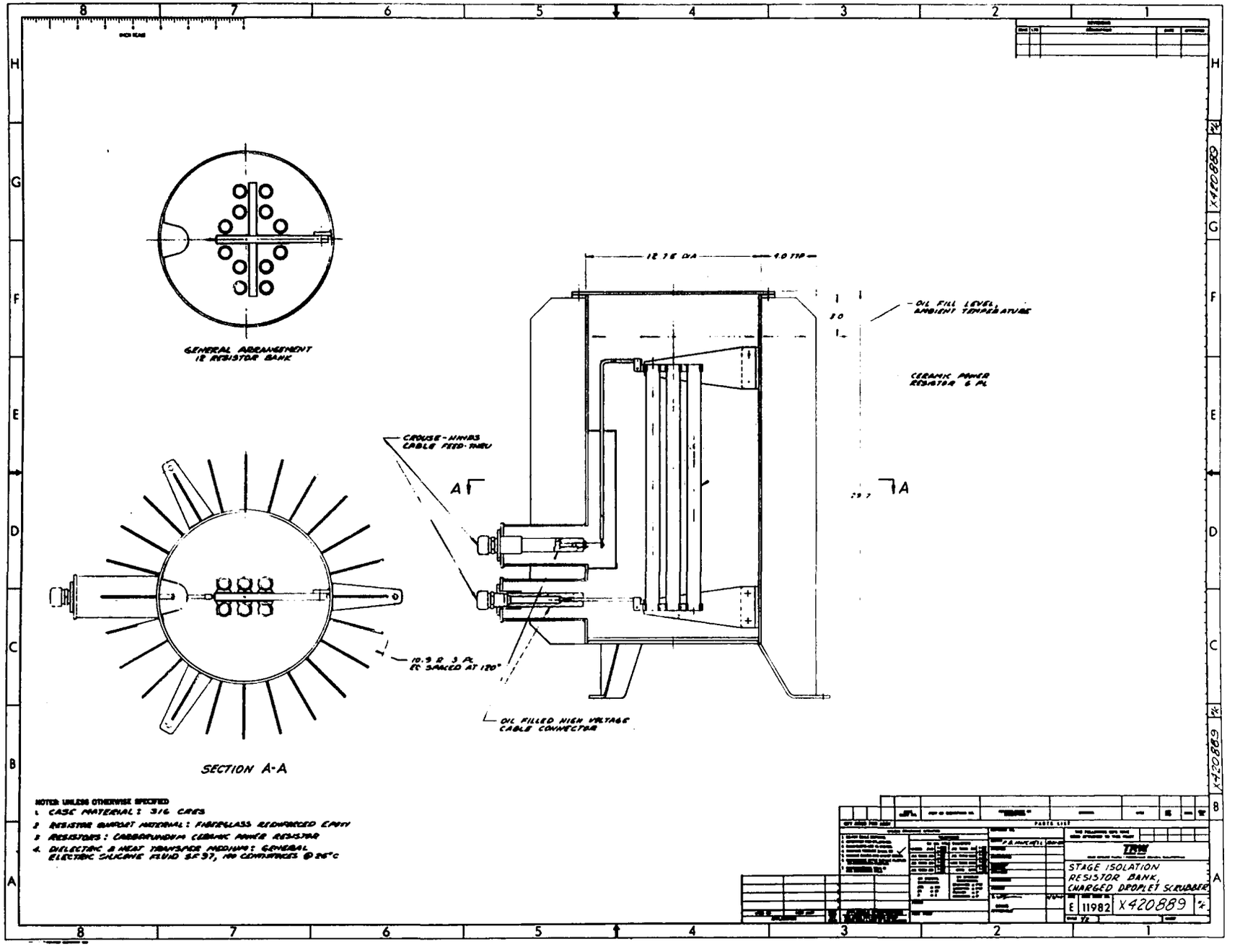

Figure 18. Isolation resistor bank.

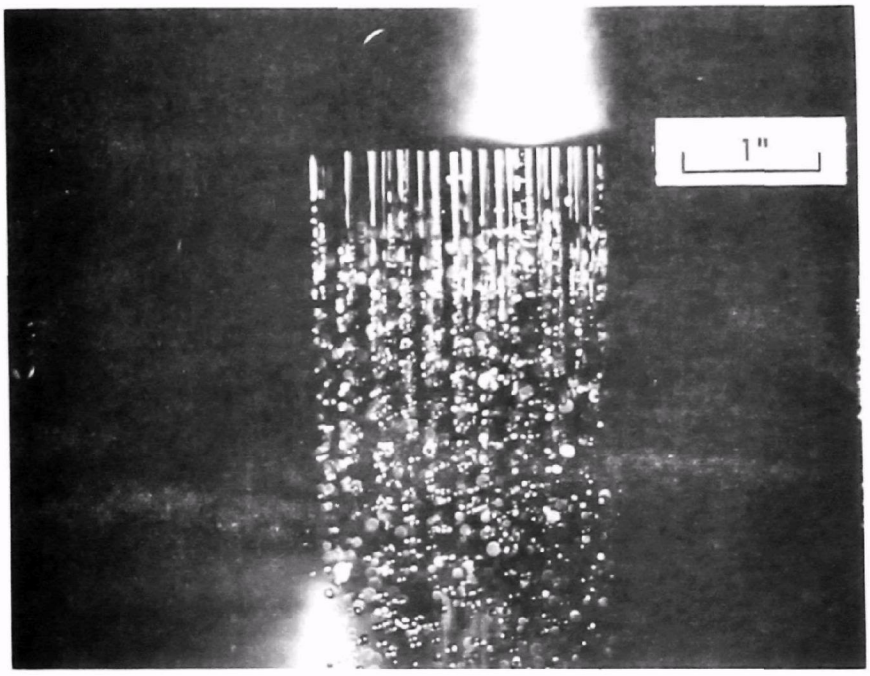

Figure 19. Shower head nozzle at zero potential.

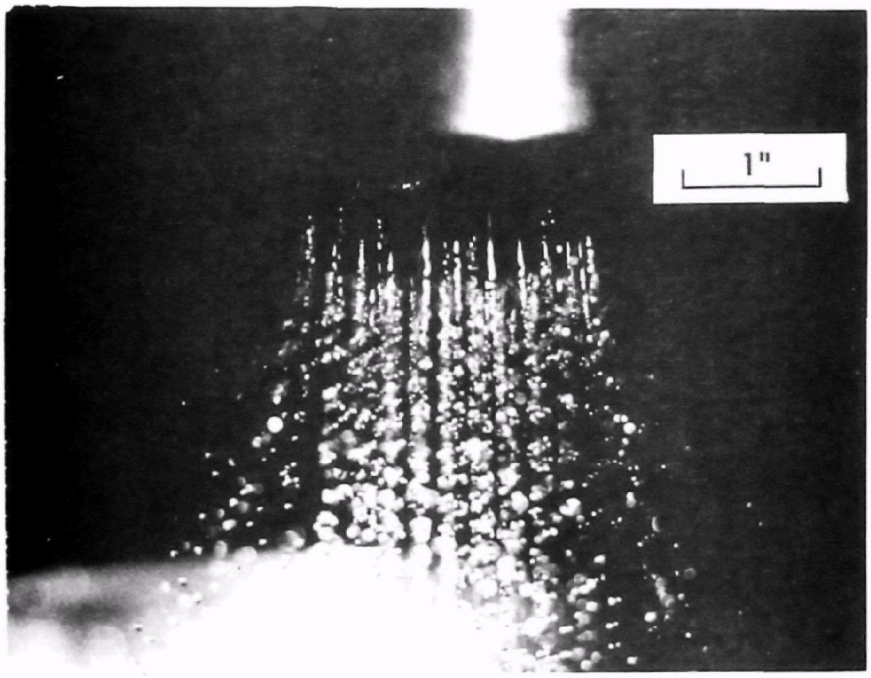

Figure 20. Shower head nozzle at -40 KV.

Figure 21. Swirl nozzle at zero potential.

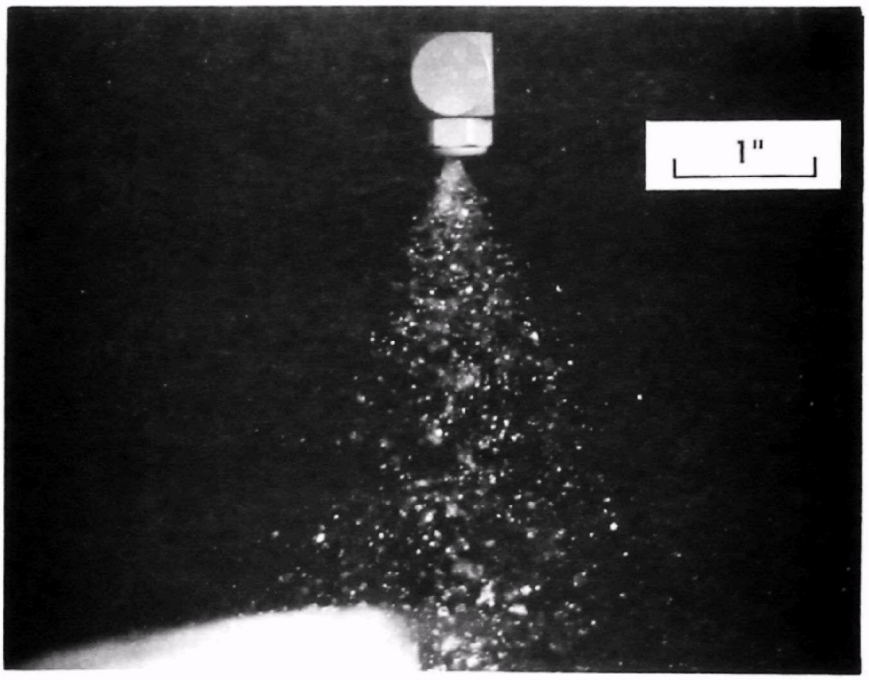

Figure 22. Swirl nozzle at -40 KV.

were operated at 2.1 ℓ/min (0.55 gpm) and were located 102 mm (4 in.) above the water collecting container. A voltage differential of up to 40 KV was maintained between the nozzle and collector. No leakage current was observed with a meter having a 100 μA sensitivity. The water used was doped with sodium chloride and had a conductivity of 60,000 μmho/cm. Other nozzle tests were conducted with tap water having a conductivity of 500 μmho/cm and with water doped with a surfactant having a surface tension of 4.0×10^{-2} N/m. No leakage current on breakdown was noted in any of the tests with -40 KV applied to the water collector.

The flow velocity of the water leaving the tubes of the shower head nozzle is less than the streaming velocity. The streaming velocity is defined as that velocity corresponding to a stream kinetic energy equal to the energy required to generate the new surface in the flowing stream. The minimum streaming velocity, v_m, can be expressed as:

$$v_m = \frac{8\sigma}{d\rho}^{1/2}$$

Where

σ surface tension of the liquid

ρ liquid density

d = flow tube outer or inner diameter, depending on the material wettability

The flow tubes used in the test were wetting and had a 1.59 mm (0.0625 in) O.D. The corresponding maximum velocity before streaming is 0.6 m/s (∿2 ft/sec). Since the stream velocity is low, the momentum is low and as can be seen by comparing the difference in droplet trajectories in Figures 19 and 20 the electrostatic forces alter the droplet flow path. The flow tubes are used in this type of nozzle rather than holes to insure that the water streams cannot agglomerate and form a continuous streamer. Also, the flow tubes have a finite length so that some back pressure is developed for flow control. The shower head nozzle has demonstrated the capability of supplying water across a large potential difference without breakdown; however, the nozzles become large for full-scale CDS units.

The swirl nozzle was tested for isolation because they would be easy to scale to full size systems. The nozzle shown in Figures 21 and 22 has a nominal 1.98 mm (0.078 in.) diameter orifice. The water flow velocity is approximately 11 m/s (∿ 37 ft/sec). The flow velocity is about 20 times that of the shower head nozzle; therefore, the water is leaving with more momentum. As can be seen by comparing Figures 21 and 22 the electrostatic forces with applied voltage has negligible affect on flow pattern.

A full-scale swirl type nozzle was also tested. It had an included spray angle of 60^{o} and a flow rate of 45.4 ℓ/min (12 gpm) at 703 g/cm^2 (10 psi) inlet pressure. The test was conducted under the same conditions as

the subscale units with similar results. There was no measurable current drain at maximum water flow and with a voltage differential of 50 KV.

A considerable quantity of air is entrained in the high velocity water jet. This entrained air causes fogging when the water droplets impinge in the collecting container. The fog is eliminated by using a funnel shaped water interceptor within the collector. With this configuration the entrained air moving ahead of the droplet shower exits the collector container on the outside of the water interceptor. The sprayed water has had a chance to agglomerate on the funnel surface while still allowing forward flow of the entrained air. The air then makes a 180° turn prior to exiting which prevents re-entrainment of water. Figure 23 presents the isolation tank design.

Stage Isolation Resistors

Two types of fixed resistors were evaluated for the application. One was a wire wound configuration, the other an extruded ceramic power resistor. After evaluation of the individual specifications, the ceramic configuration was selected because of the higher operating temperature capability and the fact that it is essentially non-inductive. Figure 24 presents a photo of the ceramic resistor chosen for the design. Typically, the maximum operating range is 20 to 350°C.

To minimize the resistor bank housing volume requirements and to minimize the temperature rise during state operating condition, the resistor would be immersed in a silicone fluid to improve the heat dissipation rate. The liquid chosen for this purpose is General Electric SF-96 silicone fluid which has a temperature operating limit of 260°C and a dielectric constant of 2.75.

The resistor bank is designed to operate at an ambient temperature of up to 38°C and accommodate a temperature rise within the bank of approximately 93°C.

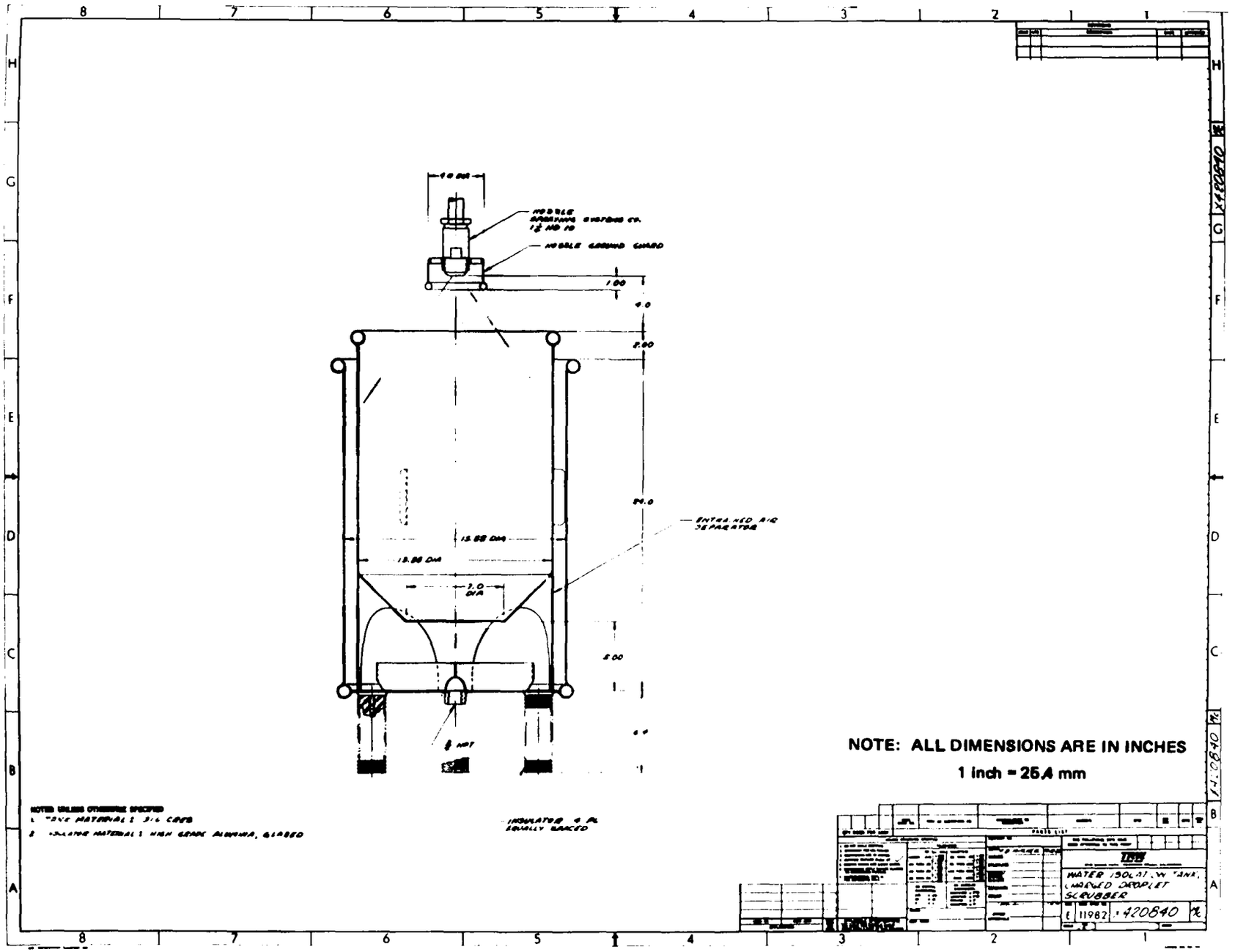

Figure 23. Water isolation tank.

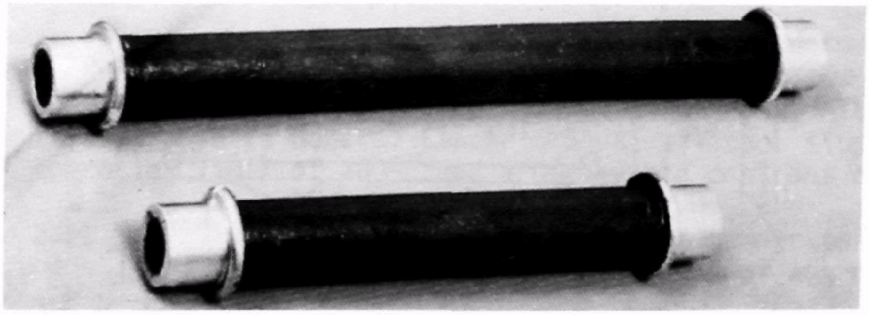

Figure 24. Ceramic resistor.

SECTION 6

EQUIPMENT CORROSION

INTRODUCTION

A flue gas corrosion study was performed as part of the Charged Droplet Scrubber program funded jointly by the EPA and TRW. The objectives of the study were to:

- Obtain quantitative data on the performance of 316 CRES (austenitic stainless steel) of which the main structure and components are constructed.
- Investigate the feasibility of coatings as a means of improving the performance of materials exposed to coke oven flue gas environments.
- Investigate the feasibility of metallic and non-metallic liners for scrubber construction.
- Investigate alternate materials, both metals and non-metals, for CDS component and structure applications.

The approach is to use a combination of materials test coupons, coated portions of the CDS structure and components and electronic corrosion probes to assess the performance of the test materials under actual scrubber operating conditions. At approximately the midpoint in the run, the specimens were removed, inspected and analyzed. A rough screening was performed and the remaining candidate material specimens replaced for continued testing. At the end of the test operation, the remaining specimens were removed and analyzed.

The type of test materials, coatings and probes and their locations are described in Appendix B. Also shown in the appendix is a diagram of the CDS unit.

Coupon test samples (metal and non-metal) were installed in the upper casing (hood) and in the lower casing under the baffles. The lower casing location produced the most severe service since the temperatures of the samples can reach that of the incoming gas stream and the wash water is only partially effective due to the screening caused by the baffles. Some of the samples were coated or lined with organic materials.

Coatings were applied to the electrode access doors, electrodes, wash couplings, upper casing (hood) surfaces, and lower casing surfaces as well as test coupons.

The electronic corrosion meter (Corrosometer, Magna Corp.) probes were used to serve as an in-process indicator/monitor for corrosion behavior. In addition, the Corrosometer data was compared to corrosion data from test coupons.

Analysis techniques employed included visual inspection, weight change determinations, metallographic examination, and hardness measurements.

CONCLUSIONS

Of the metallic coupons tested, the commercially pure titanium, Ti-0.2 Pd and Incology 825 alloys performed best. Hastelloy C-4, TI - Code 12, and Inconel 617 had very good corrosion resistance when exposed to the lower casing gas stream but were attacked in the upper casing gas stream. The chemical lead samples performed satisfactory in the lower casing and lead lining of the casing appears to be a strong candidate for a long life design. The 316 CRES samples showed fair corrosion resistance in both the upper and lower casing gas streams.

The pitting/crevice behavior of the stainless steels and nickel alloys roughly follows the molybdenum content. Thus, the relative performance in order of increasing corrosion resistance would be predicted to be:

> Ni (0 percent Mo), 304 CRES (0 percent Mo), Inconel 601 (0 percent Mo), 316 CRES (3 percent Mo), Incoloy 825 (3 percent Mo), Inconel 617 (9 percent Mo) and Hastelloy C (16 percent Mo).

This sequence held quite well for the samples tested in the lower casing gas stream except that Incoloy 825 performed better than Inconel 617. However, in the upper casing gas stream, the Hastelloy-C coupon was severely attached with its relative performance falling between that of pure nickel and Inconel 601. No explanation for this behavior has been identified at this time.

In general, the corrosive attack was more severe for metallic coupons exposed to the upper casing gas stream than those in the lower casing. The upper casing coupons were not exposed to the amount of water as were coupons in the lower casing since they were above the electrode headers. Therefore, the coupons were in a moist atmosphere with temperatures in the 18.2°C to 33.8°C range, but did not get the cleaning/diluting effect which the lower casing samples experienced.

Therefore, the chloride concentration would be expected to be higher on the upper coupons which would tend to promote pitting and crevice corrosion in the stainless steels and nickel alloys. In addition, the moisture clinging to the coupons would tend to collect and concentrate sulfuric acid. That is, as water evaporated the higher boiling point of the sulfuric acid causes the concentration to increase. Figure 65 shows the boiling point curve for

sulfuric acid. It is not clear which factors caused the pitting attack of the Ti-Code-12 coupon in the upper casing. This alloy is specifically formulated to retard pitting and crevice attack.

The sulfuric acid concentration on coupons in the lower casing would be expected to be high. However, some on wetting/washing of the samples would occur even though the baffles partially screened the coupons from the water flow, so that some dilution would occur. In cases, where dilution did not occur, sulfuric acid concentration of the order of 70 percent is possible .

The wall temperatures run cooler than the gas temperatures and, all other other parameters being equal, the corrosion rates would be expected to be lower than for the coupons. This was borne out by the corrosion meter measurements in the upper casing and in the lower casing below the baffles for the 316 CRES. The probe located in the lower casing above the baffle showed a higher rate, Table 17, but no coupons were mounted in this region so that a direct comparison can not be made.

None of the coating systems tested were able to survive the CDS environment. The combination of temperature, gas velocity, and chemical environment caused blistering, debonding or cracking. The epoxy EA 919 coating gave some degree of protection to the electrode headers (which run cool due to the internal water flow) and the upper casing doors. However, long term survival is unlikely.

The elastrometric liner materials subjected to the gas stream checked or cracked. However, some of the elastrometric materials performed well as gaskets, seals and baffle shims. Viton rubber showed excellent resistance in these configurations and neoprene elastromer performed well as a seal in the upper casing. A Teflon/glass fabric (Armalon) liner was applied to an upper casing door and showed no signs of degradation. Vinyl shrink tubing performed well over electrode header connectors since the temperature in these regions was quite low due to water flow inside the electrodes.

Of the fiberglass reinforced plastic panels, only the polybutadiene showed acceptable resistance. Again the combination of temperature (up to 177°C) and concentrated sulfuric acid was too aggressive an environment. It is possible that some of these materials, specifically Ashland 197/3 and Ashland 800, would perform satisfactorily on the walls where the temperatures are lower and the washing action of the water would prevent high concentrations of sulfuric acid to form.

The overall performances of the various materials are shown in Table 19.

RECOMMENDATIONS

Based upon the inspection and analysis, preliminary recommendations have been made for materials and design changes and maintenance procedures for coke oven application units. The recommendations are divided into short term (up to two years), intermediate term (two- to ten years), and long term, (greater than ten years) life requirements.

Two Year Service

- 316 CRES upper and lower casings, doors and hood. Inspect periodically. Local repairs as necessary (weld-on doublers).
- 316 CRES electrodes. If perforation occurs, replace with titanium electrodes as they fail.
- Viton door seals.
- Viton baffle shims.
- 316 CRES wash system.
- 316 CRES baffles. Replace as required.

Two-To-Ten Year Service

- pH control and inhibitors.

Long-Term Service

- Lower casing lined with lead.
- Lead lined baffles.
- Upper casing and doors lined with lead, Hypalon elastomer sheet, or neoprene elastomer sheet.
- Titanium electrodes, headers, couplings, wash system, collector plates.
- Viton door seals and baffle shims.

INSPECTION AND ANALYSIS

The test coupons from the upper and lower casing were removed at midpoint and analyzed. A summary of the observations is given in Tables 14 and 15. The coupons which exhibited severe degradation were screened from the program and testing of these materials was discontinued.

Stainless Steel

The corrosion resistant stainless steels (CRES) subjected to the lower casing environment exhibited pitting and crevice corrosion attack. 304 CRES was more severely attacked than 316 CRES, see Figures 25 and 26. The 304 CRES specimens showed attack ranging from small multiple pits to cracking of the specimen in the most heavily pitted regions, Figure 25. Some 316 CRES specimens were only lightly attacked, or not attacked at all, while others showed extensive pitting over the entire coupon surface, Figure 26. Crevice attack was normally present around the attachment bolt holes.

TABLE 14. CONDITION OF MATERIAL TEST COUPONS - LOWER CASING

ROW-LOCATION	SAMPLE NO.	REMARKS
1-1	S-( )C	Surface attack
1-2	S-23K	Coating peeled
2-1	304-18	Slight surface attack
2-2	S-14W	Coating failed
2-3	304-7PS	Coating peeled
2-4	Ti-12-1	Missing
2-5	Ti-PD-1	No attack
2-6	Ti-1	Slight surface etch
2-7	304-17	Surface attack-cracks or pits
2-8	Ni-5	Pitted
2-9	304-10RO	Coating failed
2-10	S-1T	Coating blistered
2-11	304-16	Slight attack
3-1	316-18	No visual attack
3-2	S-13RO	Coating failed
3-3	304-3T	Coating peeled at edge, some blisters
3-4	I825-5	No attack
3-5	Ni-1	Badly pitted
3-6	316-17	No attack
3-7	1617-1	No attack
3-8	I607-2	Pitted
3-9	316-13W	Coating failed
3-10	S-8PS	Coating blistered
3-11	316-16	Pitted
4-1	316-4E	Coating failed
4-2	315-12RO	Coating failed
4-3	AT382/05	Surface etching, cracking & crazing
4-4	AT711-1	Surface etching, cracking & crazing
4-5	AT382-1	Surface etching, cracking & crazing
4-6	AT580-1	Surface etching, cracking & crazing
4-7	317-7PS	Coating blistered
4-8	316-AW	Coating failed
4-9	316-1T	Coating delaminated at edges
5-1	ASH 7241-29	Surface etched
5-2	ASH 72L-22	Missing
5-3	ASH 7240-39	Surfaced etched
5-4	ASH 197/3AT-5	Missing
5-5	ASH 800-25	Sample cracked & etched
5-6	ASH 197/3-5	Some edge attack
5-7	ASH 800FR-20	One face etched
6-1	ASH 800PR-21	Some surface etch
6-2	ASH 197/3-4	Some edge attack
6-3	ASH 800-24	Some surface etch
6-4	ASH 197/3AT-6	Some edge attack

(continued)

TABLE 14. (continued)

ROW-LOCATION	SAMPLE NO.	REMARKS
6-5	ASH 7240-40	Edges etched
6-6	ASH 72L-21	Surface and edge etch
6-7	ASH 7241-30	Edges etched
7-1	HY-180	Missing
7-2	HY-132	Slight discoloration
7-3	P33-1	Delaminated - failed
7-4	C31-1	Delaminated - failed
8-1	Pb-2	No attack
8-2	Pb-1	No attack
9-1	316-( )NB	Checking, rubber hardened
9-2	316-( )NB	Checking, rubber hardened
9-3	S-( ) NB	Checking, rubber hardened
9-4	S-( ) NB	Checking, rubber hardened
9-5	316-26N	Coating failed
9-6	316-25N	Coating failed
9-7	S-18N	Coating failed
9-8	S-17N	Coating failed
9-9	316-29H	Local failure - blisters
9-10	316-28H	Local failure - blisters
9-11	S-( )H	Coating failed
9-12	S-( )H	Coating failed
10-1	316-22	No attack
10-2	304-9PS	Some peeling at corners
10-3	Ti-2	No attack
10-4	TiPd-2	No attack
10-5	Ti-12-2	No attack
10-6	316-11RO	Coating failed
10-7	304-1T	Some peeling at edge
10-8	304-12	No attack
11-1	304-16RO	Missing
11-2	S-5E	Coating failed
11-3	I601-4	Pitted
11-4	I1617-3	No attack
11-5	316-23	No attack
11-6	304-21	Some pitting
11-7	316-8PS	Peeling at corners
11-8	I825-2	No attack
11-9	304-5E	Coating failed
11-10	S11RO	Coating failed
12-1	304-20	Slight attack
12-2	S-3T	Coating blistered

(continued)

TABLE 14. (concluded)

ROW-LOCATION	SAMPLE NO.	REMARKS
12-3	Ni-3	Pitted
12-4	304-14W	Coating failed
12-5	316-6E	Coating failed
12-6	316-3T	No attack
12-7	S-16W	Coating failed
12-8	304-15W	Coating failed
12-9	S-10PS	Blistered
12-10	316-20	Some attack
13-1	304-28K	Coating peeled
13-2	Hast B-1	No attack - some darkening
13-3	Hast C-1	No attack
13-4	S-( )C	Surface etched
14-1	S-24K	Coating peeled
14-2	304-29K	Coating peeled
15-1	4092-1	Surface etched
16-1	4030-1	Surface etched
17-1	4020-1	Surface etched and flaked off

The CRES sample in the upper casing showed similar behavior with the 304 CRES pitting over most of the exposed surface and the 316 CRES showing some pitting and crevice attack near the attachment holes. Figures 27 and 28 show the appearance of typical 304 CRES and 316 CRES coupons, respectively.

Nickel Alloys

Pure nickel samples were severely attacked by the CDS environment. Extremely heavy pitting and crevice corrosion was noted on all lower casing specimens, Figure 29. The Inconel 601 specimens also showed severe attack. Intergranular corrosion caused grains to spall off the surface which resulted in multiple pits, Figure 30. The bolt attachment areas were attacked by crevice corrosion. The nickel alloys containing high amounts of molybdenum, Inconel 617, Incoloy 825, Hastelloy C-4 and Hastelloy B, were not attacked, although some discolorization was noted on the Hastelloy B coupon, Figures 31 and 32.

The nickel and Inconel 601 specimens exposed to the upper casing environment were pitted over their surfaces as shown in Figures 33 and 34. In contrast to their performance in the lower casing, Incoloy 825 and Inconel 617 all showed evidence of pitting attack in the upper casing, see Figures 35 and 36. The Hastelloy C sample was badly pitted even though it showed excellent resistance to attack in the lower casing, see Figure 36.

TABLE 15. CONDITION OF MATERIAL TEST COUPONS - UPPER CASING (HOOD)

ROW-LOCATION	SAMPLE NO.	REMARKS
1-1	304-2T	Coating blistered, delamination
1-2	304-13W	Coating failed
1-3	304-8PS	Coating blistered, peeled
1-4	304-11RO	Coating failed
1-5	304-4E	Coating failed
1-6	Hastelloy C	Surfaced pitted
1-7	I825-1	Surfaced roughened
1-8	I601-3	Surfaced pitted
2-1	Ti PD-3	Discoloration
2-2	Ti-12-3	Some pitting
2-3	316-19	Edges pitted
2-4	304-24	Pitting, crevice attack
2-5	Ni-2	Pitting attack
2-6	I617-2	Pitting attack
2-7	Ti-12	Discoloration
2-8	316-2T	Coating blistered, delamination
2-9	316-15W	Coating failed
2-10	316-9PS	Coating blistered
2-11	316-10RO	Coating failed
3-1	316-21	Good
3-2	304-19	Pitting attack
3-3	S-4E	Coating failed
3-4	S-12RO	Coating failed
3-5	S-9PS	Missing
3-6	S-5W	Coating failed
3-7	S-2T	Coating peeled
3-8	316-5E	Coating failed

Titanium Alloys

The commercially pure titanium coupons and the Ti-0.2 Pd and Ti-Code 12 coupons all showed good resistance to attack in the lower casing. Some slight surface etching was noted, Figure 37. Otherwise, the surfaces appeared normal except for some staining which was removable with a non-metallic brush and detergent. The Ti and Ti-0.2 Pd coupons in the upper casing also exhibited excellent resistance to attack, Figure 38. However, the Ti-Code 12 coupon was pitted after exposure to the upper casing environment.

Lead

The chemical lead specimens were discolored due to the formation of a surface film but had not sustained pitting or crevice attack. The film was adherent and very difficult to remove by brushing and washing, Figure 39. All specimens were mounted in the lower casing.

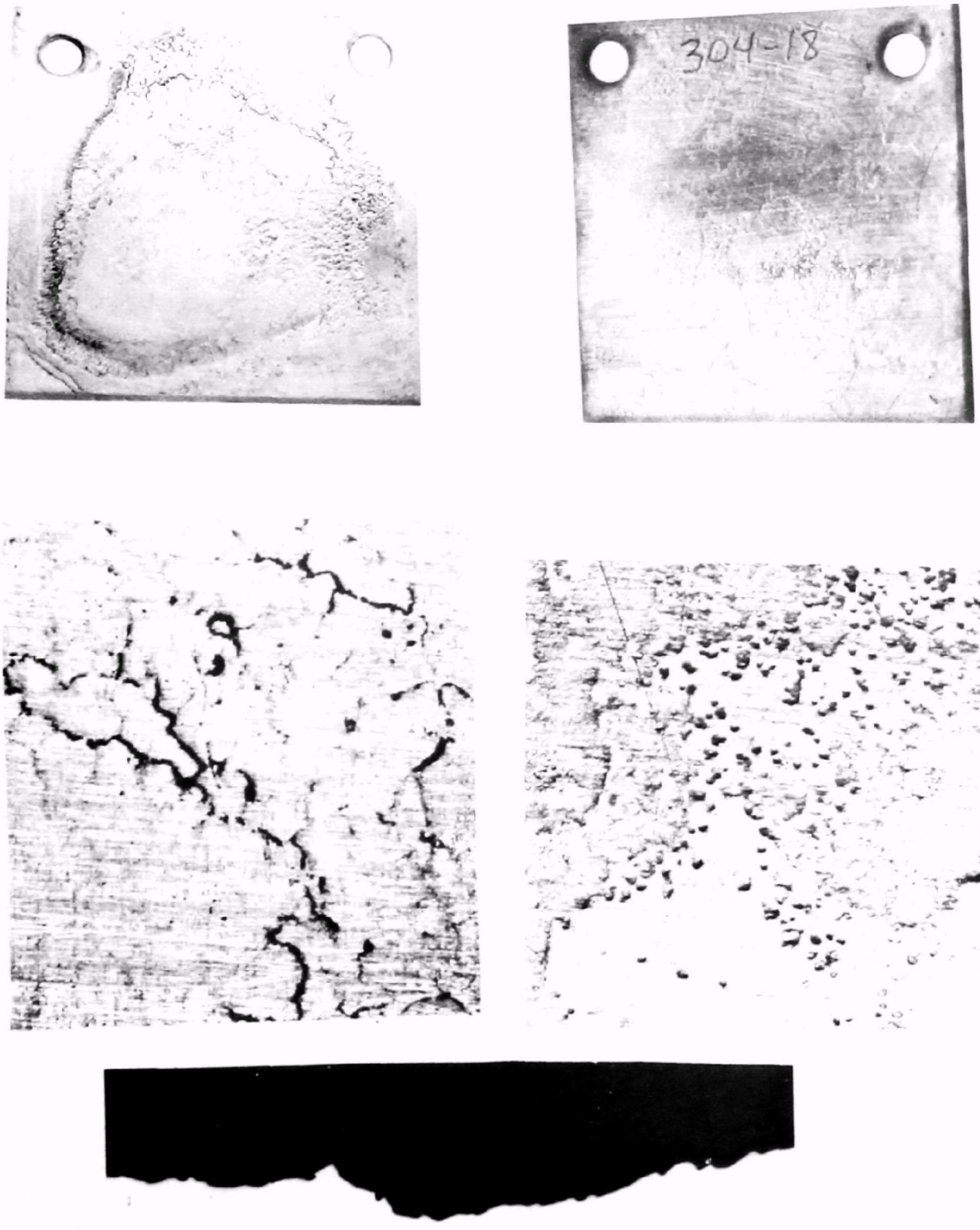

Figure 25. Coupon 304-17 (left) and 304-18 (right). Severe pitting attack with 304-17 showing cracks in heavily pitted regions. Micrograph showing section through pitted area. Lower casing.

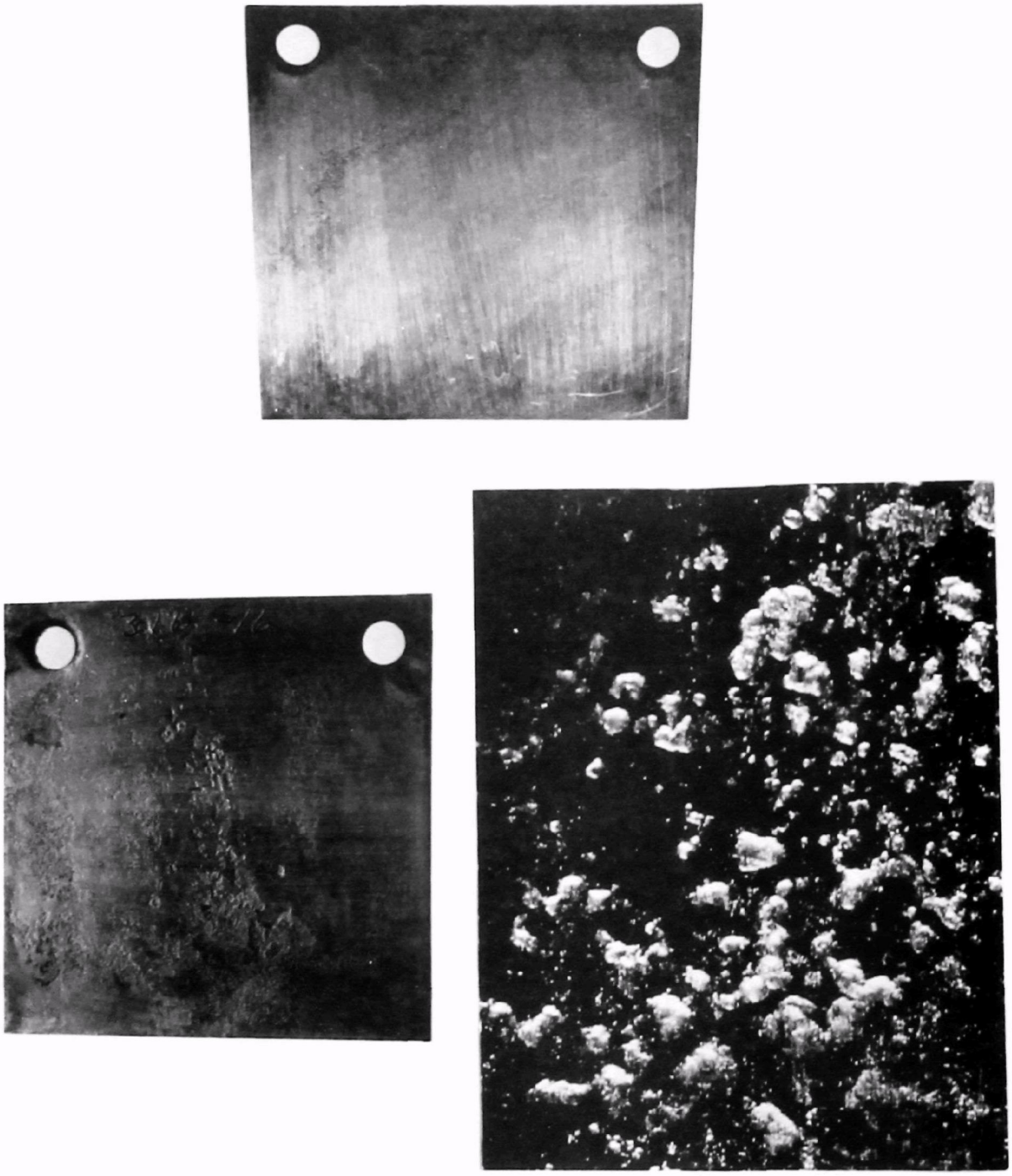

Figure 26. Coupons 316-23 (top) showing mild attack and 316-16 (bottom) which has extensive pitting attack. Lower casing.

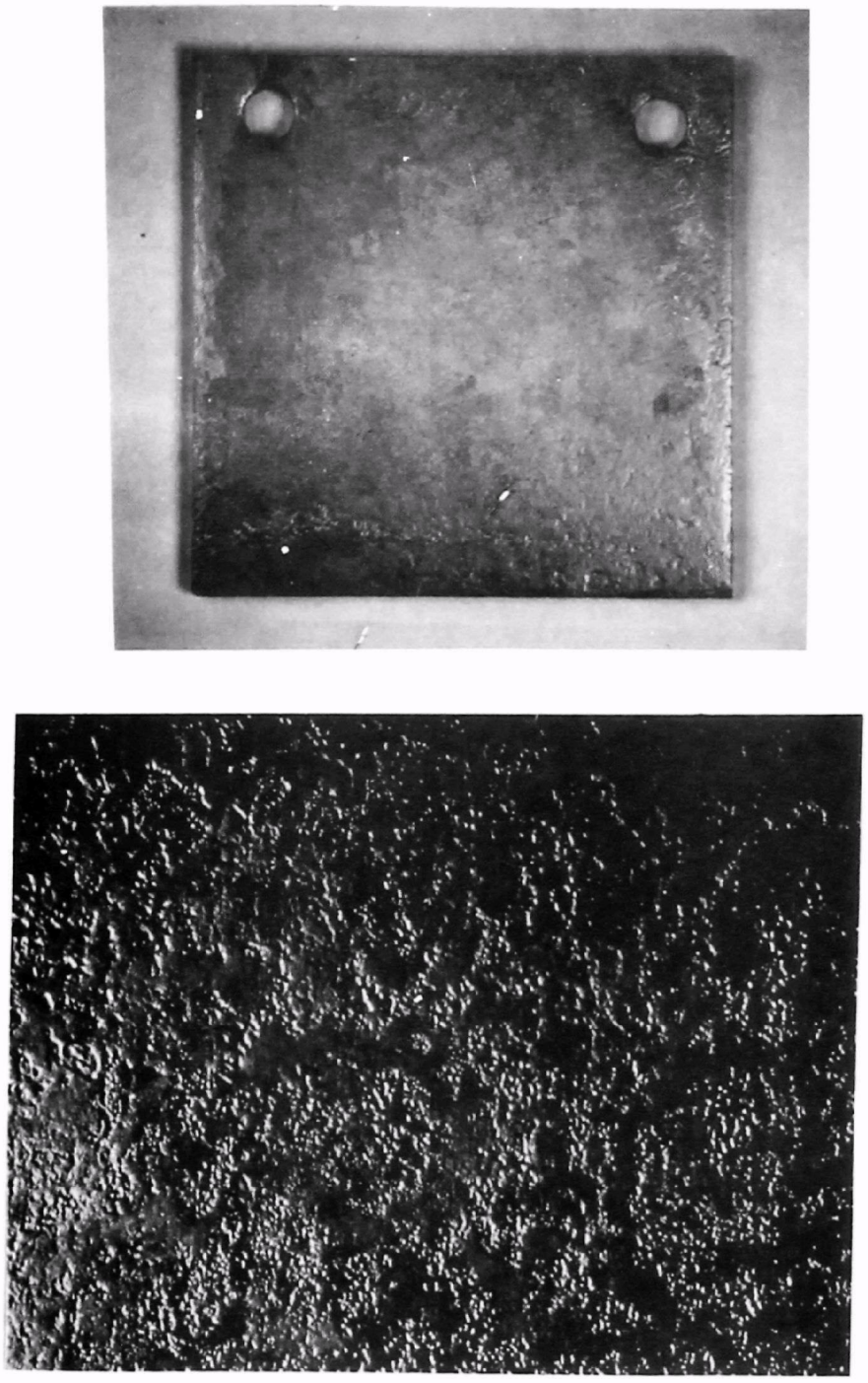

Figure 27. Coupon 304-24. Pitting and crevice corrosion. Upper casing.

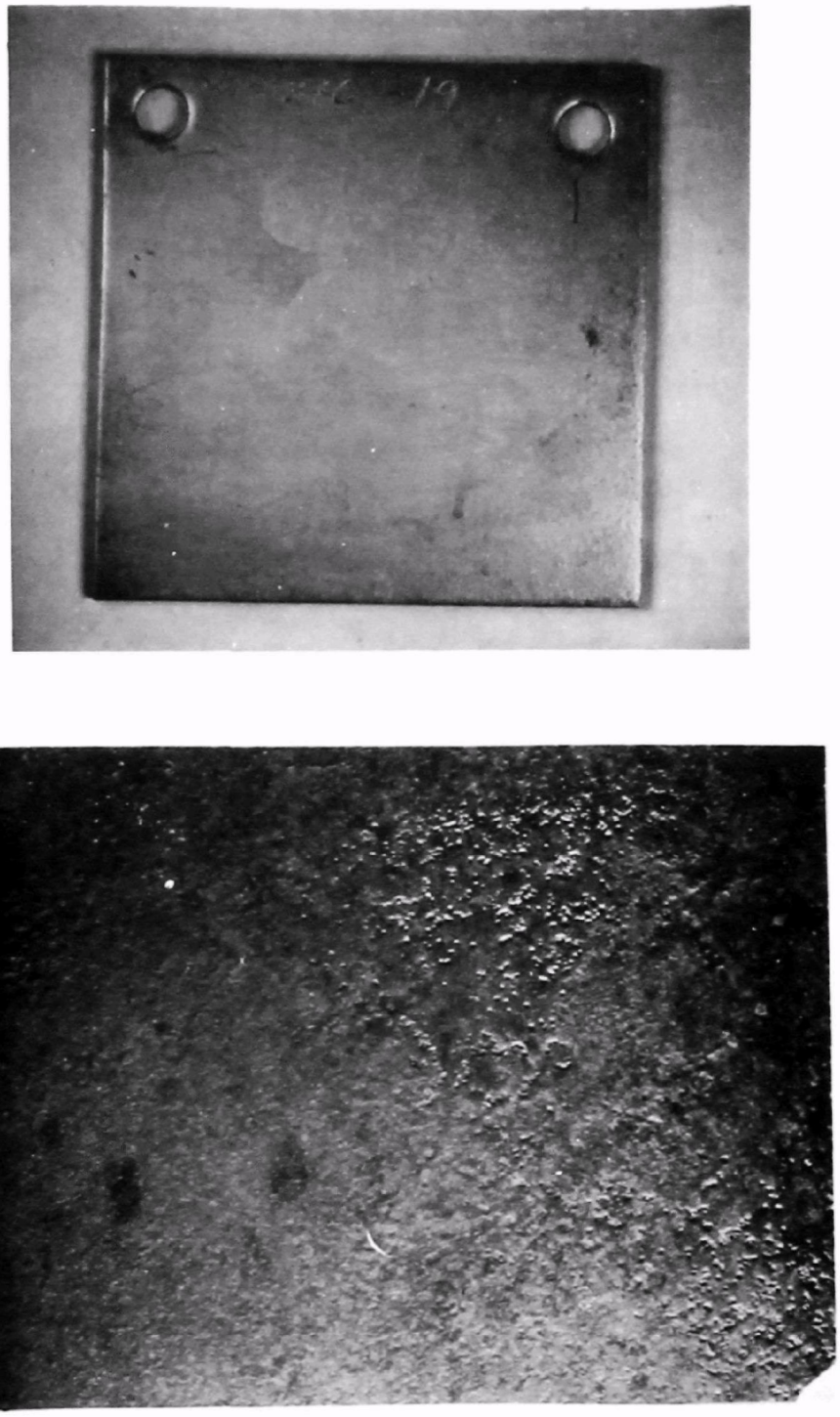

Figure 28. Coupon 316-19. Some pitting attack. Upper casing.

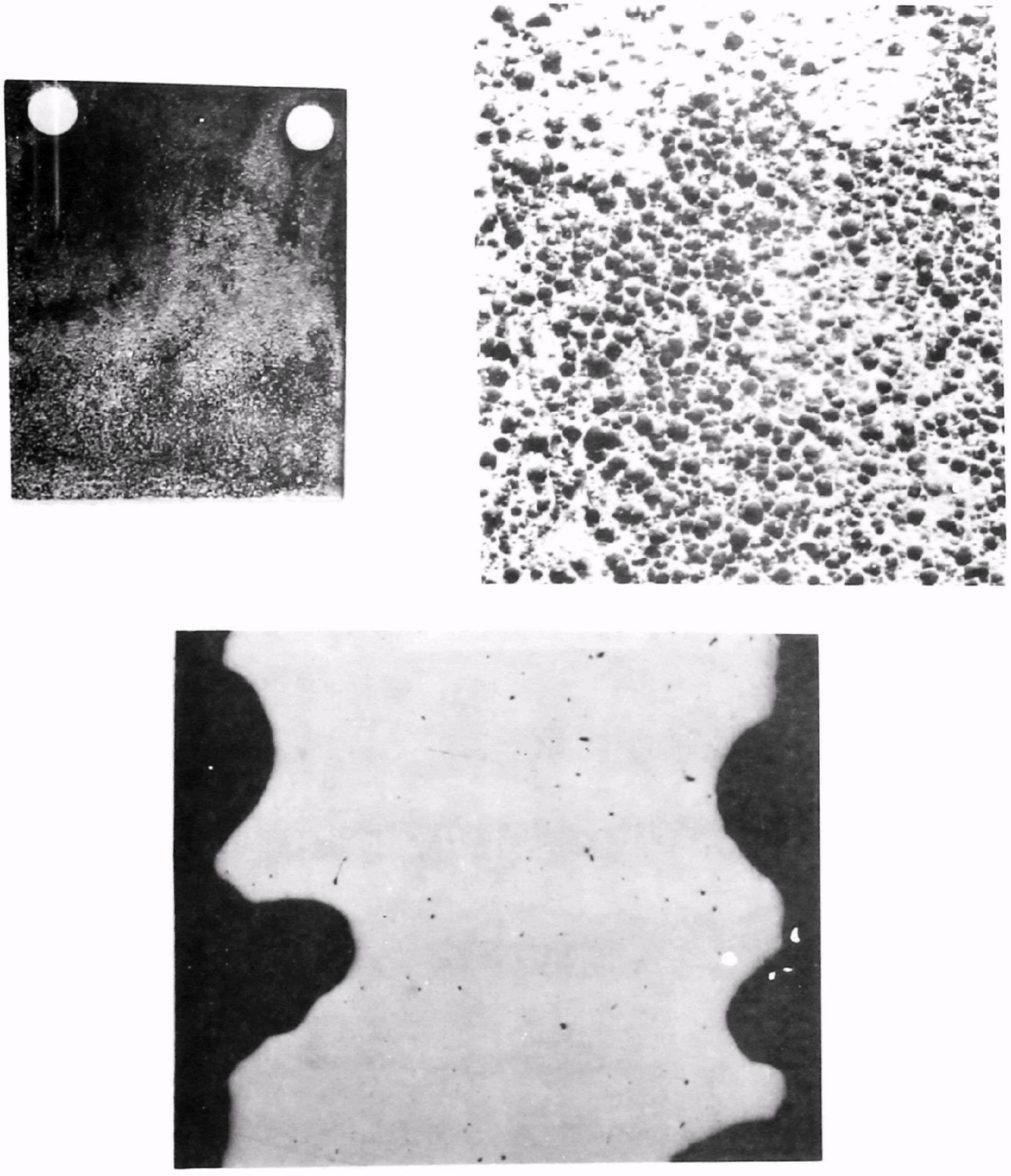

Figure 29. Coupon Ni-1. Severe pitting attack has occurred over entire surface. Lower casing.

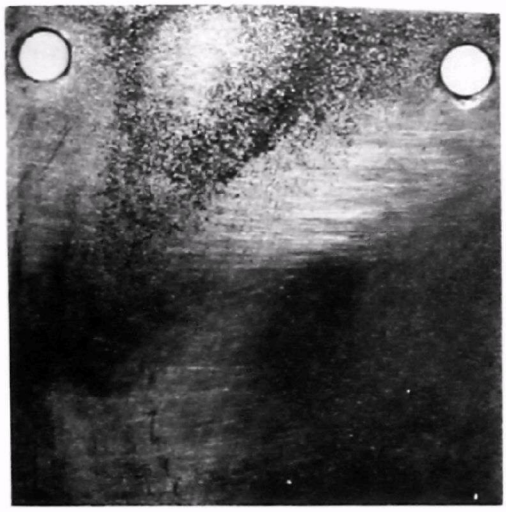

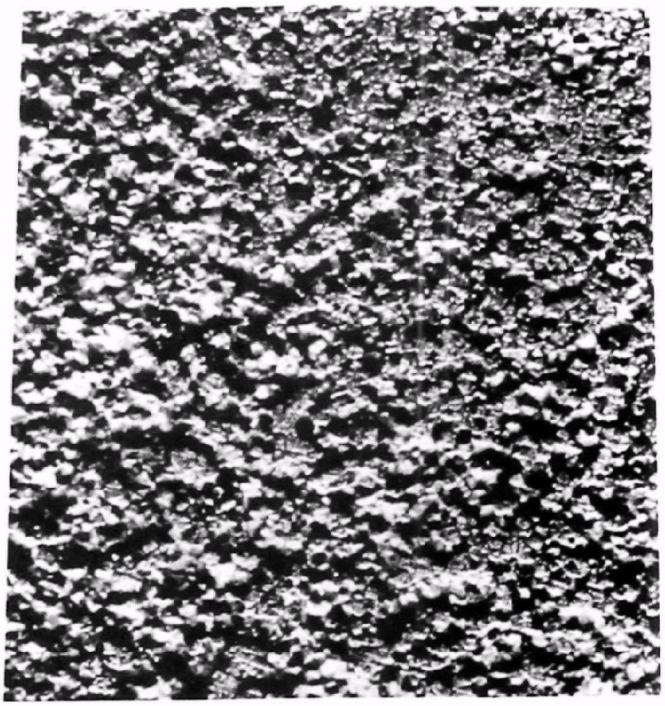

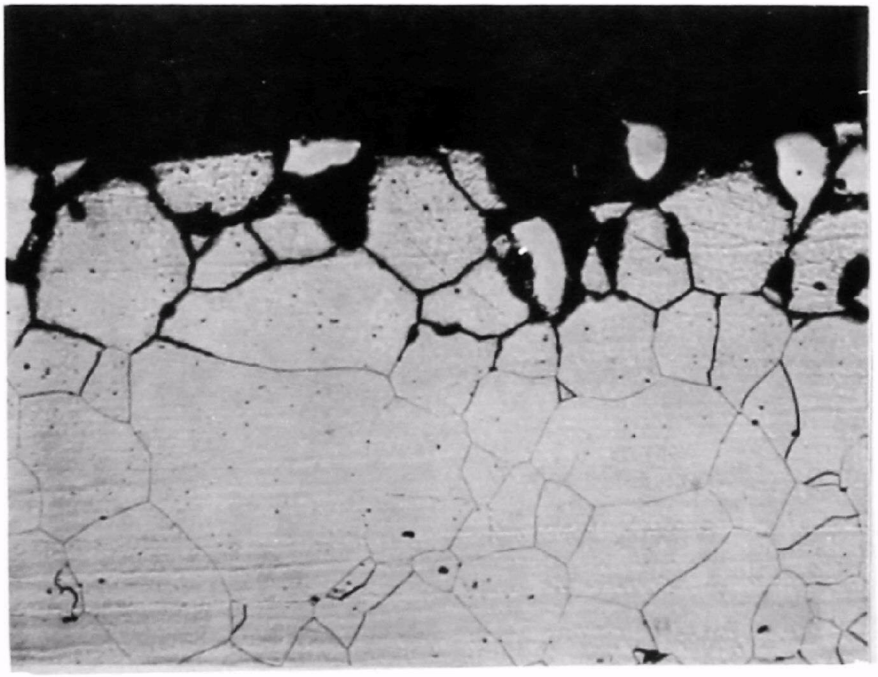

Figure 30. Coupon I6-1-2. Extremely severe intergranular attack with spalling of surface grains. Lower casing.

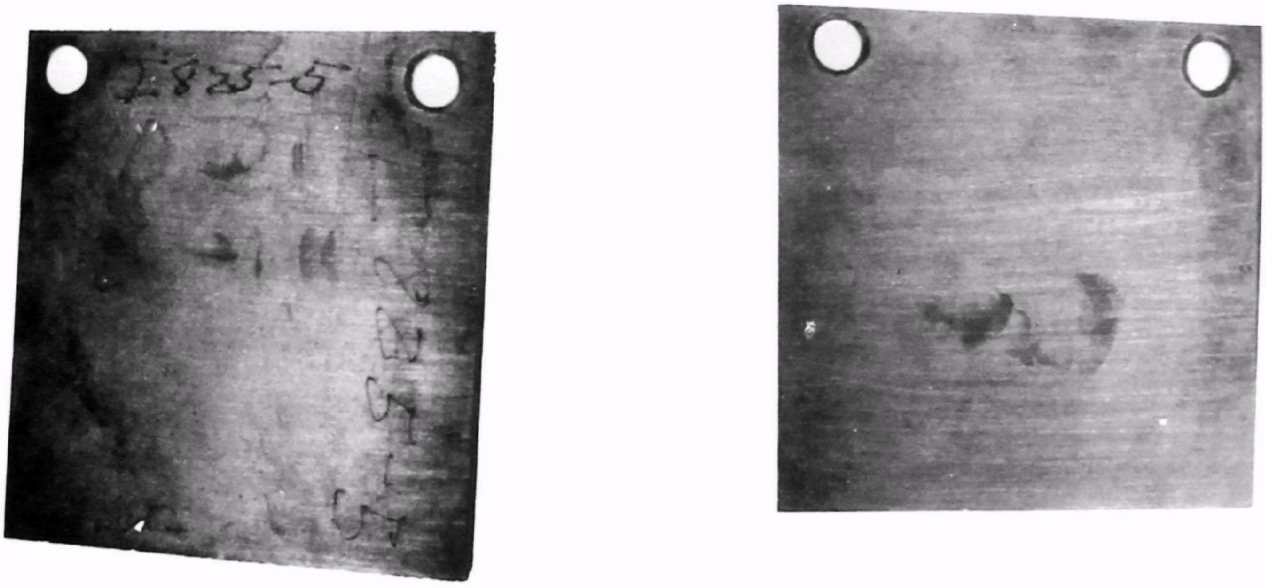

Figure 31. Coupons I825-2 (left) and 1825-5 (right). No indications of corrosive attack. Lower casing.

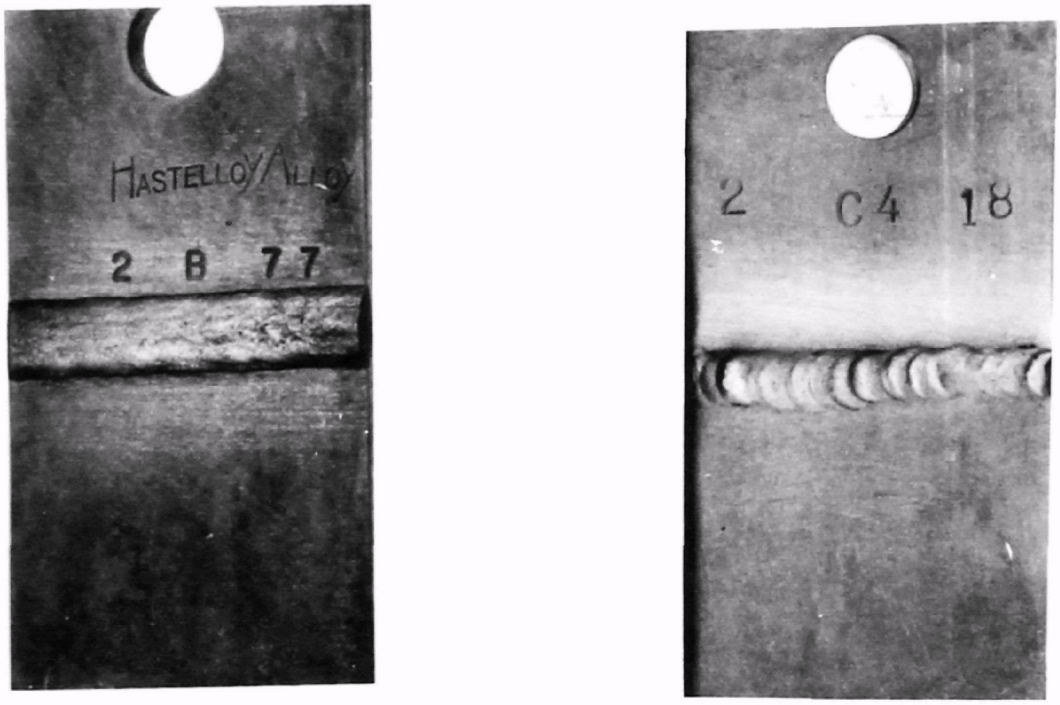

Figure 32. Coupons Hast. B-1 (left) and Hast C-1 (right). Some discoloration of the Hastelloy B specimen. Hastelloy C-4 not attacked. Lower casing.

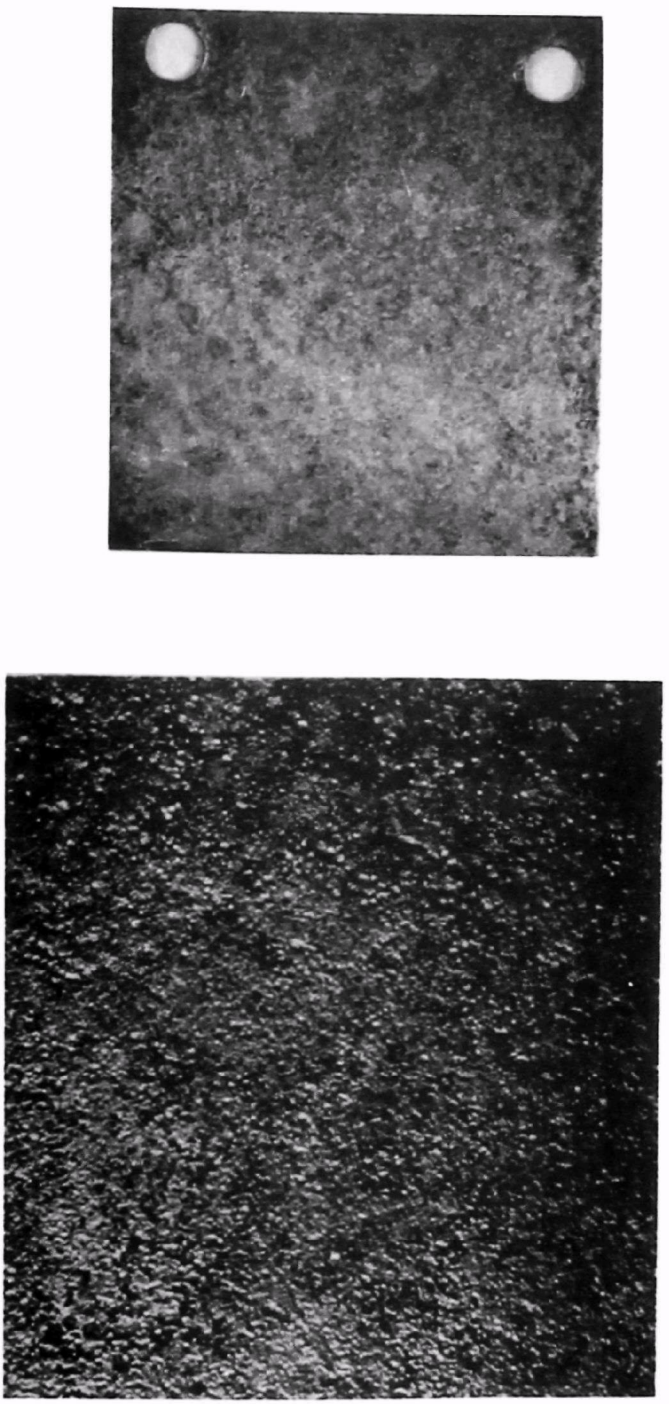

Figure 33. Coupon Ni-2. Severe pitting attack. Upper casing.

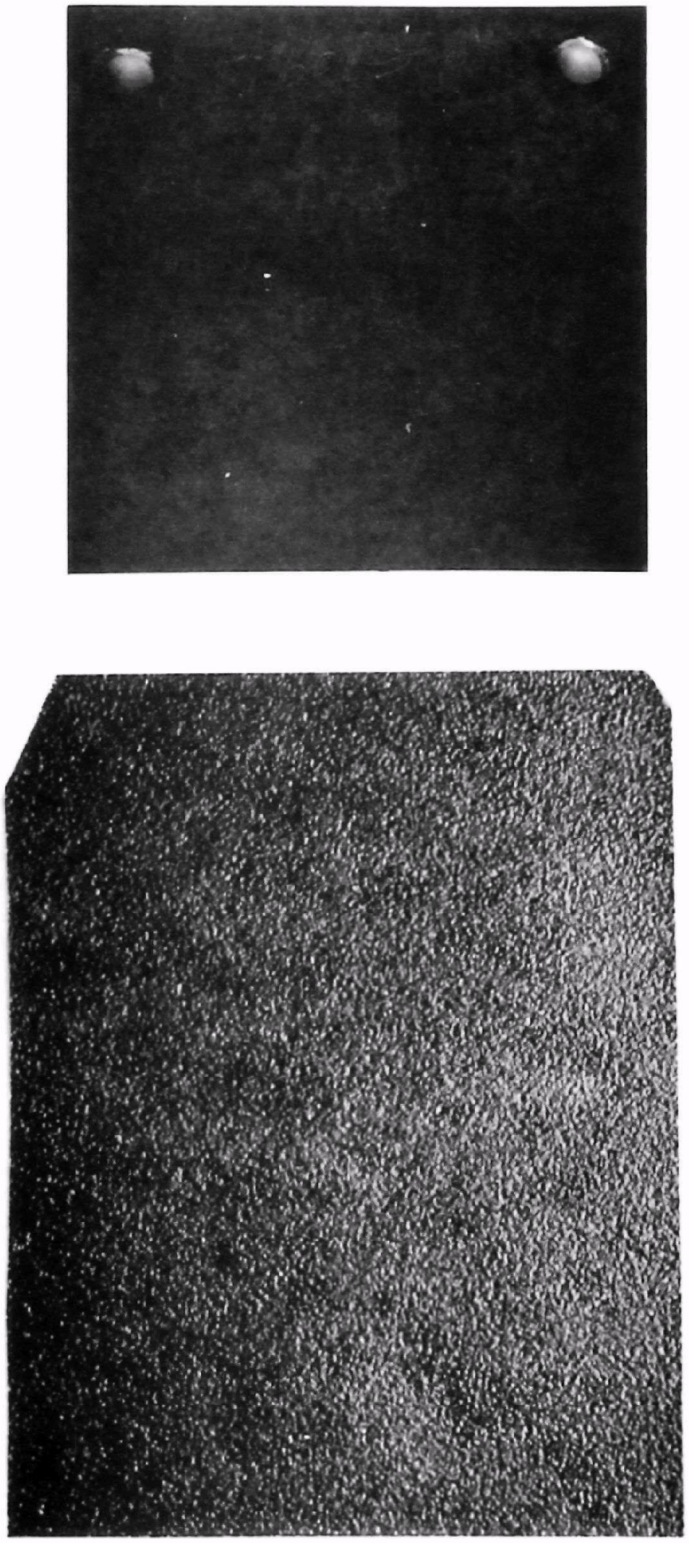

Figure 34. Coupon I601-3. Pitting attack on surface. Upper casing.

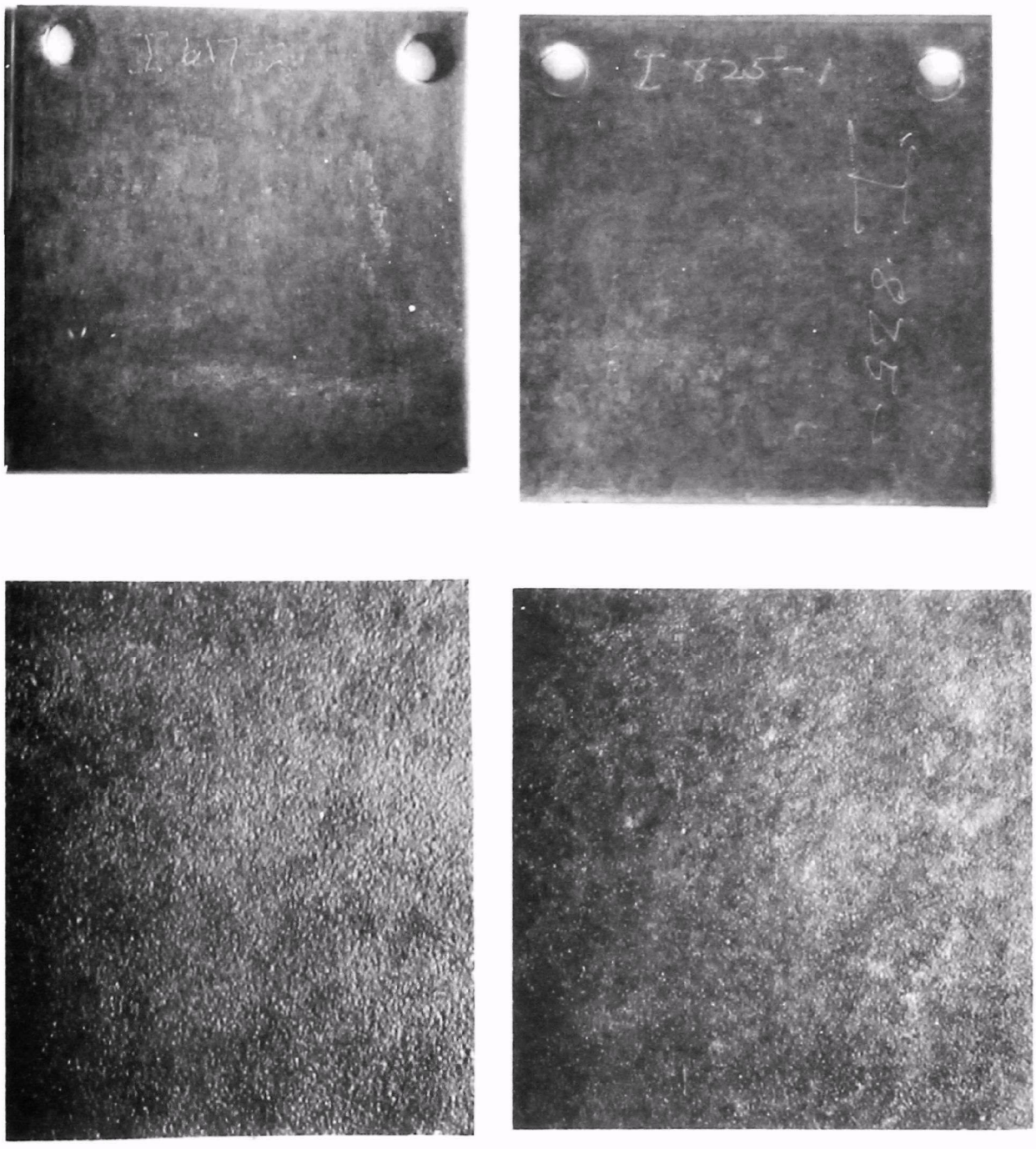

Figure 35. Coupons I617-2 (left) and I825-1 (right). Surface roughened (incipient pitting). Upper casing.

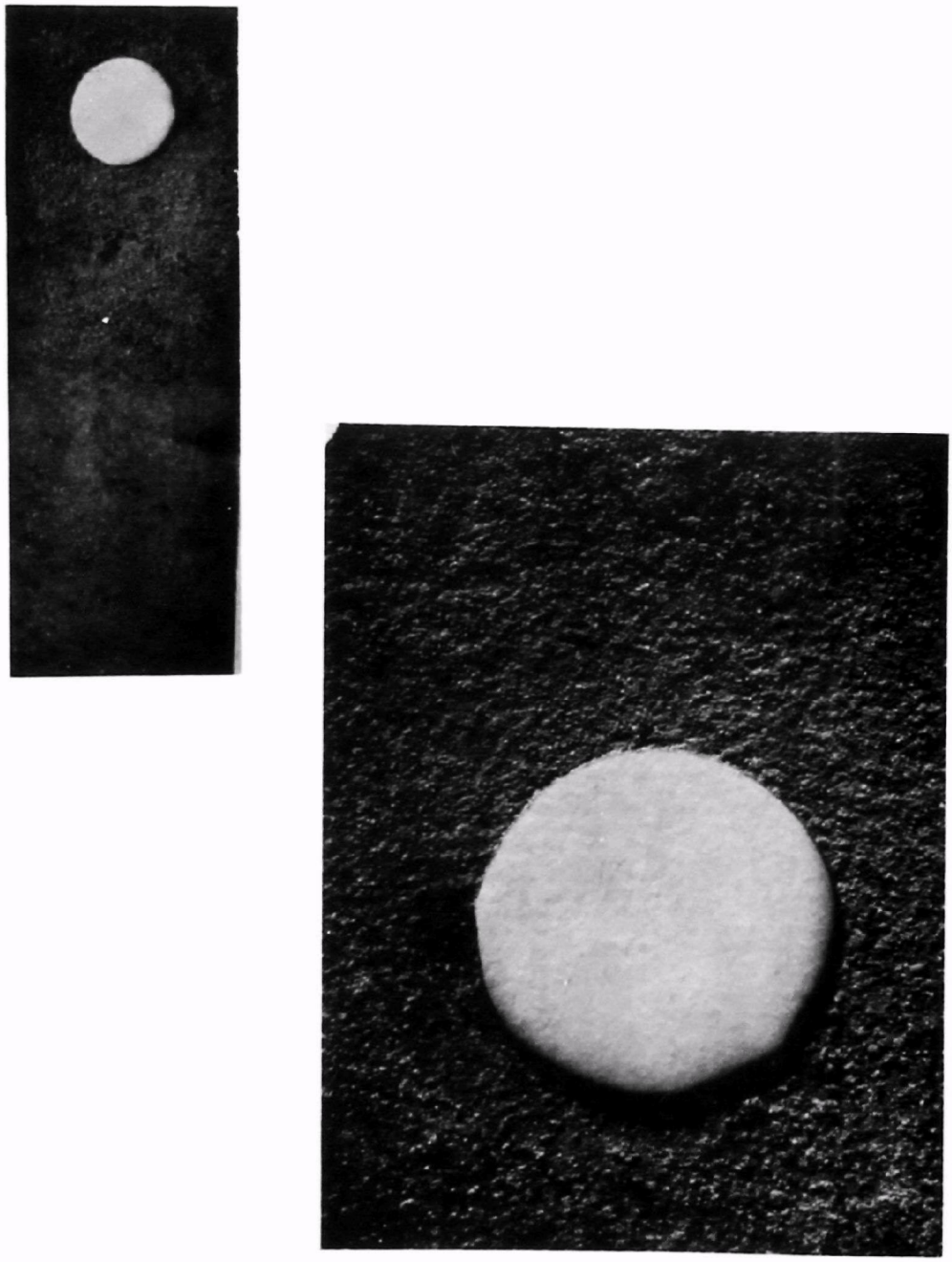

Figure 36. Hastelloy C coupon. Severe pitting attack. Upper casing.

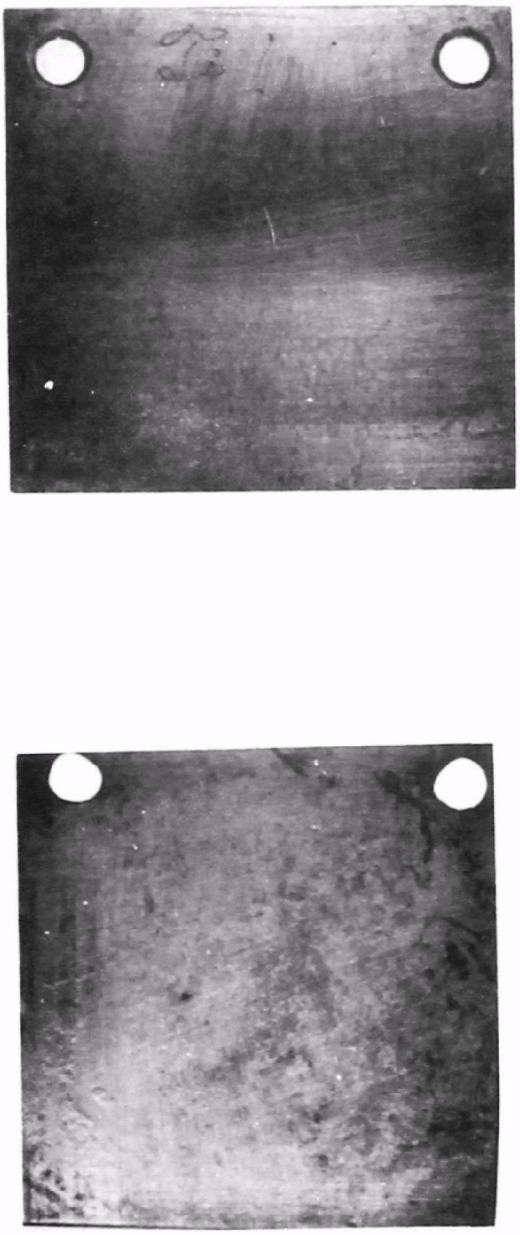

Figure 37. Coupons Ti-1 (top) and TiPd-1 (bottom). Some surface etching of titanium specimen. Lower casing.

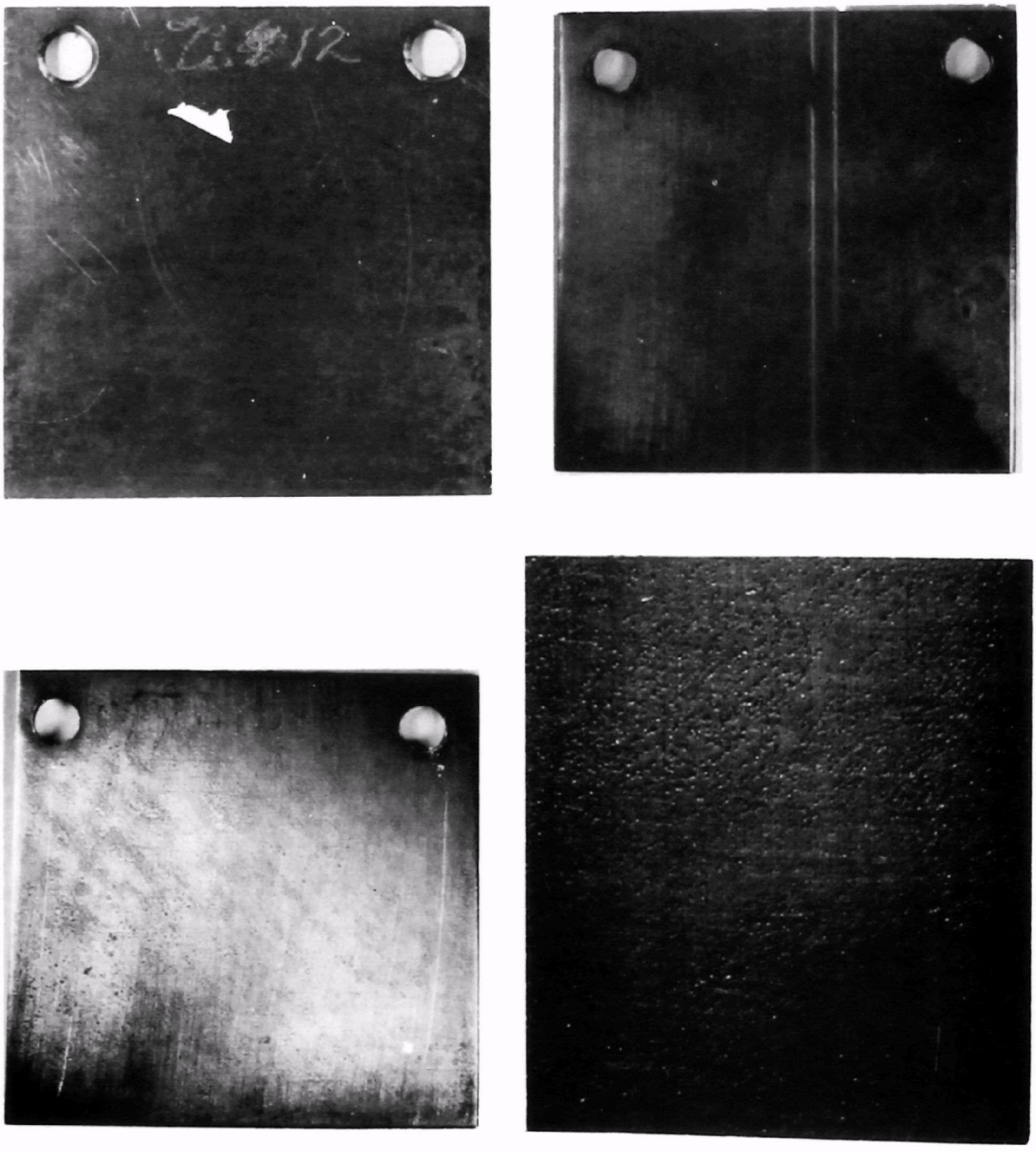

Figure 38. Coupons Ti-12 (upper left), TiPd-3 (lower left) and Ti-12-3 (upper and lower right). The Ti-12-3 coupon has pitted. Upper casing.

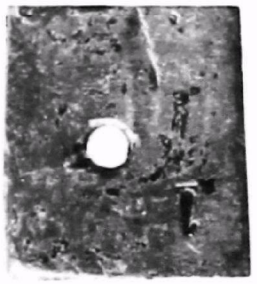

Figure 39. Coupon Pb-1. Surface film formed which was difficult to remove. Lower casing.

Non-Metallic Coatings

All of the coatings tested showed some degradation, either of the coating itself or of the coating/substrate bond. The EA919 epoxy (E), vinyl plastisol (W) and alkyd (RO) all failed by coating attack, blistering and peeling, see Figures 40 through 42. In some cases the coating disappeared from the surface of the coupons during exposure to the CDS environment. The polyvinylidene fluoride (K) coatings failed by adhesion as evidenced by blistering and peeling of the coating from the substrate, Figure 43 through 45. However, the coating materials themselves appeared to be unaffected by exposure. Both the polychloroprene (N) and polysulfonated rubber (H) coatings were attacked and cracking was noted, Figures 46 and 47.

The glass flake filled polyester (Cielcote) and filled vinylester coatings showed surface etching and, in one case, portions of the coating flaked off, Figures 48 and 49.

Twelve water spray nozzle couplings in the upper casing were coated with epoxy, alkyd, vinyl, and polyphenylene sulfide (3 each) and exposed to the normal operation environment. The epoxy, vinyl, and alkyd coatings failed while the polyphenylene sulfide coating was still intact when the test was terminated (the PS coating was damaged during the coupling removal operation). Three tested couplings are shown in Figure 51.

Coatings were applied to lower casing walls (hypalon and neoprene elastomer), upper casing doors (epoxy, alkyd, and vinyl), the electrode headers (epoxy, vinyl, and alkyd) and the upper casing walls (hypalon, neoprene, vinyl and alkyd). Only the epoxy coatings on the upper casing doors and electrode headers did not fail, although they discolored and exhibited some blistering. All of the other coatings failed, usually in the bond. It should be noted that substrate preparation was not possible and the coatings were applied in the field after solvent cleaning with acetone. Therefore, good adhesion would not be expected.

The bonded polychloroprene (neoprene) (NB) liner material showed surface checking, and cracking, Figure 50. The elastomer hardened from a shore A of 70 to 90 indicating chemical attack.

An Armalon (teflon/glass fabric) liner applied to an upper casing door showed excellent resistance to attack.

Non-Metallic Structural Panels

Fiber reinforced polyesters, vinylesters, furans, and polybutadiene were tested in panel form in the lower casing. In addition, polyvinylchloride (PVC) was tested as shrink tubing and polyhexafluoropropylene (Viton) as gasketing material.

The polyesters showed degrees of degradation ranging from surface etching to delamination as shown in Figures 52 through 58. The vinylester panel showed some surface etching and edge attack, Figure 59. The furans also

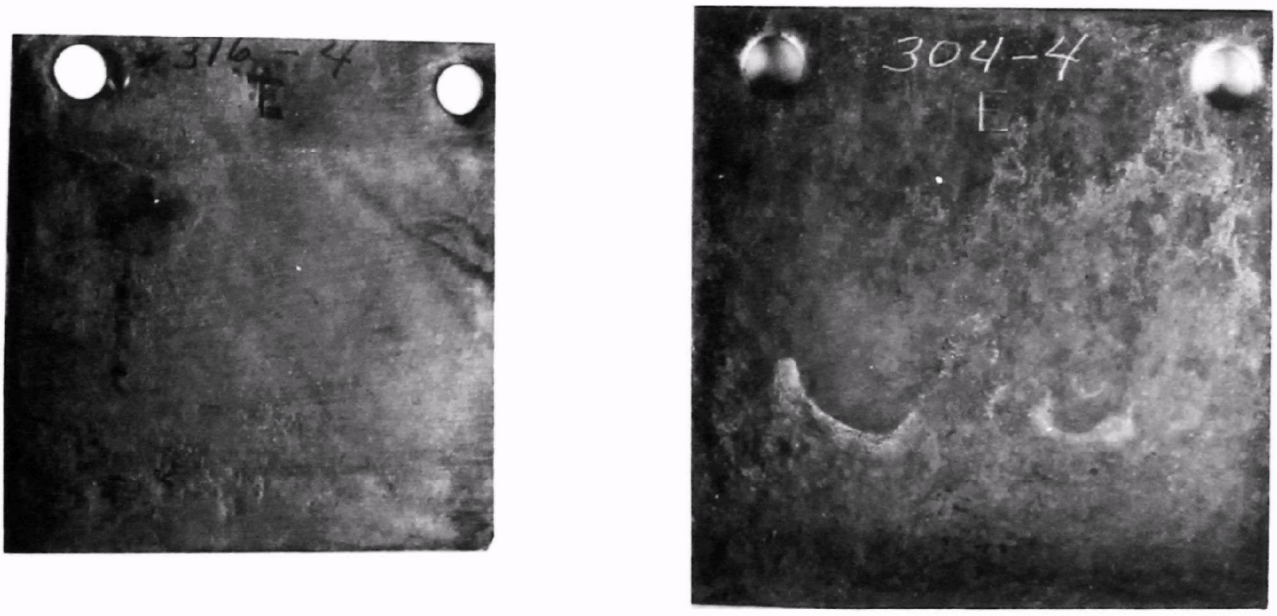

Figure 40. Coupons 316-4E (left) lower casing and 304-4E (right), upper casing. EA 919 epoxy coating has failed exposing substrate.

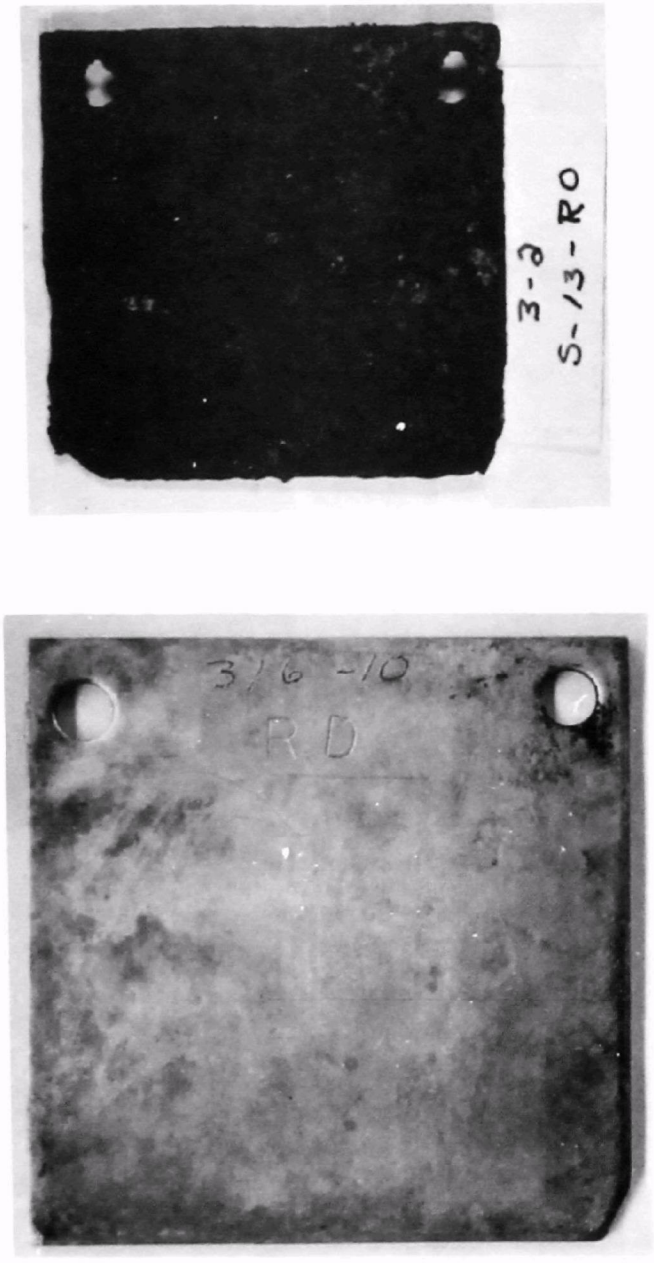

Figure 41. Coupons S-13RO (top) lower casing and 316-10RO (bottom) upper casing. Coating failed exposing substrate.

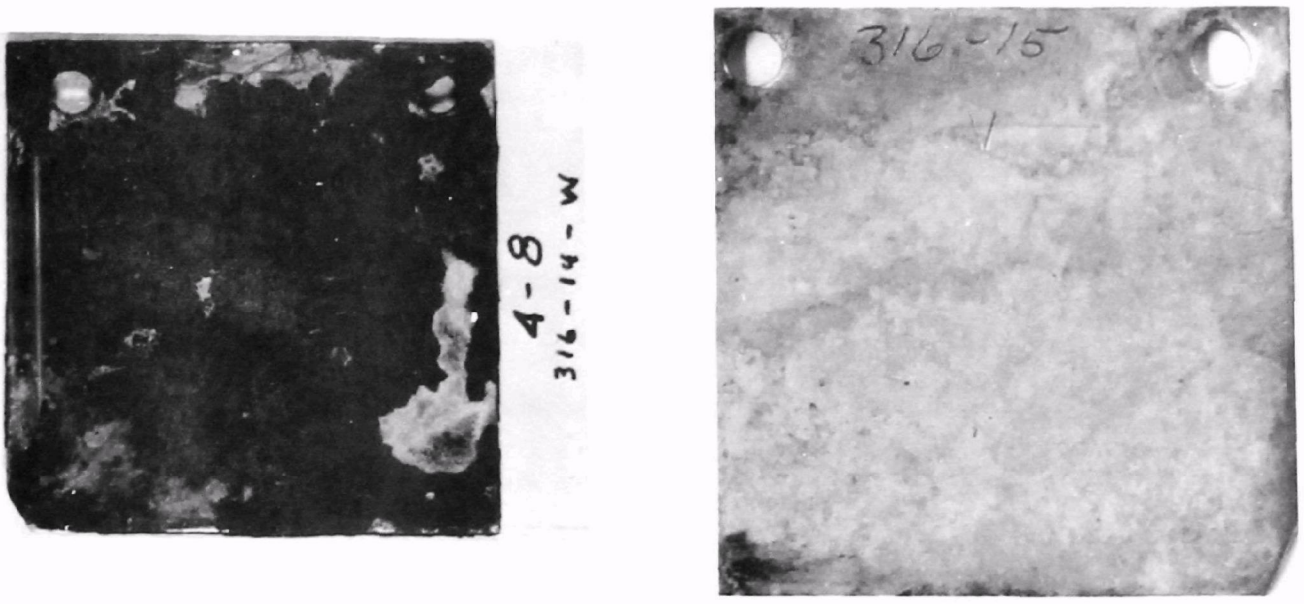

Figure 42. Coupons 316-14W (left) lower casing and 216-15W (right) upper casing. Coating failed exposing substrate.

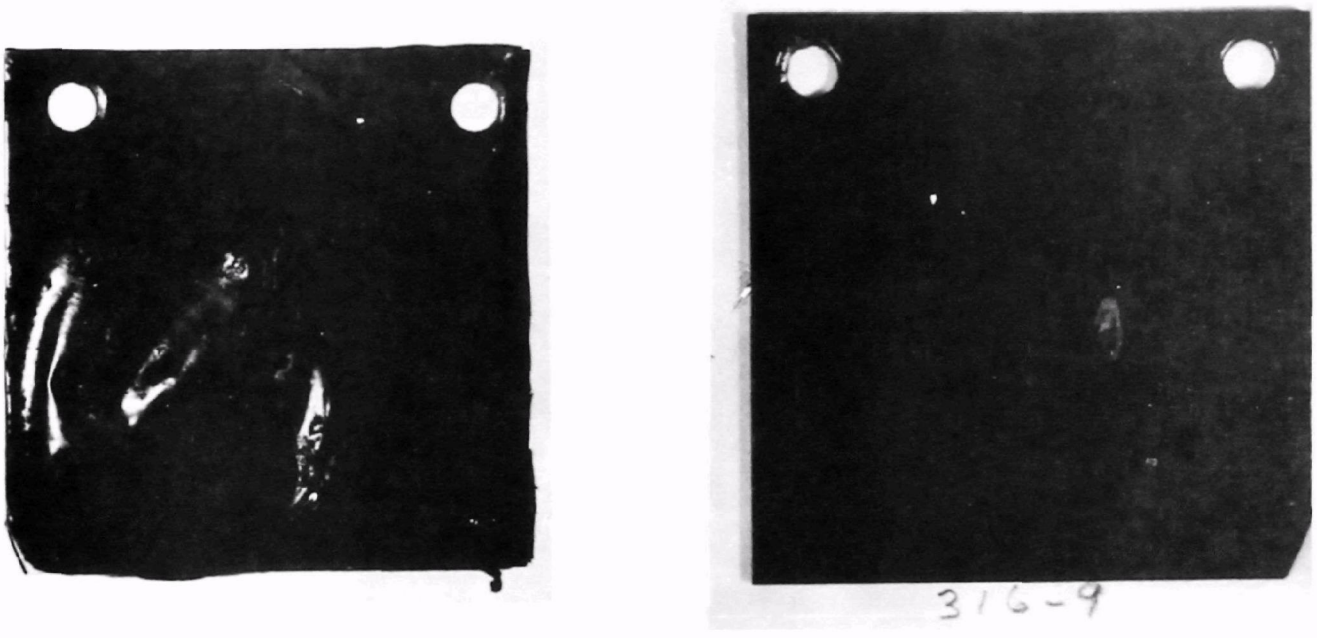

Figure 43. Coupons 316-7PS (left) lower casing and 316-19PS (right) upper casing. Coating failed in adhesion causing blistering and delamination.

Figure 44. Coupons 304-3T and S1-T (upper) lower casing and 216-2T upper casing. Coating failed in adhesion causing blistering.

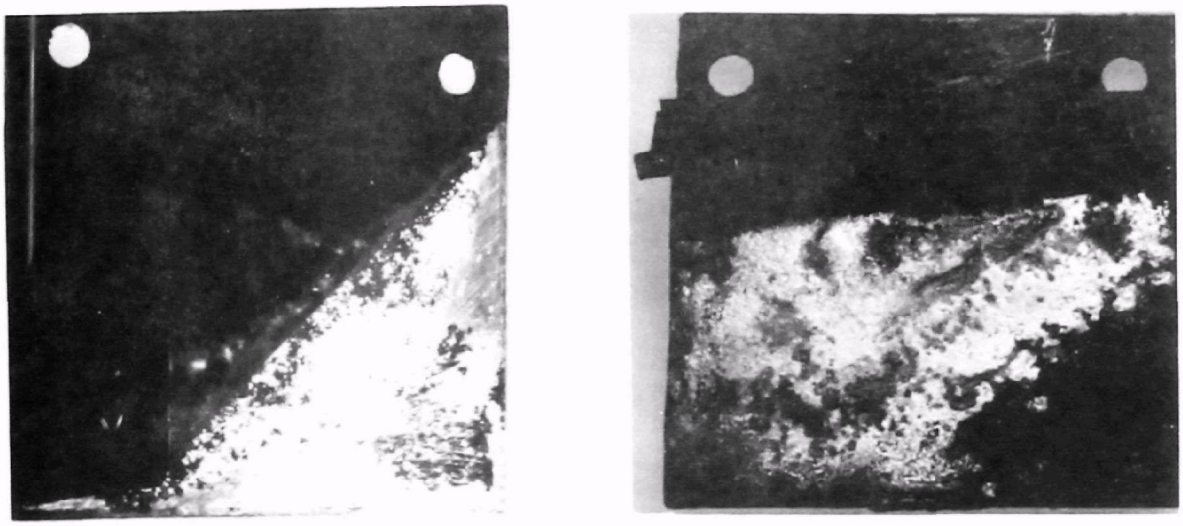

Figure 45. Coupons 304-28K (left) and S-24K (upper) lower casing. Bond failed causing delamination.

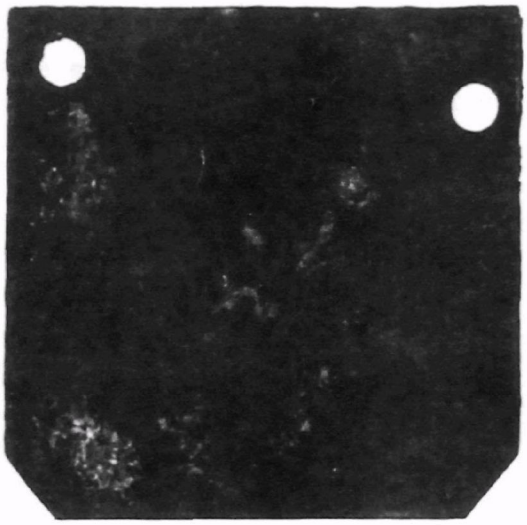

Figure 46. Coupon S-18N lower casing. Coating cracked and delaminated.

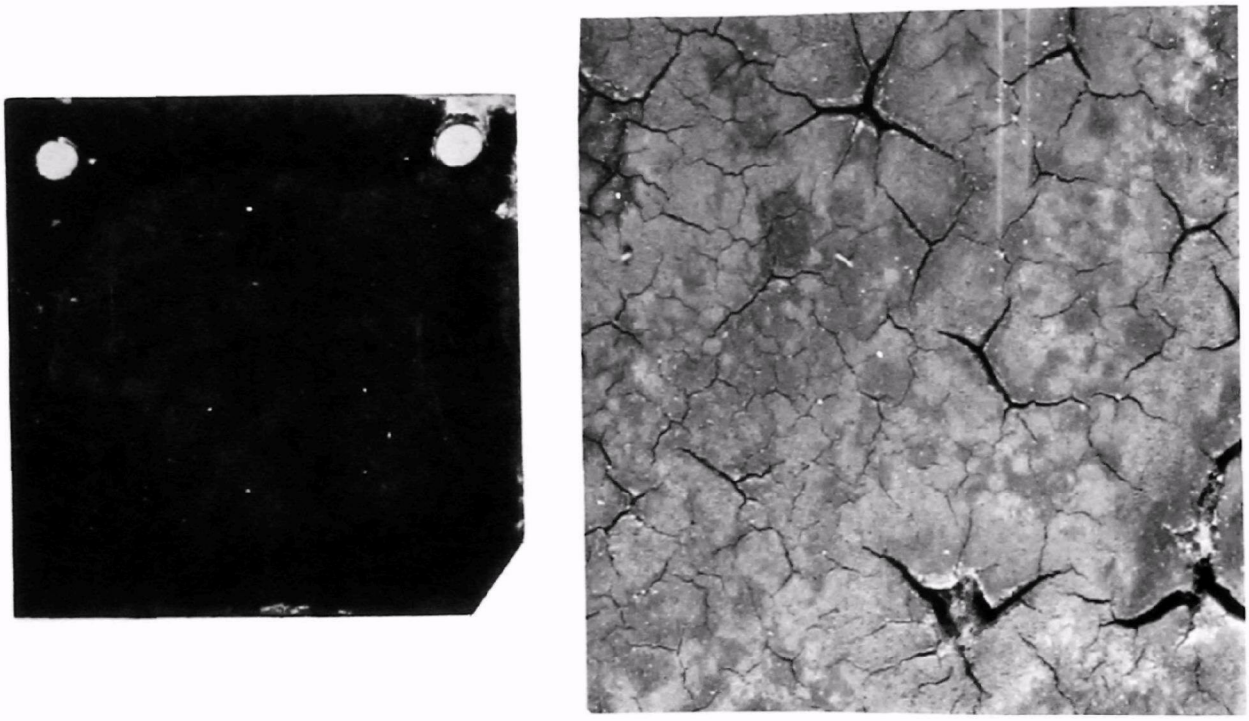

Figure 47. Coupon 316-28H lower casing. Surface etched and cracked.

Figure 48. Steel coated with glass flake filled polyester (ceilcote) Surface has been etched by the gases.

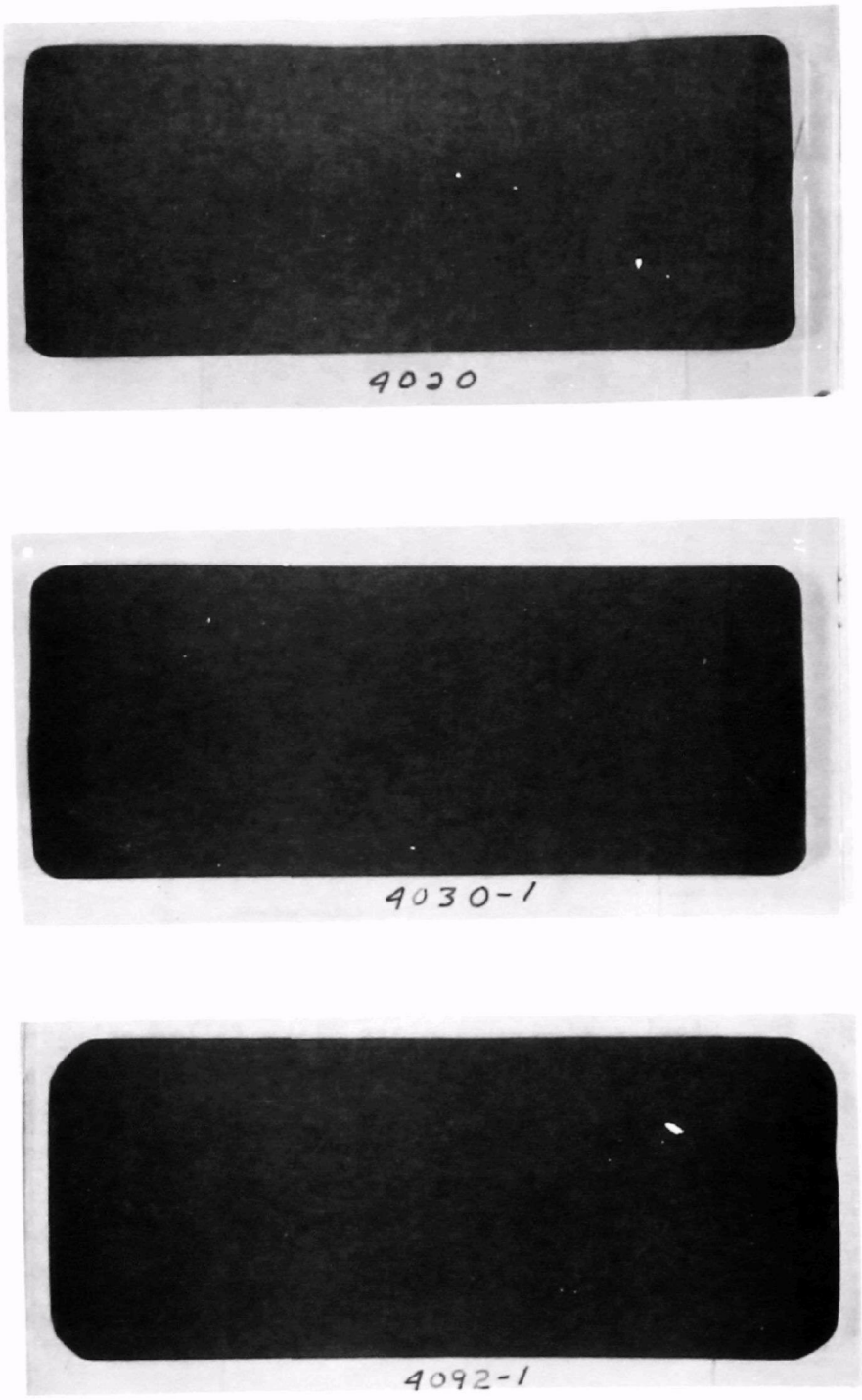

Figure 49. Steel coated with glass filled vinylesters. Surfaces have been etched. 4030-1 sample shows coating failure by chipping off at attachment hole.

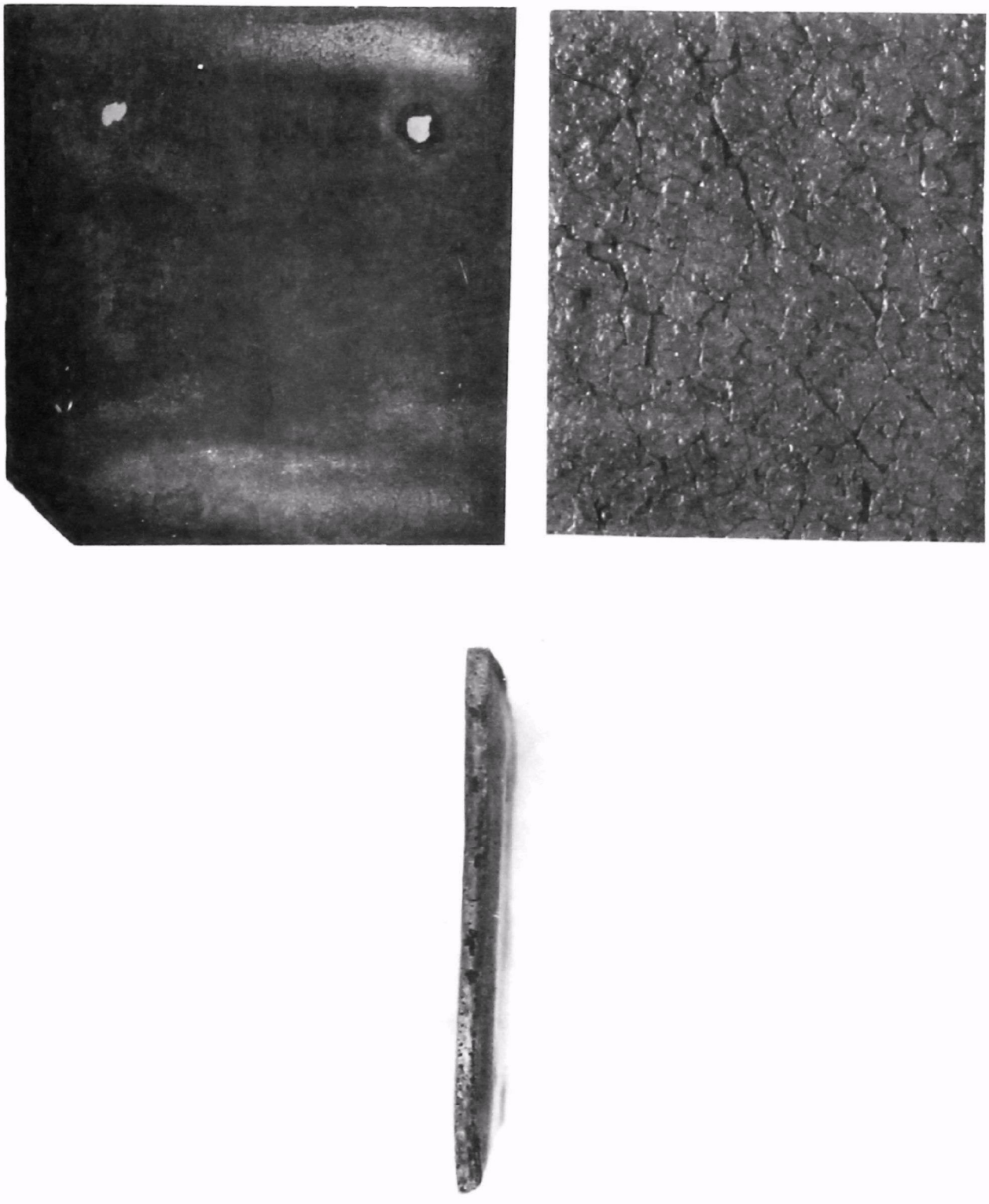

Figure 50. Coupon 316-NB. Neoprene elastomer liner shows surface cracking (checking). Lower casing.

Figure 51. Water spray nozzle couplings from upper casing. Couplings are coated with polyphenlyene sulfide (PS), alkyd (RO), vinyl (W) and epoxy (919). The PS coating was intact (although damaged during the removal operation). The other coatings failed.

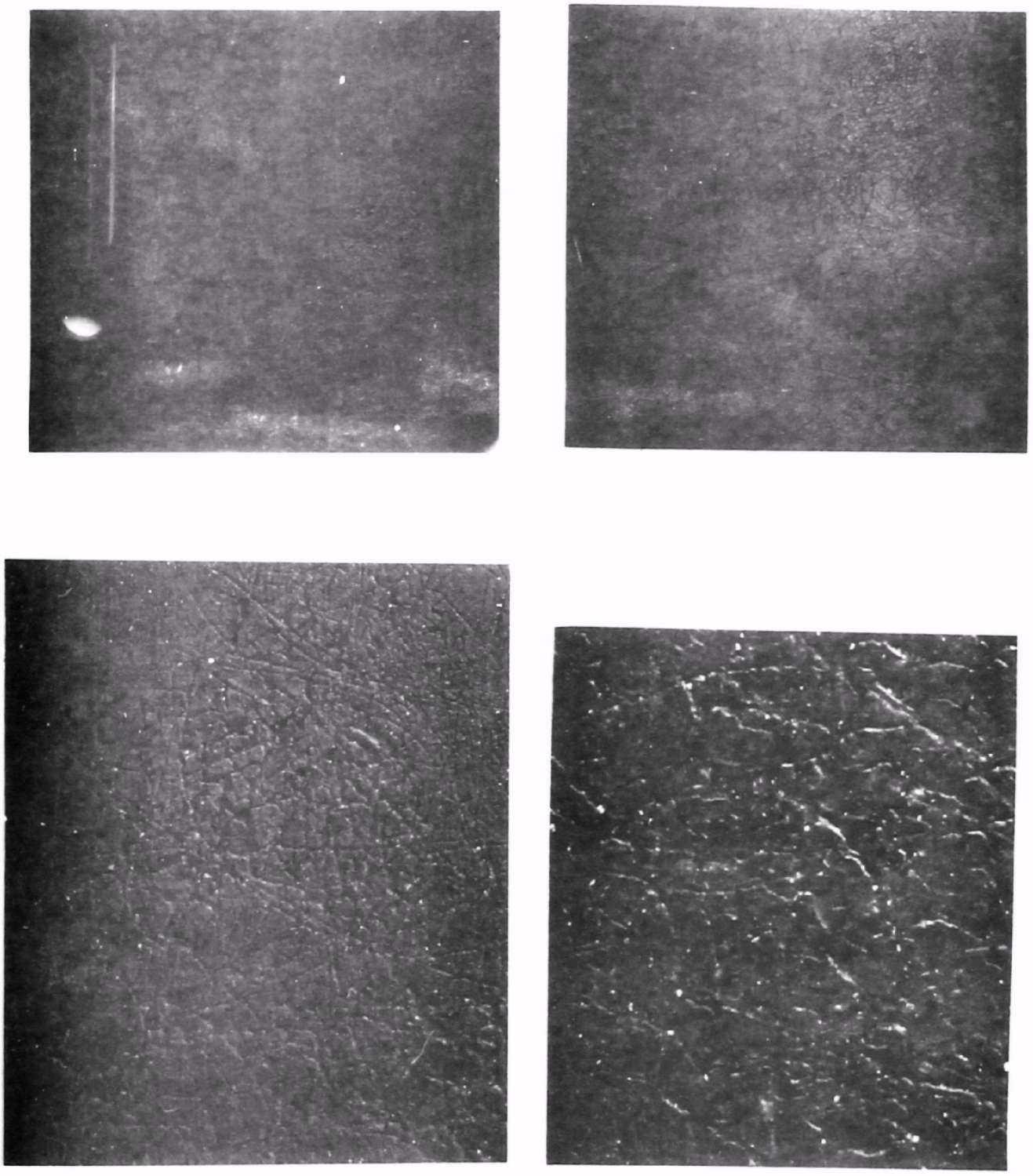

Figure 52. Coupons AT382-1 (left) and AT382/05 (right) bisphenol polyesters. Surface checking and cracking. Lower casing.

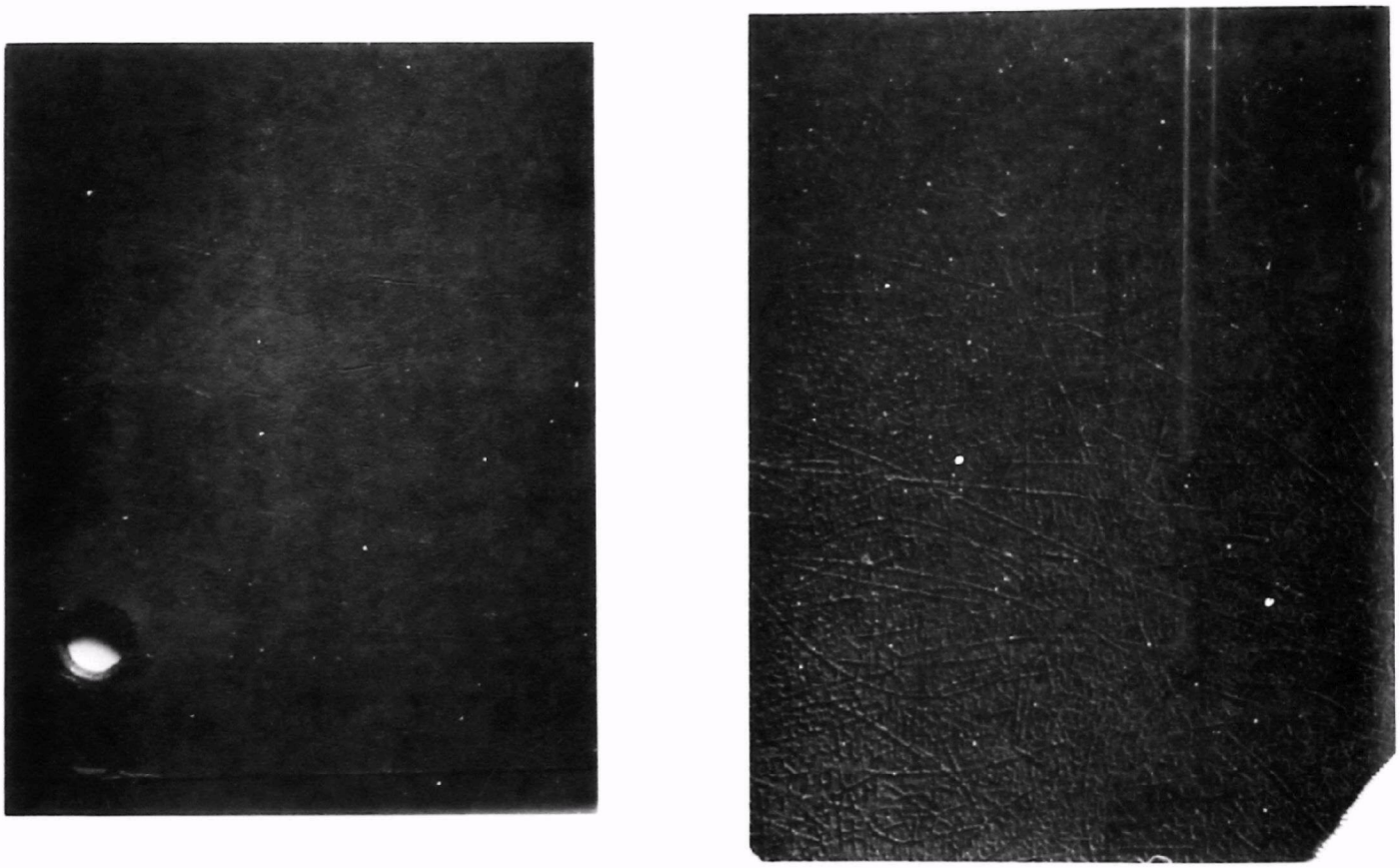

Figure 53. Coupon AT-11-1 flame retarded polyester. Surface etching and checking. Lower casing.

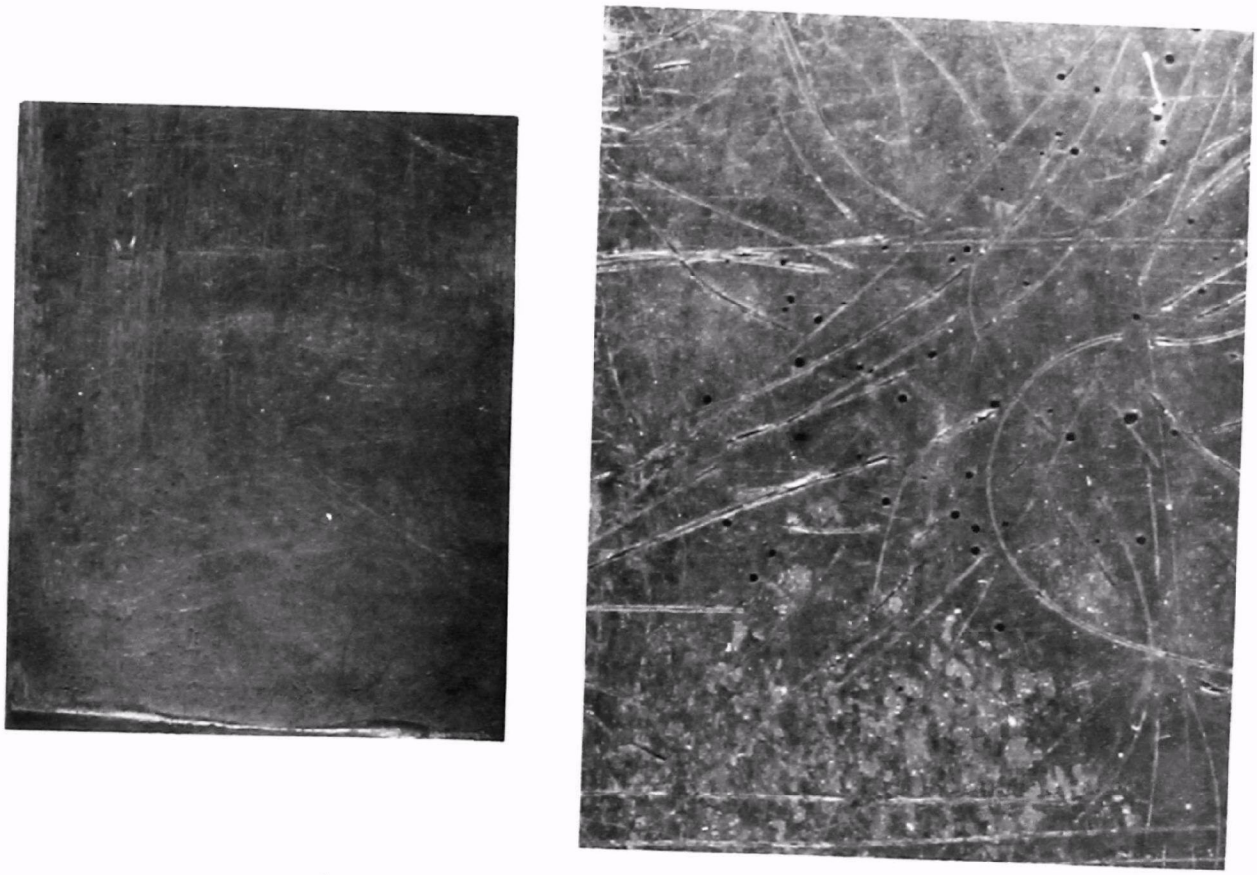

Figure 54. Coupon ASH7240-40 IPA polyester. Surface attack, pits and cracks. Lower casing.

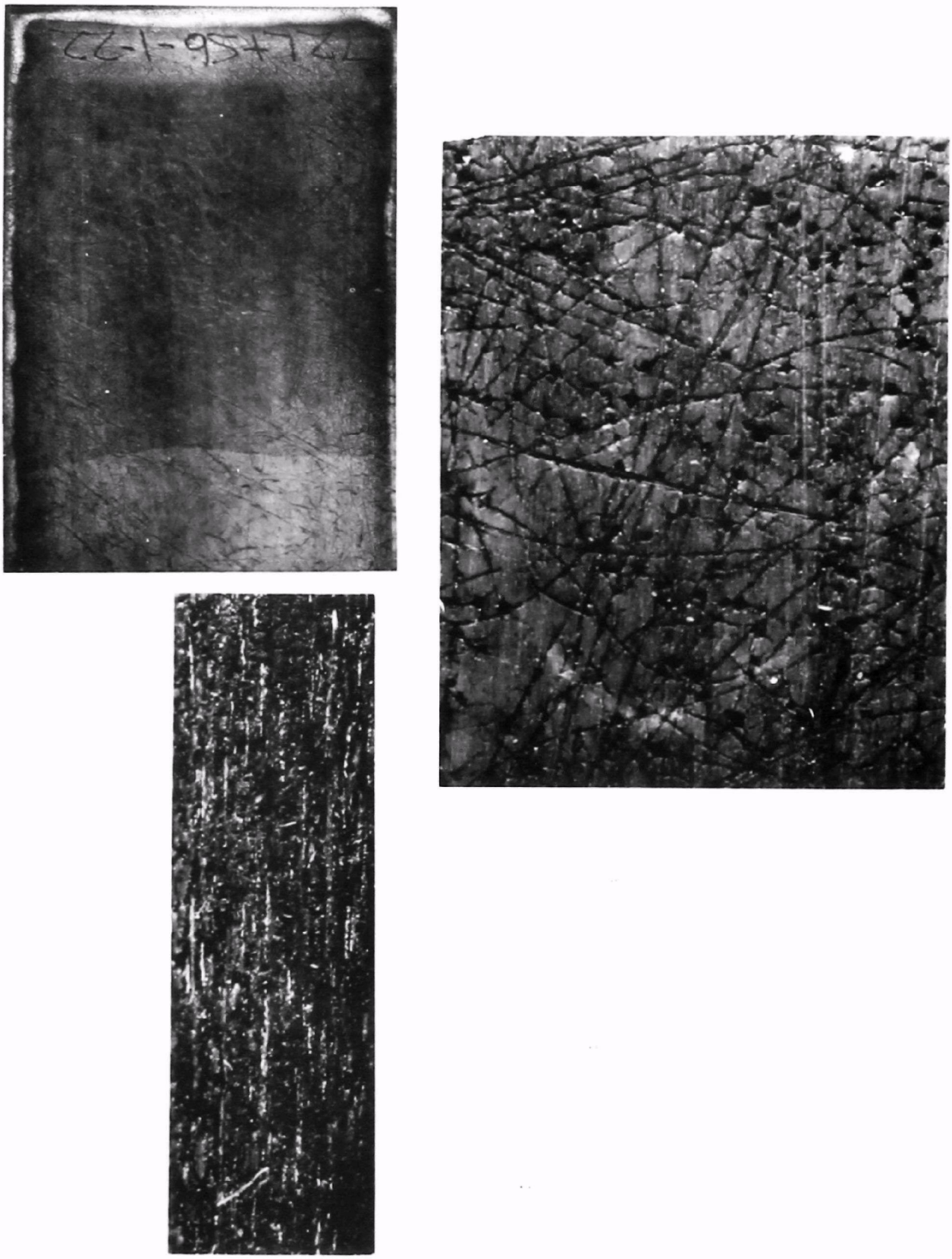

Figure 55. Coupon ASH7241-29 IPA polyester. Surface etching, cracking and pitting. Lower casing.

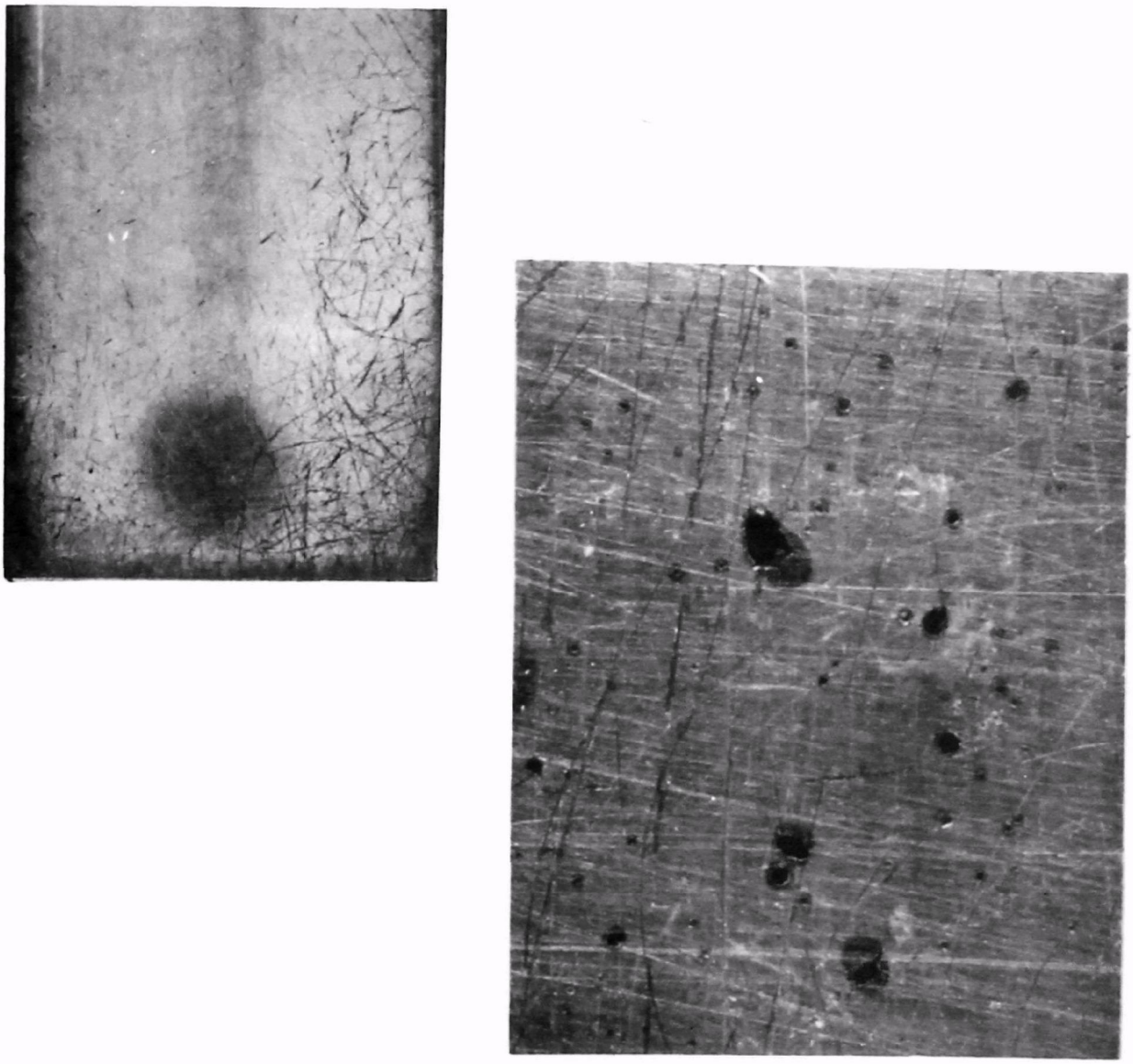

Figure 56. Coupon ASH 197/3-5 polyester. Surface etching, pitting and crazing. Lower casing.

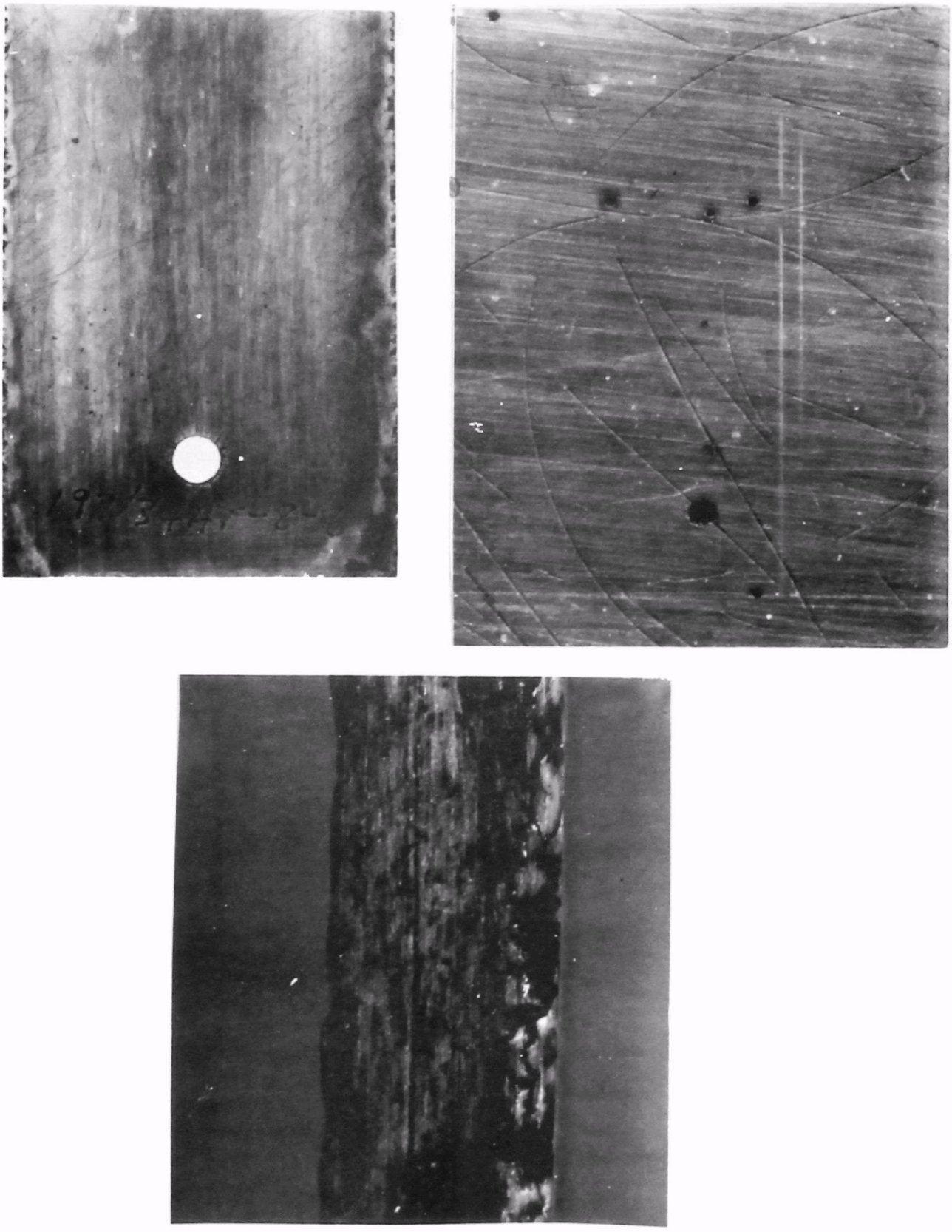

Figure 57. Coupon ASH 197/3AT-6 polyester. Surface crazing and pitting. Lower casing.

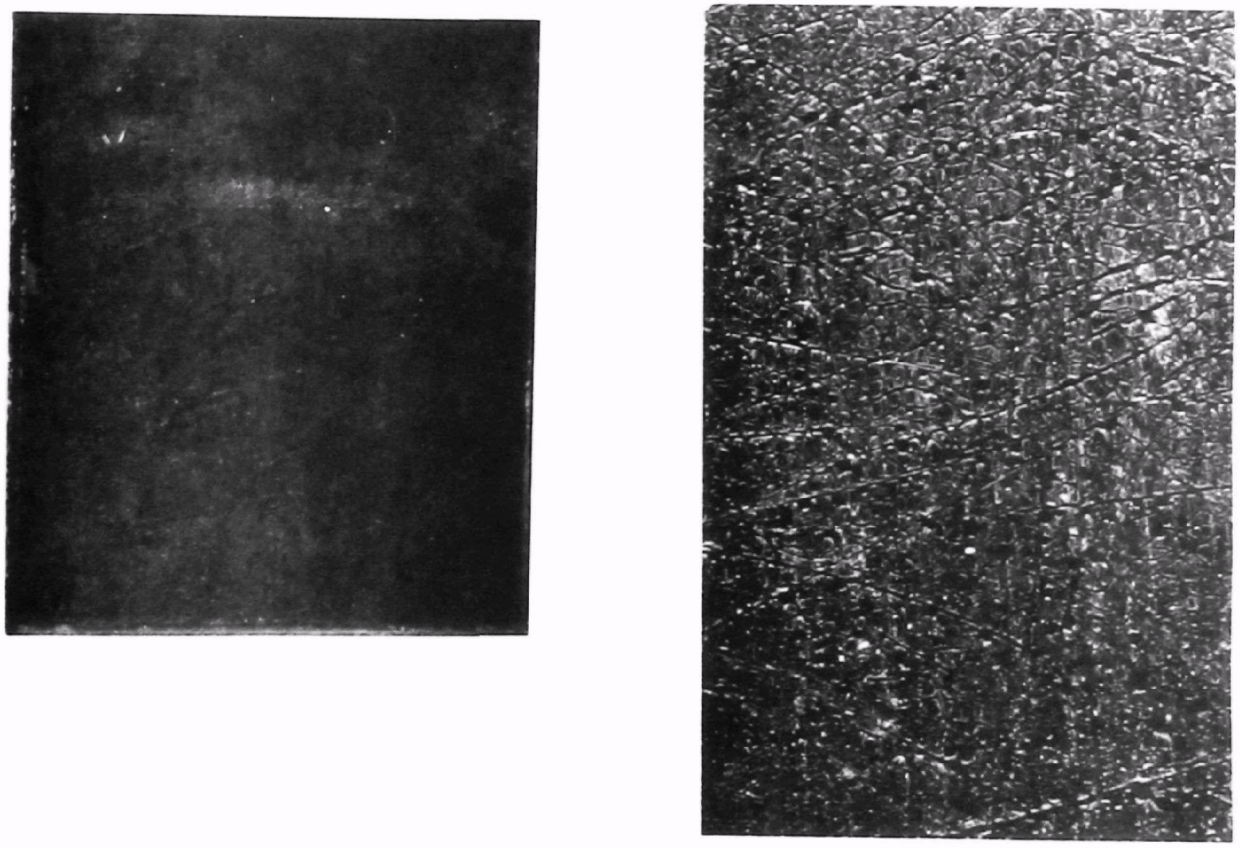

Figure 58. Coupon ASH 72L-21 flame retarded polyester. Surface checking, cracking and pitting. Lower casing.

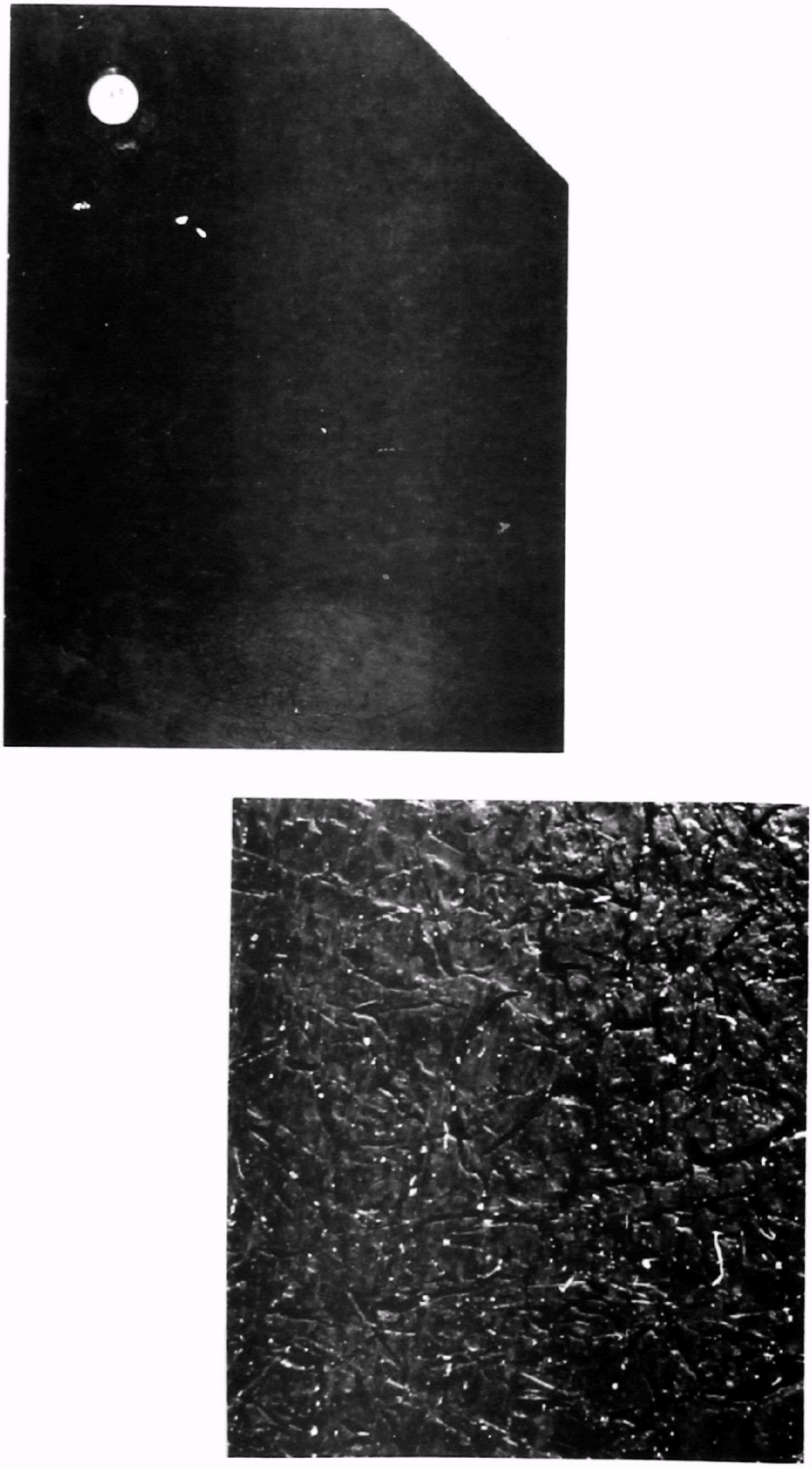

Figure 59. Coupon AT580-1 bisphenol vinylester. Surface cracked and etched. Lower casing.

showed surface etching and edge attack, Figure 60. The polybutadiene panel discolored and showed some minor pitting near the edge, Figure 61.

The PVC shrink tubing was installed over water spray couplings and electrode couplings and showed visible signs of degradation.

The temperature of the shrink tubing was low due to water flow. Some signs of crevice corrosion of the stainless steel was noted under some of the shrink tubing liners.

The viton seals showed no degradation due to exposure to the CDS operating conditions.

Braced Nozzle/Grommet Joint

In order to provide a more reliable joint between the electrode nozzles and the mounting grommets, a brazed configuration was tested. It was also hoped that less arcing, and resulting erosion of the nozzles, would occur with a positive electrical path between nozzle and grommet. Excessive arcing had resulted in failure of some nozzles after a baffle support failure.[1]

Several nozzle/grommet assemblies were crimped and vacuum brazed at TRW using Gapasil No. 9 (Ga-Pd-Si) braze alloy.* After initial process development problems, good flow and filletting was obtained, Figure 62. The nozzle assemblies were installed on several electrodes and exposed to the CDS environment for approximately 100 hours. The braze fillet was attacked preferentially along second phase particles, Figure 63. The braze on the water side of the crimp appeared to be slightly attacked at the exposed edge but otherwise intact. The nozzles showed no evidence of attack.

Weight Change Measurements

The metallic specimens were weighted before and after exposure to determine weight change. These data are shown in Table 16. In this Table, uniform corrosion rates are shown which were calculated from the weight change data. Note that the nickel and Inconel 601 samples pitted badly so that the uniform corrosion value given for these metals should not be used except for a qualitative comparison. The uniform corrosion rate for 316 CRES was determined from specimens which showed little or no pitting attack. The best resistance to attack was exhibited by titanium, Inconel 617, and Incoloy 825.

Electronic Corrosion Meter Data

Five electronic corrosion probes (Magna Corporation 21343/W40/8020 with 316 CRES elements) were installed on the north side of the north CDS unit. The data taken are shown in Table 17. Figure 64 shows the Corrosometer probes used in the test.

*Western Gold and Platinum, Inc.

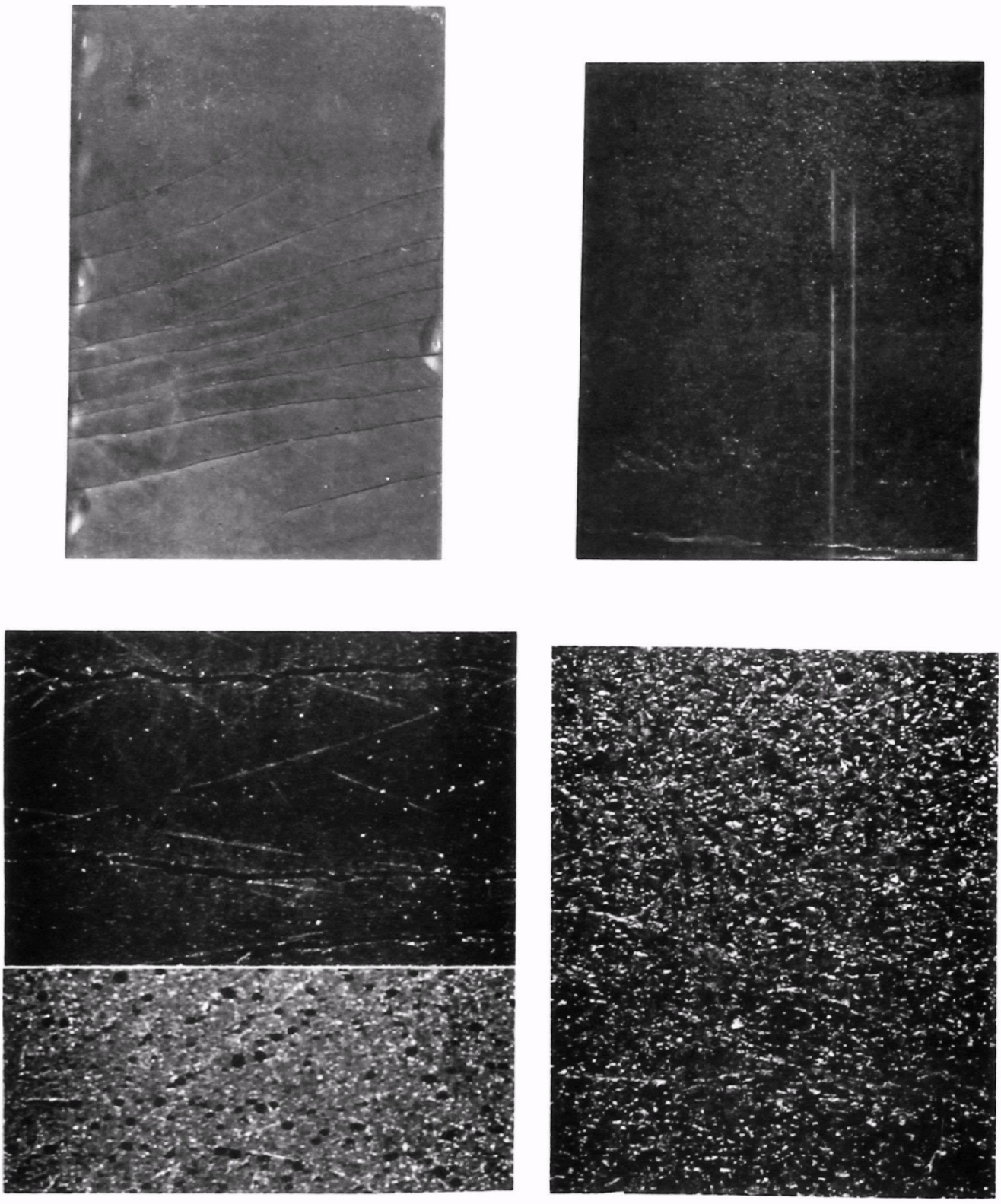

Figure 60. Coupons ASH800-28 furan (left) and ASH800FR-20 flame retarded furan. Surface cracking, checking and pitting. Lower casing.

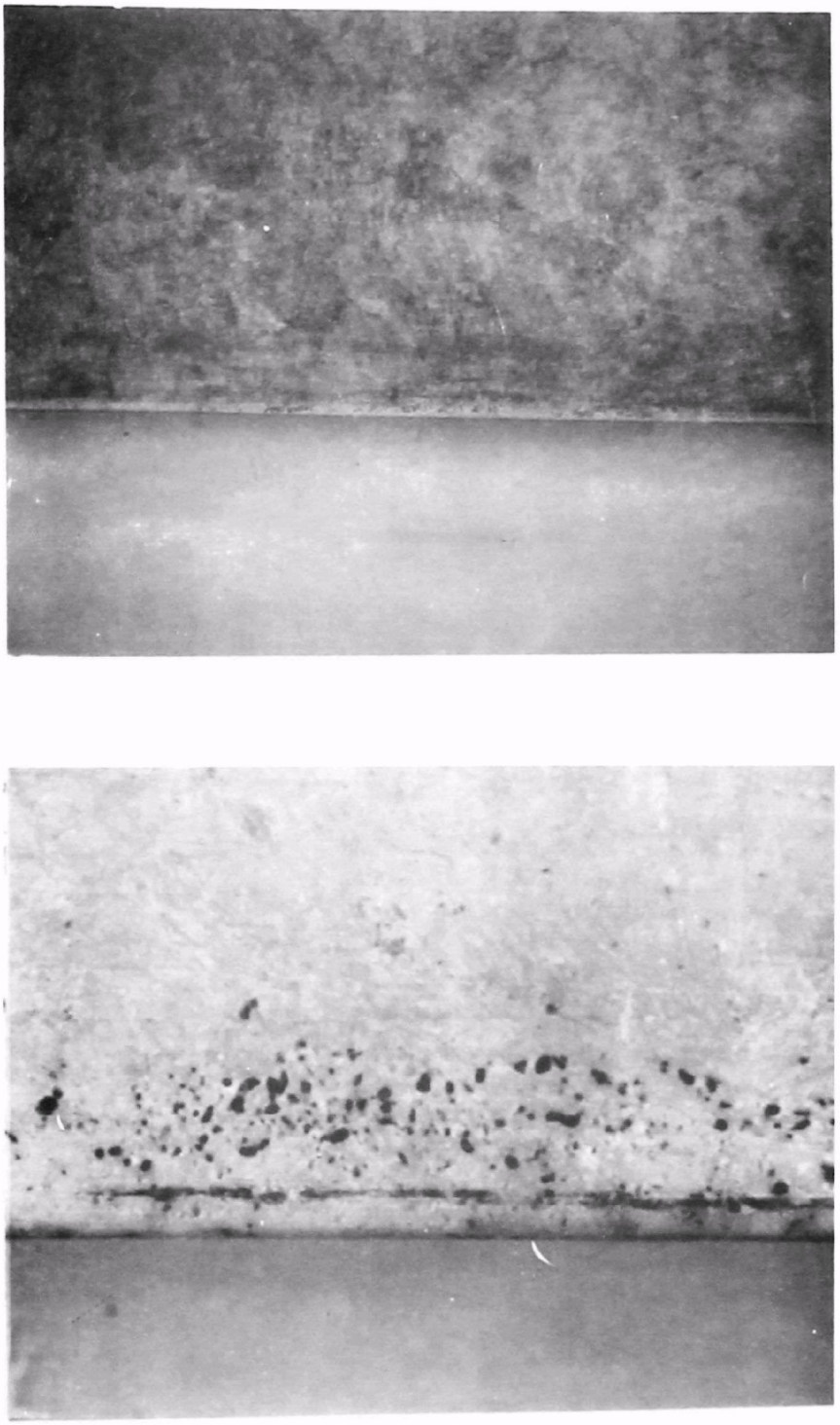

Figure 61. Coupon HY132 polybutadiene. Some pitting attack at edge. Lower casing.

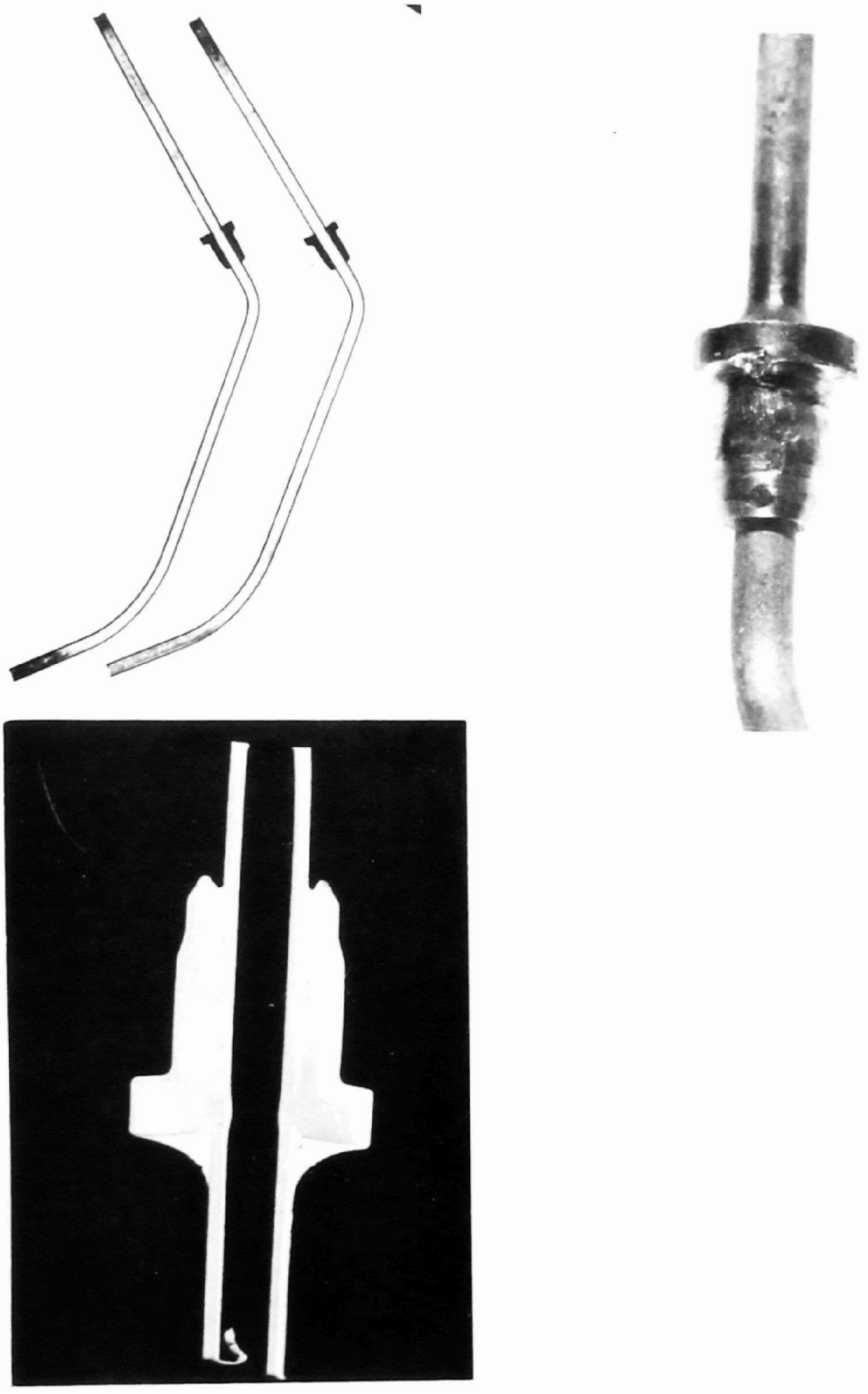

Figure 62. Nozzle/grommet joints. Crimped only (left) and brazed (right).

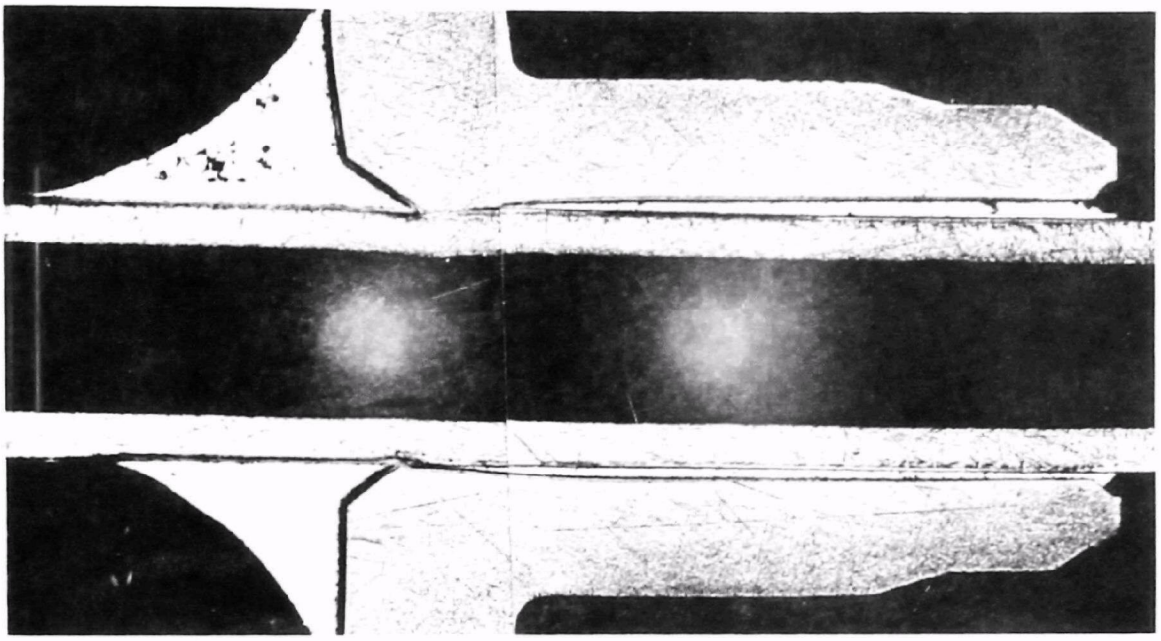

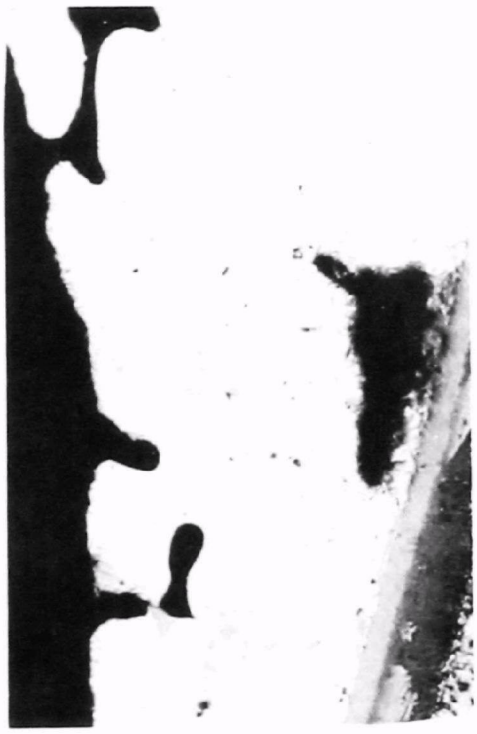

Figure 63. Appearance of brazed joint after exposure of 100 hours. Brazed fillet attacked along second phase. Joint inboard (toward the header) of crimp unaffected.

TABLE 16. WEIGHT CHANGE OF METALLIC TEST COUPONS

MATERIAL TESTING	LOWER CASING			UPPER CASING		
	NO. OF COUPONS	AVE. WT. LOSS (g)	UNIFORM CORROSION RATE (mmpy)	NO. OF COUPONS	AVE. WT. LOSS (g)	UNIFORM CORROSION RATE (mmpy)
316 CRES	5	0.2950	0.135	2	0.5361	0.241
Nickel	3 (P)	12.1532	5.790	1 (P)	9.0497	3.683 (P)
Inconel 601	2 (P)	1.1154	0.500	1 (P)	0.9463	0.201 (P)
Inconel 617	2	0.3828	0.165	1	0.7537	0.328
Incoloy 825	2	0.1798	0.079	1	0.5064	0.226
Hastelloy B	1	3.397	1.186	-	-	-
Hastelloy C-4	1	0.1807	0.061	1 (P)	1.6599	1.407 (P)
C.P. Titanium	2	0.0794	0.063	1	0.2329	0.188
Chemical Lead	2	0.3311	0.244	-	-	-

(P) Pitting attack - uniform corrosion rates should be used for qualitative comparison only.

TABLE 17. CORROSOMETER DATA

PROBE NO.	LOCATION	UNIFORM CORROSION RATE (mmpy)
1	A - CDS Inlet Duct	0.012
2	C - Lower Casing - East End	0.093
3	D - Lower Casing - West End, Above Baffles	0.309
4	L - Upper Casing - East End	0.041
6	K - Upper Casing - West End	0.038

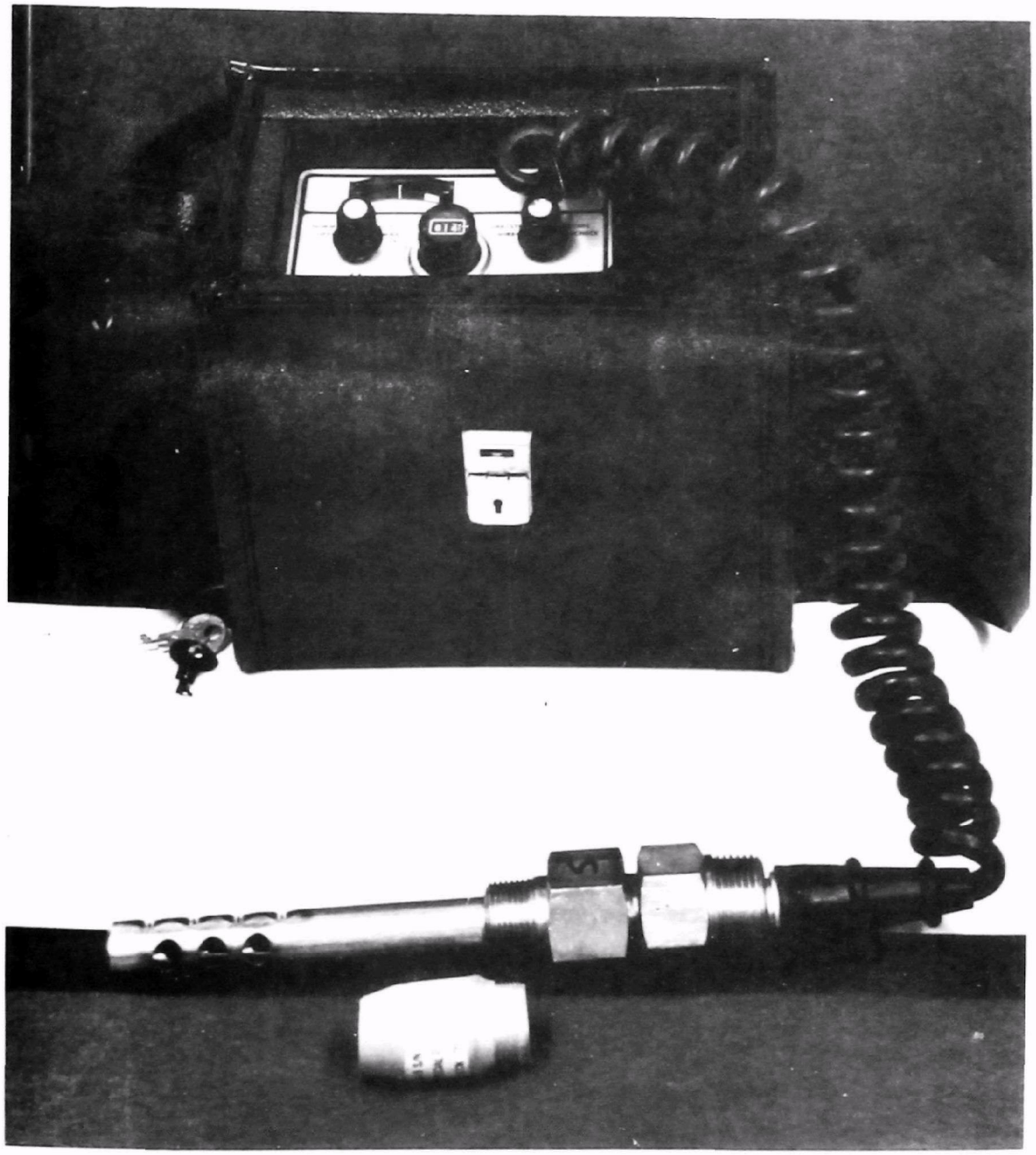

Figure 64. Electronic corrosion meter (Magna Corporation CK-3) and type of probe (2143/W40/8020) used for the in-process corrosion rate measurements.

Thermal/Chemical Environment

Inlet gas temperature for the north unit was recorded at the same time that Corrosometer readings were taken. The temperature probe located near port A indicated that the inlet gas temperature ranged from 175.5°C to 190.5°C. In order to assess the wall temperatures of different parts of the unit, a thermal profile was run by inserting probes into the Corrosometer ports in the lower casing and the stage area. In addition, upper casing wall temperature was taken at three points on the south side of the unit. The results are shown in Table 18.

Carbonaceous deposits were found on walls, doors, internal structures, baffles and test coupons. An analysis of the deposit indicates up to 1.7 weight percent chloride is present. When water is added to the deposit, the resulting solution exhibits a pH of between 1 and 2.

The coke gas stream contains C, SO_2, H_2S, O_2, NOx, CH_3, H_2, HCN, S, CO, CO_2, N_2 and possibly other hydrocarbons. Water reacts in the gas stream to form sulfuric acid and, to a lesser extent, carbonic acid, nitric acid and other corrosive fluids.

Wastewater and domestic feed water samples were analyzed to establish the chemistry before and during CDS operation. The data sheets are included in Appendix C. The key changes include:

a) The chloride content dropped from 60 ppm (domestic water) to about 25 ppm (wastewater).

b) The sulfate content increased from approximately 10 ppm to 220 to 286 ppm.

TABLE 18. WALL TEMPERATURES OF NORTH CDS UNIT

PORT	LOCATION	TEMPERATURE (°C)
A	Inlet Duct	142
B	Lower Casing-West End (Below Baffles)	136
C	Lower Casing-East End (Below Baffles)	84
D	Lower Casing-Midpoint (Above Baffles)	97
I	Collection Section-West End (Upper (Door #2))	50
F	West End (Lower (Door #2))	45
H	Midpoint (Middle (Door #5))	66
G	East End (Lower (Door #9))	53
-	Upper Casing-West End (Above Door #2)	68
-	Upper Casing-Midpoint (Above Door #4)	79
-	Upper Casing-East End (Above Door #9)	59

TABLE 19. SUMMARY OF MATERIALS PERFORMANCE

MATERIAL	EXCELLENT	GOOD	FAIR	POOR
		Lower Casing - Gas Stream		
Metals	Titanium C/P Ti - .2 Pd Ti - Code 12 Hastelloy C-4 Incoloy 825	Chemical Lead Inconel 617	316 CRES (P) Hastelloy B	304 CRES (P) Nickel (P) Inconel (I) 601
Coatings				Teflon (A) Kynar (A) Polyphenylene Sulfide (A) Epoxy (A) (T) Vinyl (A) (T) Alkyd (A) (T) Hypalon (A) (T) Neoprene (A) (T)
Liner			Neoprene (T)	
Reinforced and Filled Coatings				Ceilcote 252 (T) (C) Plasites: 4020 (T) (C) (A) 4030 (T) (C) 4092 (T) (C)

(continued)

TABLE 19 (continued)

MATERIAL	EXCELLENT	GOOD	FAIR	POOR
Lower Casing - Gas Stream				
Fiberglass Reinforced Plastic	Hystl 6793-132		Ashland 197/3 (T) (C) Ashland 800 (T) (C)	Ashland 7240 (T) (C) Ashland 72 (T) (C) ATLAC 382 (T) (C) ATLAC 711 (T) (C) ATLAC 580 (T) (C) Corralite 31-345 (T) (C)
Lower Casing - Walls				
Coatings				Hypalon (A) Neoprene (A)
Baffle Shims	Viton			
Upper Casing - Doors				
Coatings			Epoxy (A)	Alkyd (A) Vinyl (A)
Liner	Armalon Teflon/Glass Fabric			
Seals	Viton			

(continued)

TABLE 19 (continued)

MATERIAL	EXCELLENT	GOOD	FAIR	POOR
Electrode Headers				
Coatings			Epoxy (A)	Vinyl (A) Alkyd (A)
Sleeving	Vinyl Shrink Tubing			
Seals	Viton "O" Rings			
Upper Casing (Hood)				
Seal (Upper Casing Hood)	Neoprene			
Coatings				Hypalon (A) Neoprene (A) Vinyl (A) Alkyd (A) (T)
Upper Casing - Gas Stream				
Metals	Ti (C.P.) Ti - 0.2 Pd	Incoloy 825	Inconel 617 316 CRES	304 CRES (P) Nickel (P) Inconel 601 (I) Ti - Code 12 Hastelloy C

(continued)

TABLE 19 (continued)

MATERIAL	EXCELLENT	GOOD	FAIR	POOR
		Upper Casing - Gas Stream		
Coatings				Teflon (A) Polyphenylene Sulfide (A) Epoxy (A) (T) Vinyl (A) (T) Alkyd (A) (T)

Key: (P) Pitting corrosion attack
(I) Intergranular corrosion attack
(A) Adhesion failure
(T) Temperature induced attack
(C) Chemical attack

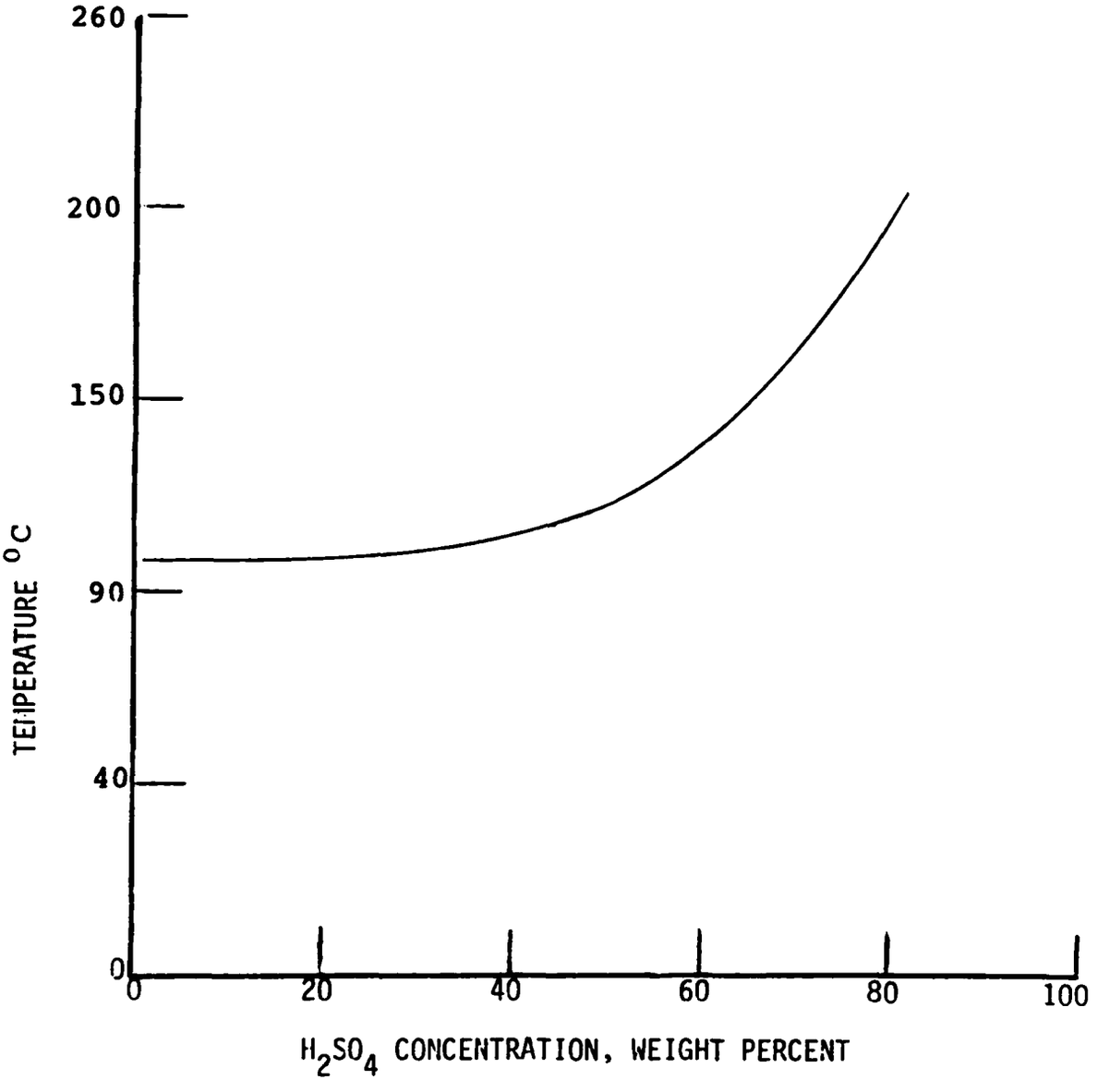

Figure 65. Boiling point of sulfuric acid in solution with water.

c) The pH decreased from 7.96 to 2.43 to 2.53.

d) The specific conductivity at 25°C increased from 290 micromhos/cm^3 to 1200 to 1400 micromhos/cm^3.

Equipment Life

As part of the materials evaluation task, the expected life of the existing 316 CRES unit is to be predicted. It must be understood that projecting long term performance on data collected over a relatively short period is risky. However, an attempt was made to project life making some assumptions as to the type of inspection and maintenance which would be required.

The behavior of the 316 CRES alloy as tested can be summarized as uniform corrosion rate ranging from 0.04 to 0.31 mmpy and a tendency to pit. The measured pit depths on 316 coupons were of order of 5.0×10^{-5} which, if a linear growth rate is assured, would result in pit growth rate of approximately 1 mmpy.

Two conditions must be considered; viz., (1) the thinning of the walls to a point where the structure is unsound, and (2) the perforation of the wall by local pitting causing gas flow disruption and emission of gas into the surrounding area. The time to the first condition can be estimated from uniform corrosion rate and the time for the second condition by a combination of uniform corrosion rate and pitting corrosion rate. Thus:

$$T_1 = \frac{t_i - t_s}{r_c}$$

$$T_2 = t_i/(r_c + r_p)$$

Where:

T_1 = time to reach minimum thickness required for strength (years)

T_2 = time to perforate wall (years)

t_s = minimum thickness required for strength (mm)

t_i = initial casing wall thickness (mm)

r_c = uniform corrosion rate (mm per year)

r_p = pitting corrosion rate (mm per year)

The initial wall thickness is 4.8 mm and the value of t_s is estimated as 2.0 mm. Assuming r_c equal to 0.30 mmpy and r_p equal to 1 mmpy, then:

T_1 = 9.3 years

T_2 = 3.6 years

Typically pitting corrosion rates vary from point to point within a structure and many samples are required to obtain a statistically meaningful average. Since the CDS configuration is such that only a relatively small number of coupons could be installed without disrupting the gas distribution and the equipment performance, the 1 mmpy rate is highly suspect. Using engineering judgment, it may be expected that some pits may grow two to three times faster than the measured rates so that a value of T_2 closer to 2 years would be more realistic.

Therefore, the anticipated behavior of the current structure is predicted as follows assuming no change in the design or process:

- 0 to 2 years: Little or no maintenance required. Periodic inspection recommended.
- 2 to 9 years: Local perforations in casing wall. Inspect on a periodic basis. Repair by welding doublers over perforated regions.
- 9 years: Some areas thinned to critical thickness. Inspect. Repair or replace structure as necessary.

SECTION 7

FLUE GAS STREAM CORROSIVES CONTROL

INTRODUCTION

The compound which is potentially the most corrosive in waste heat flue gas is gaseous sulfur dioxide. In searching for a way to neutralize the effects of the SO_2 and the resulting corrosion problem, it was determined that the most effective method would be to inject an additive to react with the SO_2 and then have the resulting particulate collected by the CDS. After careful analysis the Thermo-Chemical Mapping results, ammonia was chosen as the candidate additive.

Use of the CDS for gaseous SO_2 removal leads to several difficulties. These difficulties can be eliminated by converting the SO_2 to a solid phase prior to its entering the active cleaning volume of the CDS. This then allows the full particulate removal capability of the CDS to be utilized for SO_2 removal.

The limitations to be considered with respect to using the CDS for scrubbing gaseous phase SO_2 are:

(1) The CDS removal efficiency is limited by the gas phase surface absorption and diffusion rates within the charged drops.

(2) The total material removal will always be limited by the saturation solubility of SO_2 in the cleaning media.

(3) The outgoing waste water is acidic, thus creating potential corrosion problems in the exhaust gas ducting and waste water processing system.

The major task here was to determine if SO_2 could be reacted with moist ammonia to form solid phase $(NH_4)_2SO_4$ within the CDS. A successful demonstration of the ability to achieve the desired SO_2 reaction would then indicate the feasibility of using the CDS system for $(NH_4)_2SO_4$ particulate collection.

CONCLUSIONS AND RECOMMENDATIONS

The $NH_3 + SO_2$ reaction can remove essentially all the SO_2 from a gas stream with inlet concentrations of 500 ppm or less. A single CDS wet stage has demonstrated removal efficiencies as high as 70 percent for the particulate

reaction products at a velocity of 3.05 m/s (10 fps). Thus, a two-stage CDS should achieve better than 90 percent removal, and a four-stage unit better than 99 percent removal.

Without the NH_3 additive and operating in the corona only mode, which is essentially the operational mode for conventional electrostatic precipitators, resulted in essentially zero SO_2 removal. There is a slight removal of the corrosion causing SO_2 when the CDS is operated in the charged droplet mode.

APPROACH

The inlet gas stream consisted of ambient air mixed with 500 ppm reagent grade SO_2. The experimental approach was to inject gaseous reagent grade ammonia into the upstream inlet to the CDS.

Initially, it was thought that it would be necessary to add water vapor and corona to accelerate the NH_3/SO_2 reaction. The corona would assist the reaction indirectly by creating ozone. The resultant reaction would be as follows:

$$O_2 + \text{Corona} = 2O^{--}$$

$$O_2 + O \quad = O_3$$

$$2(NH_3) + SO_2 + H_2O + O_3 - (NH_4)_2SO_4 + O_2 \qquad (1)$$

It should also be possible to get more direct action:

$$2(HN_3) + SO_2 + H_2O + O^{--} = (NH_4)_2\ SO_4 \qquad (2)$$

During the tests it was observed that the SO_2 could be removed via other chemical reactions and without the need for a corona. This will be discussed later in more detail.

Figure 66 is a schematic of the test apparatus. The CDS duct was operated at a slightly negative pressure with the gas flow maintained by an exhaust blower located downstream of the scrubber. The gas flowed vertically downward through the CDS. An in-line damper was used to control the gas flow velocity. The exhaust gas was vented into the building exhaust system.

The CDS could be operated in any one of three modes: single wet stage, single dry corona stage or corona stage plus single wet stage. Gas injection and sampling capabilities were proved by horizontal 9.5 mm (0.375 in.) diameter perforated tubes extending across the duct inlet section. SO_2 concentrations were measured at the scrubber outlet using an Environmetrics series N5-200 SO_2/Nitrogen Oxide Analyzer. Ammonia injection rates were monitored with a conventional rotameter.

An argon laser and an off-axis photodetector located at the exit of the CDS cleaning section were used to observe particulate formation due to the SO_2+NH_3 reaction and removal due to CDS operation. The scattered intensity was displayed on a strip chart recorder connected to the photodetector output.

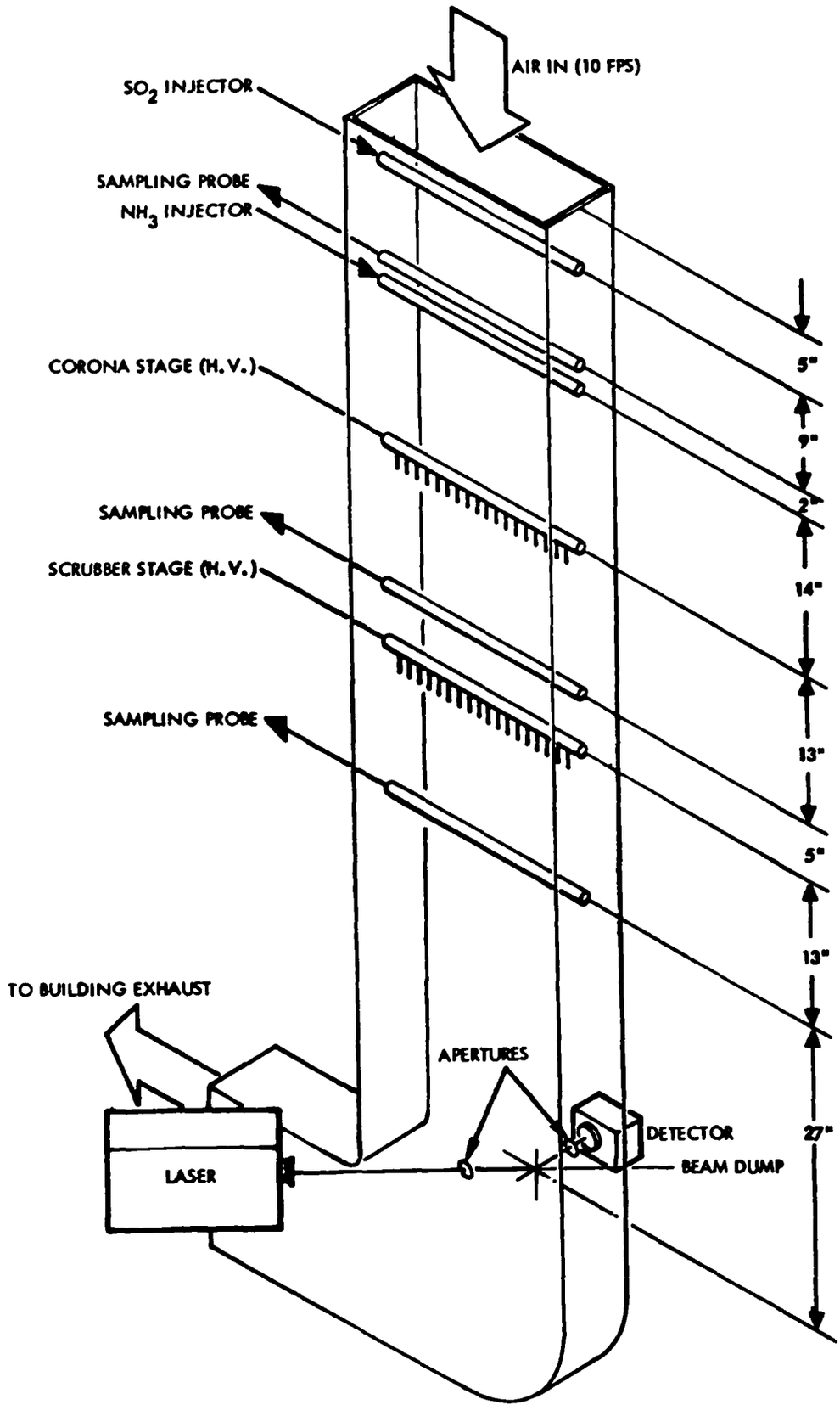

Figure 66. Experimental equipment arrangement.

The detector output was assumed to be proportional to the particle concentration at the CDS exit. Strictly speaking, this is only true if the particle sizes remain constant for all conditions and if there is negligible absorption in the scattering volume. However, the proportionality assumption is valid for the present purpose of providing an initial feasibility demonstration.

RESULTS AND DISCUSSIONS

Gas Phase SO_2 Removal

The purpose of the gas phase work was to provide a baseline set of pure gas phase SO_2 CDS operational data for comparison with later measurements with NH_3 additive. Complete mixing of the SO_2 with the inlet air did not occur until after the mixture had passed through the CDS. For this reason efficiencies were based on the outlet sampling station readings where the SO_2 concentrations were correlated with the inlet rotometer settings. The removal efficiencies were calculated from the ratios of outlet concentrations for the CDS on vs CDS off.

Table 20 summarizes the observations for the three CDS operating modes. It can be seen that the SO_2 removal fractions were of the order of or less than the probable errors in reading the total SO_2 concentration. The probable error in these cases were estimated based on the reproducibility of the SO_2 analyzer readings over the time span of the measurements. Generally, any given set of measurements would last on the order of one hour, the driving factor being the approximately 20 minute equilibration time constant of the analyzer.

Table 20 indicates a slight removal of SO_2 when the CDS operated in the charged droplet mode. Operating the CDS in the corona only mode, which is essentially the operational mode for conventional electrostatic precipitators, resulted in essentially zero removal.

Since the major removal mechanism during normal CDS operation is SO_2 absorption through the surfaces of the charged droplets, it would be expected that significant absorption also occurs on the wet collector plates. In order to confirm this mechanism, downstream SO_2 concentrations were compared for wet and dry collector plates with the CDS turned off for both cases. The results are shown in Table 21.

It is apparent from Table 21 that SO_2 absorption into the wet surfaces did occur. The magnitude of the observed effect was diminished by the fact that significant drying occurred during the 20 minute equilibration time required for the SO_2 analyzer.

Particle Formation Due to NH_3 Injection

Ammonia was injected into the SO_2 laden gas stream to produce a range of NH_3 molar concentrations varying from 1:5 to 4:1 corresponding to a range of one-tenth to twice stoichiometry for reactions (1) and (2). The SO_2 inlet

TABLE 20. CDS REMOVAL EFFICIENCY FOR GAS PHASE SO_2
(32 KV ELECTRODE VOLTAGE 3 m/s (10 fps)
GAS FLOW VELOCITY)

CONCENTRATION RANGE	LOW		MEDIUM		HIGH	
OPERATING MODE	SO_2 (ppm)	EFF. (%)	SO_2 (ppm)	EFF. (%)	SO_2 (ppm)	EFF. (%)
CDS Off	153 ±10		380 ±60		786 ±100	
Corona Only	147 ±10	4	383 ±60	3	761 ±100	3
Water Only	127 ±10	17	309 ±60	19	736 ±100	6
Corona + Water	132 ±10	14	325 ±60	14	736 ±100	6

TABLE 21. SO_2 THROUGHPUT COMPARISON FOR WET AND DRY
COLLECTOR PLATES (CDS TURNED OFF, 3 m/s (10 fps)
DUCT FLOW VELOCITY)

SCRUBBER CONDITION	DRY	WET	DRY	WET	DRY
SO_2 Throughput (ppm)	427	406	427	412	427

concentration was 1000 ppm. The gas velocity was 3 m/s (10 fps). Relative particulate concentrations at the scrubber exit were measured by the laser scattering system.

Figure 67 shows the scattered laser intensity as a function of NH_3 concentration. The apparent particle concentration decreased sharply below 2.1 molar ratio and tended to level off above 1:1. This is in good agreement with the 2:1 NH_3 to SO_2 ratio required for reaction.

SO_2 Removal By Reaction With NH_3

NH_3 was injected at molar ratios of 3.4:1, 1.7:1 and 1.2:1. In all three cases there was a heavy particulate fallout and the SO_2 concentration at the outlet would fall below the sensitivity of the SO_2 detector (5 ppm) 1 percent of the injected fraction. These measurements were carried out at nominal

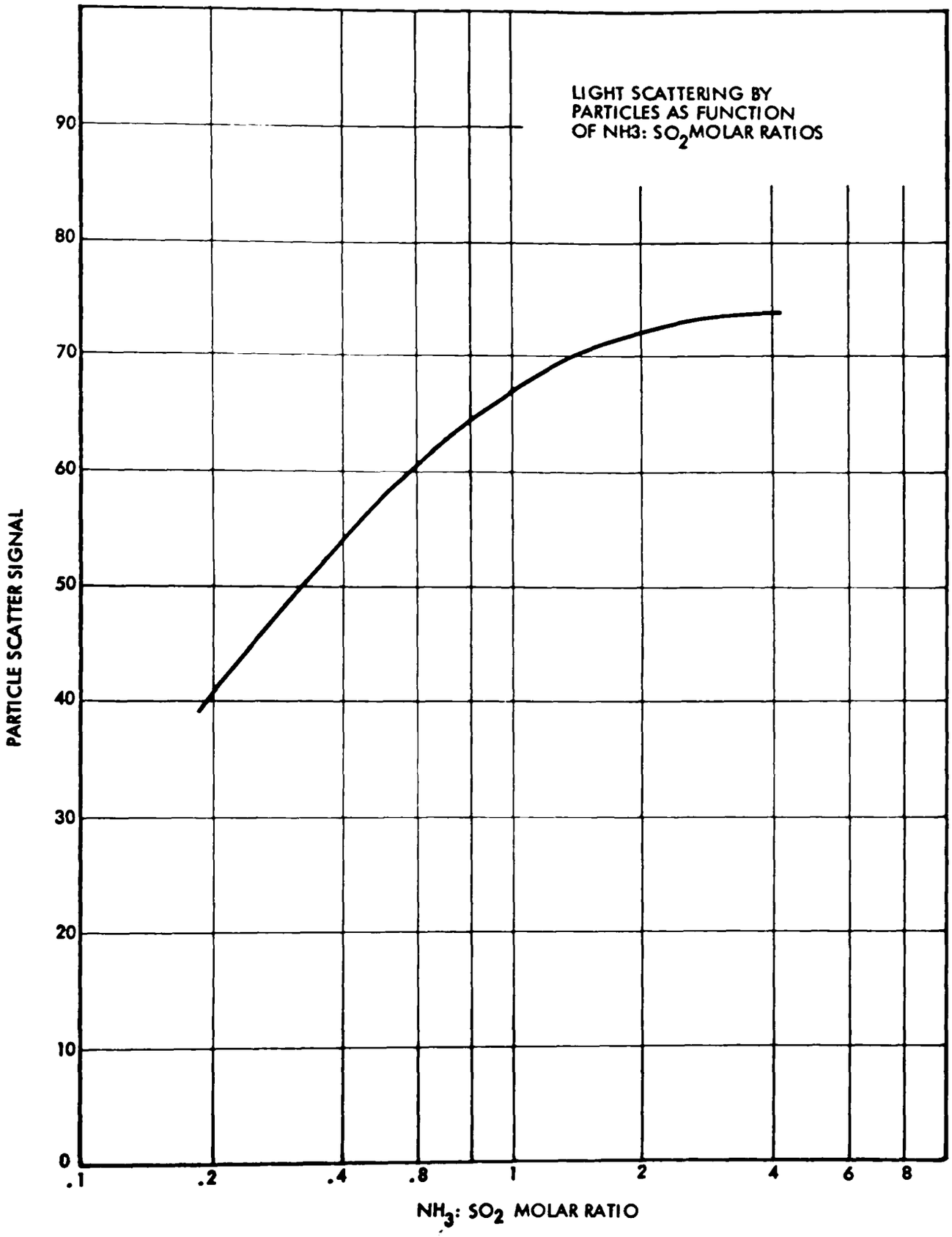

Figure 67. Particulate formation due to addition of NH_3.

500 ppm inlet SO_2 concentration. The virtual elimination of the SO_2 at even the 1:1 molar ratio is surprising since this corresponds to 1/2 of stoichimetry for the formation of $(NH_3)_2SO_4$. It is possible that SO_2 removal also occurred via the following reactions:

$$2\ SO_2 + O_2 = 2\ SO_3$$
$$NH_3 + H_2O + SO_3 = (NH_4)\ H\ SO_4 \qquad (3)$$

or

$$2\ SO_2 + O_2 + 3\ HN_3 + 2H_2O = (NH_4)_2SO_4 + (NH_4)\ HSO_4 \qquad (4)$$

These reactions would reduce the NH_3 required as compared with reactions (1) and (2). Another factor is that the porous plug of the SO_2 detector had a tendency to clog at the high particle concentrations that were created and this may have caused the instrument to read erratically low.

The net observed effect may have been due to SO_2 precipitation through reactions (3) and (4) coupled with clogging of the porous plug in the SO_2 analyzer.

It was possible to achieve better than 99 percent SO_2 removal even when no corona was employed. This indicates that either the bisulphate reaction (3) or the sulphate reaction (5) shown below occurred.

$$O_2 + SO_2 = SO_3$$
$$SO_3 + H_2O = H_2SO_4 \qquad (5)$$
$$H_2SO_4 + 2\ NH_3 = (NH_4)_2SO_4$$

Figure 68 shows the scatter signal for various operating modes of the CDS. For low molar ratios turning on either the corona stage only or water stage only increased the particle concentration over that observed with the CDS. Apparently the effect of the enhanced reaction rate due to the corona and injected water was greater than that due to particle removal by the CDS.

Once the corona stage was on, turning on the water stage could decrease the scattered signal appreciably, indicating net decreases of 30 to 70 percent in the particle concentration. The true removal efficiencies were probably higher. However, the experimental arrangement could not separate out the effect of enhancing the primary chemical reaction. Since this effect would always decrease the apparent removal efficiency, the highest efficiency observed is best representative of the true CDS capability, i.e., 70 percent removal per stage.

To summarize, it has been demonstrated that the HN_3 - SO_2 reaction can remove essentially all the SO_2 from an air duct with inlet concentrations in the 500 ppm range. A single CDS wet stage has demonstrated removal

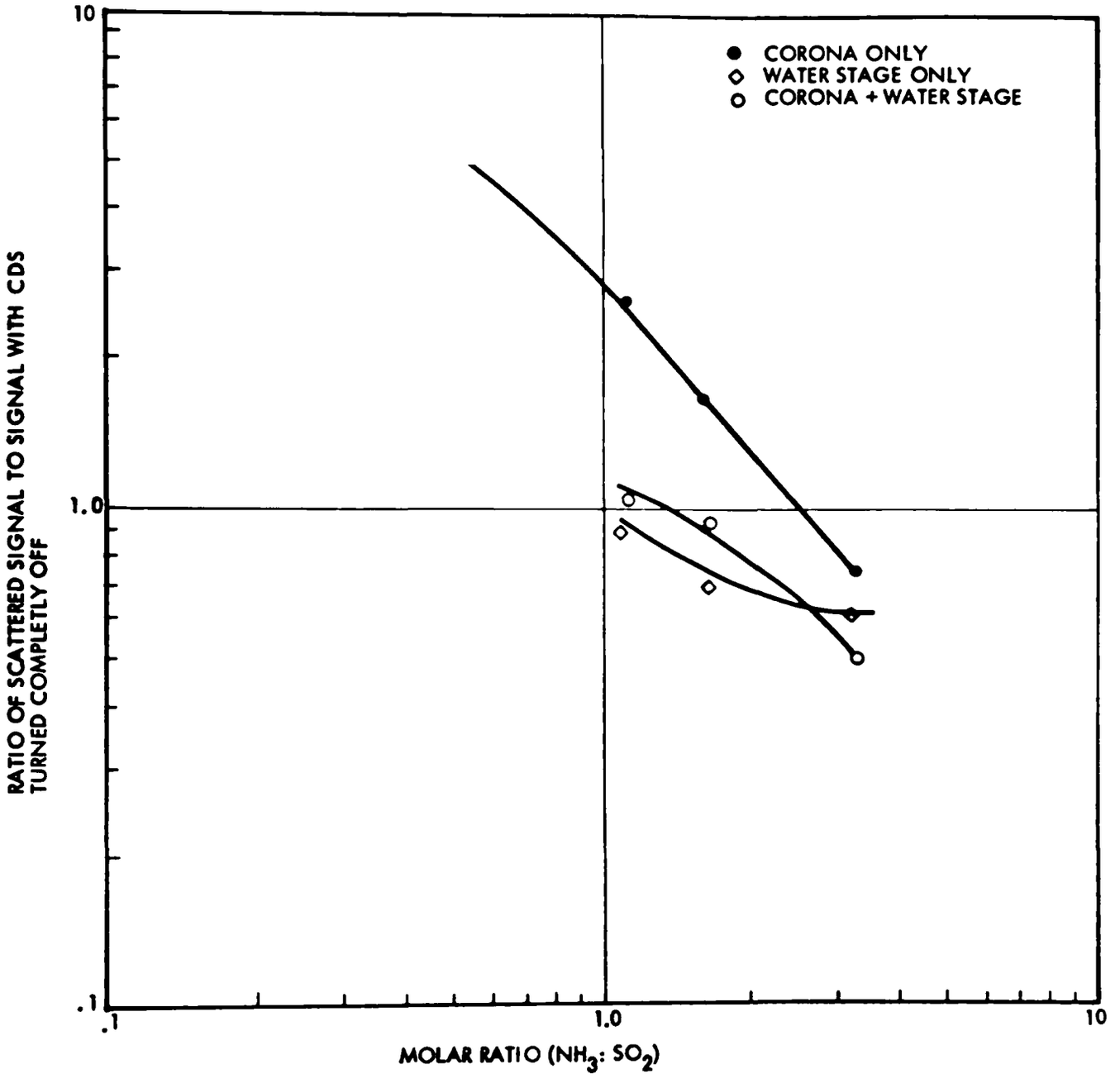

Figure 68. CDS particulate throughput for various operating modes and different NH_3:SO_2 molar ratios (3 m/s (10 fps) duct velocity, 500 ppm SO_2 inlet)

efficiencies as high as 70 percent for particulate reaction products at 3 m/s (10 fps) duct velocity. Thus, a 2 stage CDS should achieve better than 90 percent removal, and 4 stages better than 99 percent removal.

SECTION 8

ELECTRICAL SPARK QUENCHING

INTRODUCTION

When the Charged Droplet Scrubber was operated in a coke oven waste heat environment, some of the electrode nozzles were severely damaged during a relatively short exposure period. Some of the damage could be attributed to chemical attack, but the majority appeared to be the result of electrical errosion.

The principles of operation of the Charged Droplet Scrubber dictate that a direct current power source with minimum ripple be used to attain maximum droplet generation efficiency. To attain the low ripple, the CDS utilized high voltage filter capacitors. In addition, an R-C circuit is also required to facilitate arc quenching. All this additional capacitance provides a large energy reservoir which is discharged into each arc resulting in excessive nozzle wear.

In an effort to improve arc detection and limit discharge energy levels, an investigative program was initiated to explore alternative methods of control. Figure 69 presents the Pre and Post investigation CDS sparks sensing and electrical power configuration diagrams.

CONCLUSIONS

As the result of the investigative program, it has been concluded that:

1) The installation of a hard line spark sensing system which directly detects sparks, manifested by abrupt changes in electrode voltage, will significantly improve the reliability of the high voltage control system.

2) The removal of the high voltage capacitors from the arc quench R-C circuit will reduce the total energy available to an arc, but at the cost of lower particulate collecting efficiency resulting from a lower average electrode voltage. This reduction is caused by the increased ripple.

3) Sustained arcs and hence nozzle damage can be reduced by modifications to the control system. The modification will extend that power off-time that occurs in response to the control circuit cut-back command from the spark sensing system. However, this

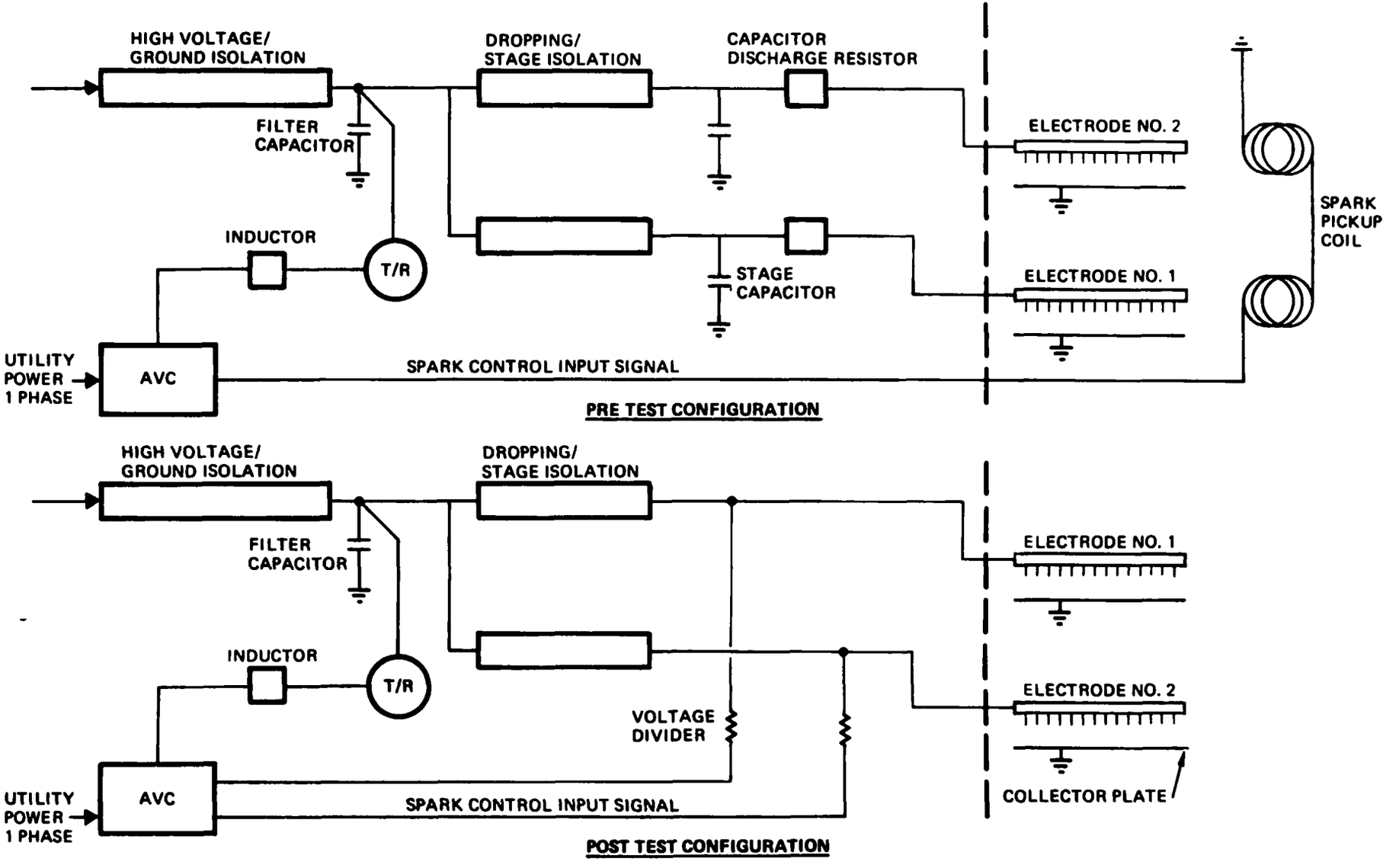

Figure 69. Charged droplet scrubber spark sensing and electrical power diagram.

also tends to reduce particulate scrubbing efficiency, although to a slight degree, because it reduces the overall on-time of the system.

4) Individual high voltage power supplies and controls sets for each stage will significantly increase system overall reliability and performance. The individual supplies will permit each stage controller to adjust the electrode voltage level for that stage without effecting the others. This would tend to allow the stages exposed to the high particulate concentrations to operate at a lower voltage while permitting the downstream stages to operate at their maximum voltage.

5) Although modification to the existing electrical power supply and control design can improve reliability and performance, the damaging effects of the filter capacitor discharge cannot be totally eliminated unless the ripple can be reduced by a means other than capacitance.

RECOMMENDATIONS

1) An alternate ripple control method should be investigated for the Charged Droplet Scrubber application. The potential benefit would be an increase in collection efficiency as the result of a higher average voltage and an increase in equipment life.

2) Individual power sets should be provided for each electrode stage for the purpose of improving system performance and reliability.

3) Replace the present design pickup coil type spark detection system with a design which directly senses abrupt voltage changes (sparks) through a voltage divider.

APPROACH

Spark Sensing

The approach taken to improve the reliability and durability of the spark sensing system was to replace the magnetically coupled coil system with one which was hardline coupled through a voltage divider. This system would have two advantages; 1) it is hardlined and therefore not susceptible to spurious electromagnetic influences, and 2) it can be placed in a location away from the hostile environment of the flue gases.

Arc Quenching

The quenching of an arc is accomplished by inhibiting current flow to the arc site. Therefore, it was postulated that this could be accomplished by modifying the automatic voltage control unit (AVC) installed as original equipment. Specifically, the Recovery Slope Control circuit would be modified such that, the power off-time would be extended for a sufficient duration that would allow the dissipation of the ionized gas surrounding the arc. If

successful, this would allow the removal of the high voltage capacitors which are presently utilized in the R-C arc quenching circuitry.

DESCRIPTION OF EXISTING SYSTEM

Spark Sensing System

The spark sensing system installed on the Charged Droplet Scrubber as original equipment consisted of a three turn wire coil located within the upper casing of the CDS and running parallel to the longitudinal axis of each stage header, Figure 70. The coil of each stage is, in turn, connected in series with the other stages and thereby provides a common signal to the spark rate control system. The coil senses the sparking occurring within the gas cleaning section of the equipment and provides a microvolt output. This signal, in turn, is amplified and used as the input to the automatic voltage controller logic circuit.

In-service experience with the coil sensing system has uncovered two significant drawbacks. Because of its antenna like characteristics it is susceptible to spurious inputs and the location requirements necessitates exposure to an extremely hostile environment with respect to temperature, moisture and corrosives.

Arc Quenching Circuit

The automatic voltage control system controls the electrode voltage using discrete input signals from the spark sensing system. However, if the frequency of sparking is sufficiently high as to appear as a steady state condition, the controller will only respond (cut-back) to the initial discharge transient. Under a constant arc condition, the controller only provides a current limiting function. Therefore, an R-C circuit is utilized to delay stage recharging, Figure 71.

This delay allows the column of ionized gas created by the arc to dissipate and minimize the possibility of a low voltage reignition.

To minimize the resistance between the transformer and electrode and still attain the necessary time constant, an additional 0.15 microfarad capacitance was required. This additional capacitance had a devastating effect on electrode nozzle wear and as a result severely impacted the equipment maintenance requirements.

DISCUSSION

Spark Sensing

Rather than install additional circuitry between the high voltage electrical compartment and the AVC, the existing voltage divider and associated wiring which is currently used for monitoring stage voltages would be utilized to carry the input signal to the spark sensing circuitry.

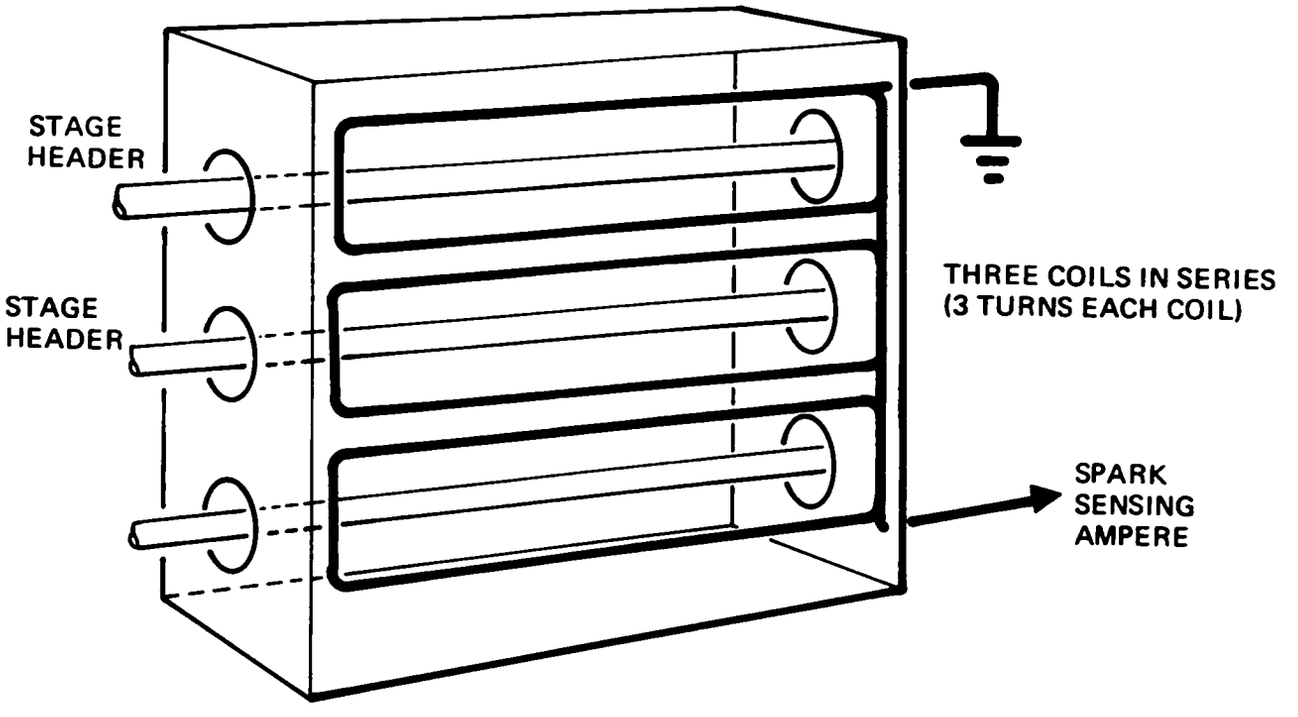

Figure 70. Spark sensing coil.

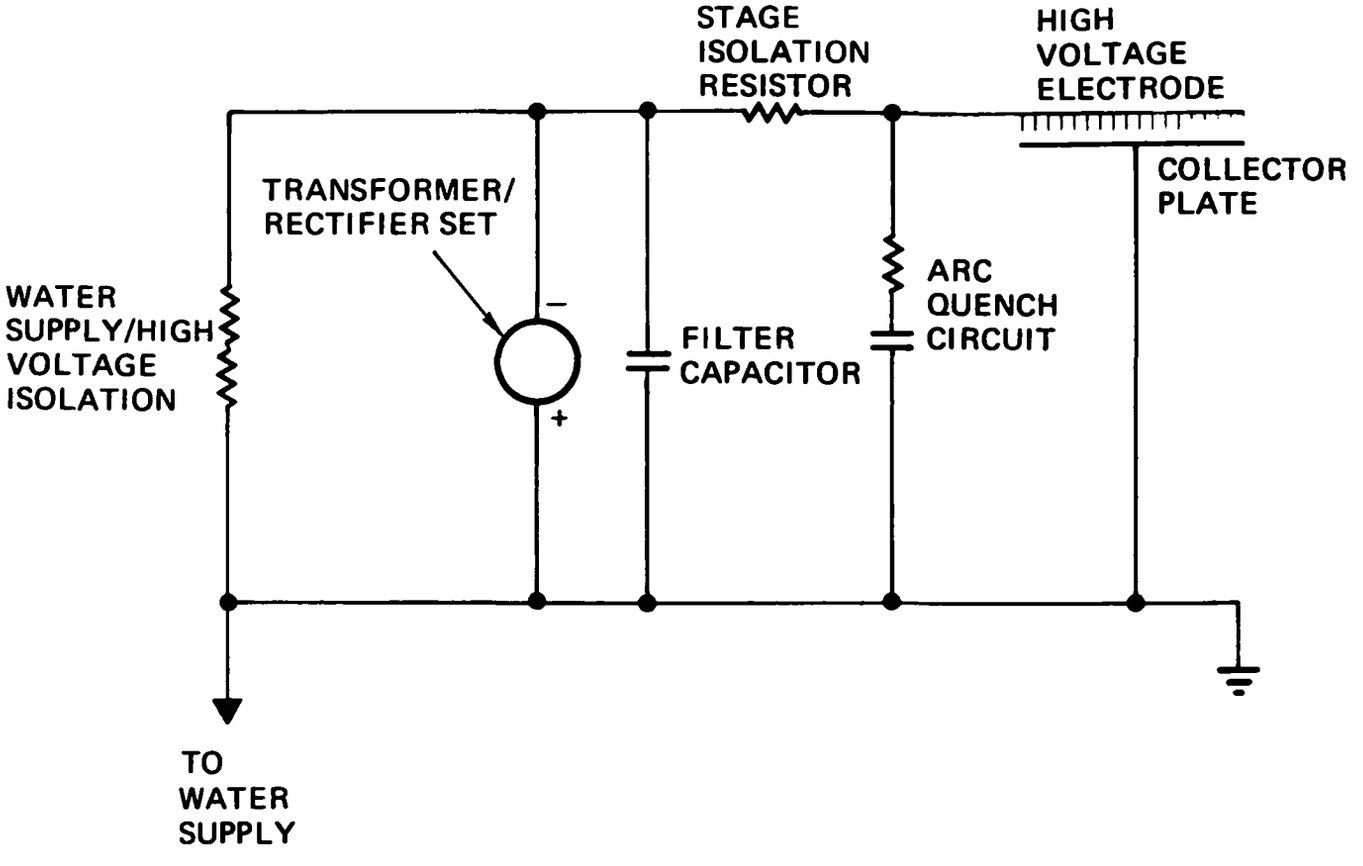

Figure 71. CDS electrical power schematic.

The signal conditioning circuitry consists of an audio amplifier, an impedance matching transformer and a blocking diode, for each electrode stage, Figure 72. Since the CDS system utilized in the development test program incorporated a common high voltage power supply design for each two stages, it is necessary that the controller responses to sparking on either or both of the two stages. Therefore, the spark signal from each individual stage must be fed in parallel, into the common controller logic circuit. For this reason the blocking diodes are used to isolate the individual sensing circuits.

Two dual channel spark sensing systems were fabricated and installed on the Charged Droplet Scrubber unit that was the subject of the redevelopment program. The test instrumentation verified that the sensing system detected all sparks and the control logic responded to all resulting input signals. The system operated over a two month period without a failure.

Arc Quenching

Initially the capacitors of each electrode stage R-C circuit were removed from the system. The change resulted in a drop of 4 KV in the average stage voltage. In addition, the frequency of sustained (lock-on) arcs increased substantially. Adjustment of existing Set-Back and Recovery-Slope controls had little effect on the frequency of lock-on arcs. The reduction in the average stage voltage was a result of a significant increase in the ripple amplitude. Although there exists an 0.075 μf capacitor in parallel with the transformer output specifically for filtering purposes, the capacitors connected to each stage perform an additional filtering function. The stage voltage ripple can possibly be reduced by increasing the high voltage filter capacitance of the transformer output or by increasing the primary circuit inductance.

The filter capacitance was increased to 0.15 μf. This resulted in a 2.5 KV increase in stage voltage. However, the energy discharged through the arc is increased substantially since; the increase is directly proportioned to the capacitance increase. The result would mean an increase in arc damage rather than a decrease. In addition, this configuration tends to decrease the stage-to-stage isolation. Although the stage isolation resistor is still in the circuit, a spark in one stage causes the common filter capacitor to discharge and thereby drop the supply voltage. The sustained arcing can be prevented by modifying the controller logic, but at the cost of a substantial increase stage off-time.

An alternate approach to lowering ripple was to increase the primary impedance. The additional impedance would increase the thyrister firing angle and result in a lower ripple and hence, allow a high average voltage to be attained at the electrodes.

The impedance was increased by the addition of a 2 mH inductor. With this addition, it was determined that the system was essentially inductance current limited. The addition of 1 mH resulted in a 2 KV increase in stage voltage. Table 22 presents a tabulation of the configurations tested and the resulting electrical characteristics. Figure 73 presents photographs of the resulting current and voltage waveforms.

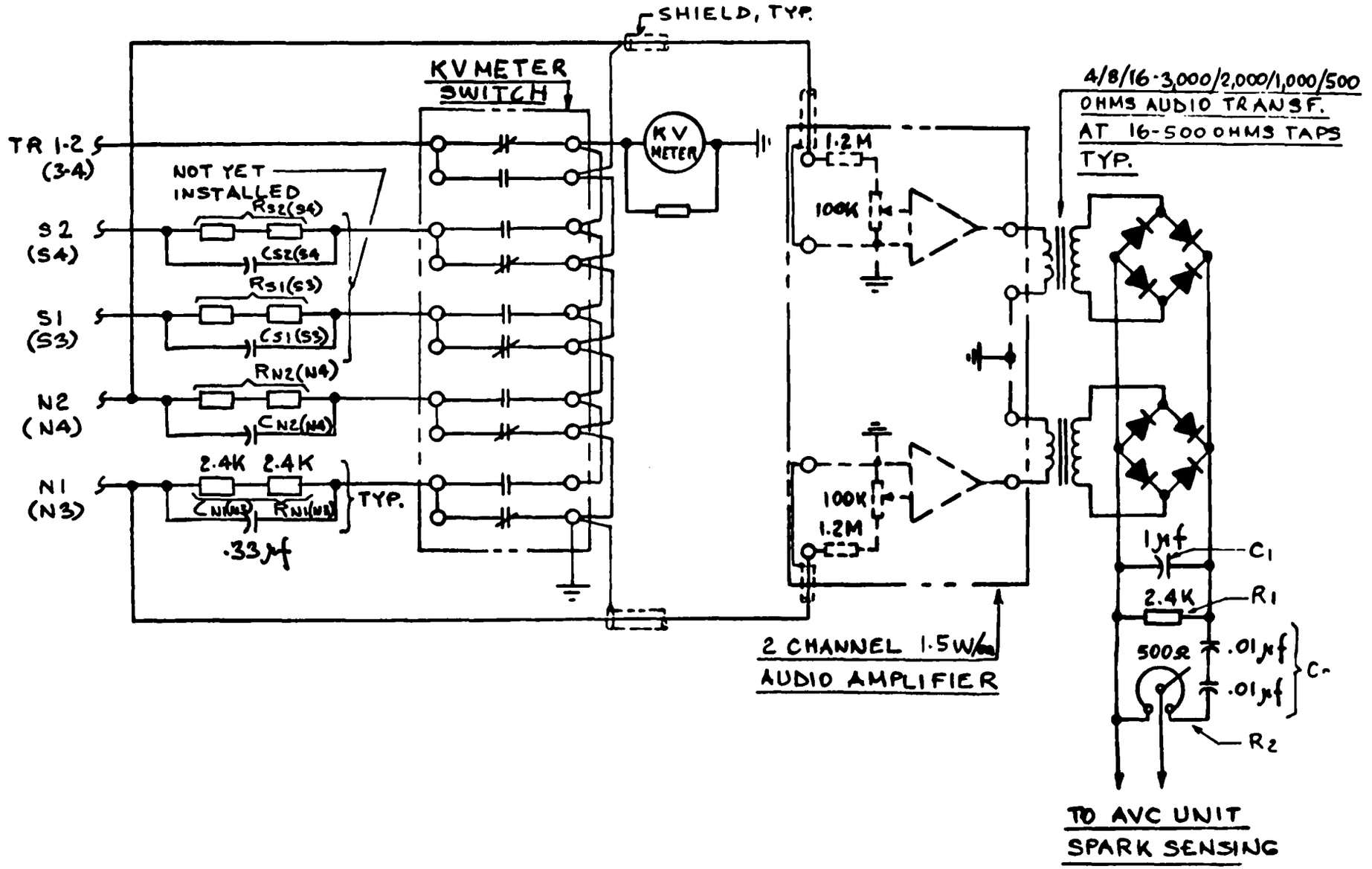

Figure 72. Charged droplet scrubber stage voltage sensed spark sensing circuit

TABLE 22. CDS PRIMARY IMPEDANCE ADDITION TEST TABLE

TEST NO.	AC		DC				SPARKS PER MIN.	LEAKAGE mAMPS	ADDED PRIMARY IMPEDANCE IN MH	REMARKS
	AMPS	VOLTS	mAMPS	T-R KV	3N KV	4N KV				
1	55	275	245	53	32.5	31.5	0	15.0	0	Photo #1, Note 2, Load Bank off.
2	104	263	242	52.5	32.5	31.0	0	14.5	0	Photo #2, Note 1, Load Bank on.
3	106	281	250	53	32.5	31.3	0	14.5	1	Photo #3, Load Bank on.
4	106	281	250	53	32.5	31.3	0	14.5	1	Photo #4, Notes 3&4, Load Bank on.
5	106	298	250	53.3	32.5	31.5	0	14.5	2	Photo Nos 5, 6 & 7, Note 5, Load Bank on.
6	106	308	250	53.8	32.5	31.5	0	14.5	3	Photo Nos 8&9, Note 6, Load Bank on.
7	50	312	240	53	32.5	31.5	0	14.0	3	Photo Nos 10&11, Load Bank off.

NOTES:

(1) In 'auto' mode stage 2N is at 33.5 KV approx.
(2) System on old spark sensing coil for this test only.
(3) Added 4.8K resistor on T-R set KV bleed line to permit photographing T-R set KV waveform.
(4) In 'auto' mode stage 3N is 35.0 KV approx.
(5) Increased current limit setting on AVC unit circuit card A2. This had very little effect. System was essentially current limited by primary inductance.
(6) Maximum voltage on stage 3N, in 'auto' and 'manual' mode, 36.5 KV.
(7) System restored to original, standard condition, except sensing resistor on T-R Set bleed line is left in.

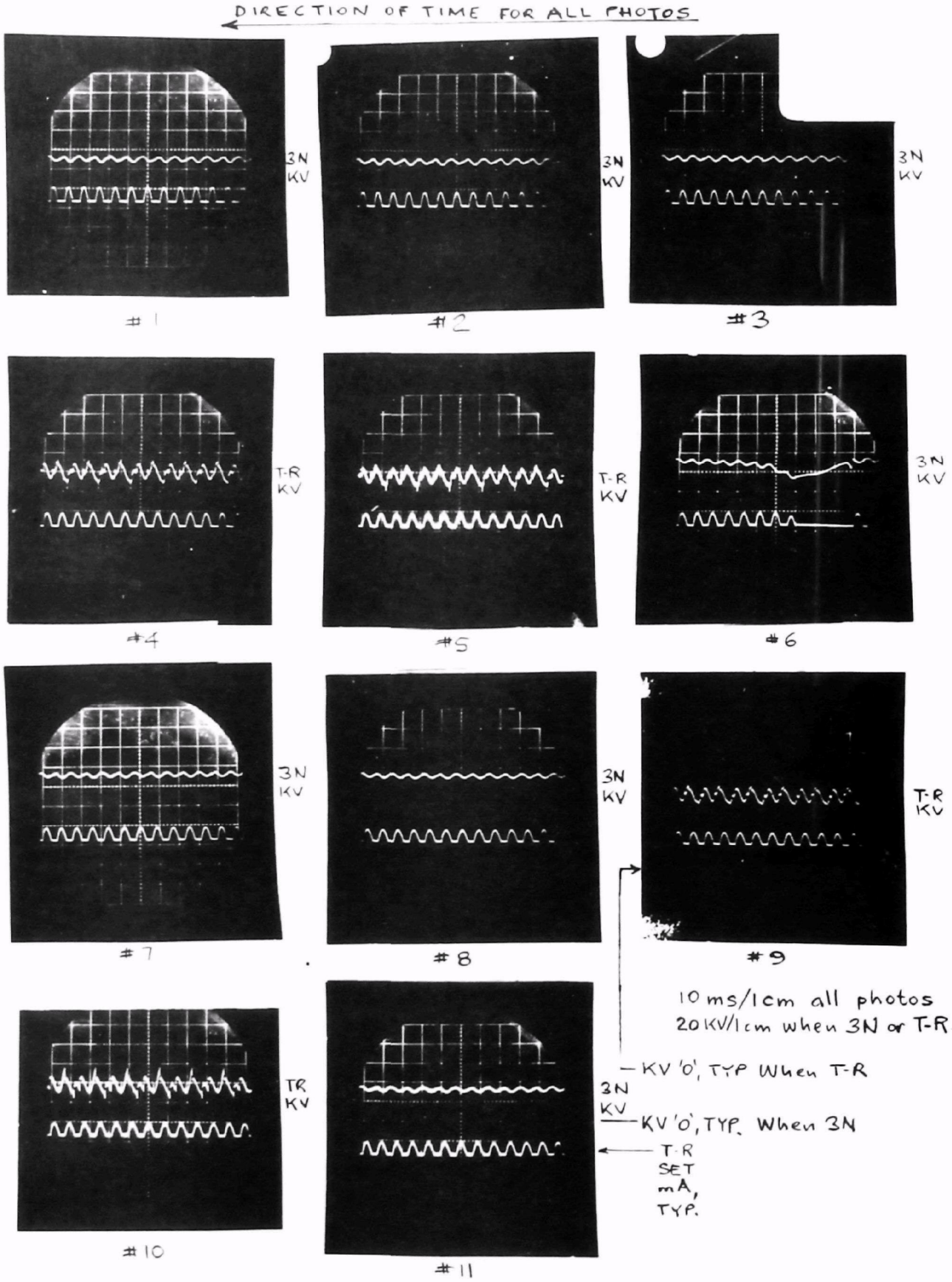

Figure 73. Oscilloscope photos of CDS primary impedance addition test

It has been determined that the existing power supply and control design can be modified to reduce ripple and present sustained arcs, but at the expense of lower collection efficiency unless individual power supplies and controls are provided for each stage.

REFERENCES

1. Maddalone, R., and N. Garner. Process Measurement Procedures: Sulfuric Acid Emissions. TRW Document No. 28055-6004-RU-01, May 1977.

2. Annual Book of ASTM Standards, Part 23. D-1193-70, Standard Specification for Reagent Water. 1971, Pg. 196.

APPENDIX A

ELECTRICAL TEST DATA

TABLE A-1. KAISER CDS GAS TEST NON-UPSET CONDITION

TIME	INLET	OPACITY	1-2	1-2	1-2	KV		KV	LEAK	S/M	3-4	3-4	3-4	KV		KV	LEAK	S/M	REMARKS
	TEMP OF	%	ACA	ACV	DCMA	1	2	TR	MA		ACA	ACV	DCMA	3	4	TR	MA		
11:15 AM	-	17	74	200	145	30	30	43	10	100-150	85	228	180	32.5	31.5	49	11.5	100-200	
11:20	-	7.5	65	180	125	29.5	29.5	40	9.5	100-200	78	215	155	32.5	30.5	47	12	100-180	NOTE 5
11:25	370	6	60	175	105	29	29	39.5	8.5	100-180	65	195	108	30	29	44	10.5	75-250	
11:30	373	5.75	60	175	110	29	29	41	10	100-180	100	270	210	35	32	54	13	100-200	NOTE 6
11:35	353	14	80	210	160	30.5	31	46	10	100-150	100	265	215	34	32	55	13	100-225	
11:40	355	12	80	200	150	30.5	30.5	44	9.5	75-150	93	255	190	34	31.5	53	12	100-200	
11:45	358	10.5	65	180	115	29	29	41	9	100-150	77	215	160	32.5	31	47	11	100-200	NOTE 7
11:50	363	10.5	60	170	105	29	29	39	8.5	100-150	75	210	150	31	29.5	45	10	100-200	
11:55	367	10	55	160	100	28	28	39	8.5	100-150	60	150	100	30	29	40.5	10	100-175	
12:00 NOON	371	12.5	50	160	100	28	28	40	9	100-150	80	250	210	33	32.5	54	13	100-175	NOTE 8
12:05 PM	351	5	80	220	170	31	31	47	10	100-150	98	270	215	34.5	33	57	13.5	100-225	
12:10	353	5	70	190	140	30	30	44	9.5	100-175	90	250	200	34	31.5	53	12.5	150-250	
12:15	357	5	65	185	120	30	30	41	9	75-175	80	225	165	32.5	31	48	11.5	100-225	
12:20	TEST 361±8	STOP 9.3±3.9													30.7±1.8				

NOTES:

1. System (including hood) washed prior to start of test.
2. Sequencer relay TDR 1 pulled to keep system on electrically during light loud.
3. Oven 22 open at both ends throughout test. Oven is relatively cool.
4. EED time at outlet, plus 4 minutes, at inlet, minus 2 minutes to that shown above.
5. Light white smoke from stack.
6. Stack clear-opacity jumped to 15% about time stages 3&4 were being read. About T+2 minutes.
7. Heavy sparking at door 7 on north side of north unit. Door 8 is relatively cool both sides. Stack clear.
8. Inlet temperature had dropped to 360°F at 12:02 PM.

ABBREVIATIONS:

1-2: Stages 1 & 2 : 3-4: Stages 3 & 4
ACA: Alternating Current Amperes
ACV: " " Voltage
DCMA: Direct " Multi-Amperes

TABLE A-2. KAISER CDS GAS TEST UPSET CONDITION

TIME	OPACITY	1-2	1-2	1-2	KV		KV	LEAK	S/M	3-4	3-4	3-4	KV		KV	LEAK	S/M	REMARKS
	% ·	ACA	ACV	DCMA	1	2	TR	MA		ACA	ACV	DCMA	3	4	TR	MA		
12:41:30 PM	55	74	200	175	30	30	44	10	100-150	100	285	240	35	33.5	53	14	100-250	
12:46:30	47	-	-	-	-	-	-	-	-	-	-	-	-	-	-	-	-	NOTE 3
12:51:30	38	60	174	60	29	29	40	10	100-150	75	220	160	33	31	44	12	100-200	NOTE 3
12:56:30	35	-	-	-	-	-	-	-	-	-	-	-	-	-	-	-	-	
01:01:30	19	85	225	180	32	32	46	11.5	100-200	105	290	260	35.5	34	58	15	100-200	NOTE 4
01:05:15	-	-	-	-	-	-	-	-	-	-	-	-	-	-	-	-	-	NOTE 5
01:06:30	10	-	-	-	-	-	-	-	-	-	-	-	-	-	-	-	-	
01:11:30	20	77	210	150	31	32	44	10.5	100-150	98	265	220	35	33	54	14.5	100-200	NOTE 6
01:16:30	41	75	210	150	31	30	43	11	100-150	95	265	220	34	32	53	14	100-200	NOTE 7
	33±15																	
01:20:00	TEST OFF STACK LIGHT GREY																	

NOTES:

1. Unit washed down prior to start of test.
2. EED time is 3.5 minutes ahead of times noted above.
3. Grey oil plume.
4. Very little plume.
5. Off of "high" on opacity meter sequencer relay TDR 1 had been removed to keep unit on line.
6. Fan running time 1805.0 hours.
7. Brownish grey stack (particulate).

ABBREVIATIONS:

1-2: Stages 1 & 2 : 3-4: Stages 3 & 4
ACA: Alternating Current Amperes
ACV: " "
DCMA: Direct " Multi-Amperes

APPENDIX B

STATUS OF FLUE GAS CORROSION STUDY - KAISER STEEL, FONTANA

TRW
DEFENSE AND SPACE SYSTEMS GROUP
ONE SPACE PARK · REDONDO BEACH · CALIFORNIA 90278

INTEROFFICE CORRESPONDENCE 5515.2.77-451

TO: R. Hession CC: DATE: November 1, 1977

SUBJECT: Status of Flue Gas Corrosion Study - Kaiser Steel, Fontana.

FROM: L.A.Rosales/M.P.Bianchi

BLDG	MAIL STA.	EXT.
01	2220	52630

INTRODUCTION

The "Coke Oven Waste Heat Flue Gas Corrosion Study" is in-progress, see Appendix. Subtask I is complete. Subtask II and IV are in-progress and some preliminary work is being accomplished on Subtask III. A description of work completed to date is included below.

SUBTASK I

Several candidate metallic and non-metallic materials have been selected for test in the Kaiser Steel North CDS unit. The metallic materials include 316 CRES (the material of which the units are constructed), 304 CRES, titanium, and several nickel-base superalloys. In addition, mild steel coupons were selected as a substrate for candidate coating systems. The 304 CRES alloy was chosen as a candidate since it is more sensitive to chloride pitting attack than 316 CRES and would give an indication of excessive chloride build up in the system. The nickel alloys were chosen for their resistance to sulfuric acid attack. Several alloys were chosen for study which included various Cr-Mo-Fe compositions. Commercially pure titanium is known to possess outstanding corrosion resistance to most media and has performed well in sulfuric acid environments. It is not affected by the presence of chlorides. Two titanium alloys which possess outstanding crevice corrosion resistance, Ti-0.2 Pd and Ti Code 12, were also included in the test. Chemical lead, widely used in sulfuric acid applications, was also included for test.

The non-metallic materials selected for test were chosen for their resistance to chemical attack, temperature resistance, ease of application and fabrication, as well as availability. The thermoset resins are the polyesters, an epoxy, vinyl esters, and furans either in the form of fiberglass reinforced structural composites or filled and unfilled coatings. The thermoplastic resins are polyvinylchloride (PVC), alkyds, polyvinyllidene fluoride (KYNAR), polyphenylene sulfide, and teflon as coatings, shrink tubing, and a reinforced liner.

The elastomers are neoprene, Hypalon, and viton as coatings, liners, and seal and shims. The substrates for the liners and coatings are mild steel and 304 and 316 stainless steels.

SUBTASK II

Two inch square coupons were made of all test materials. Some of these were coated using the appropriate methods. In addition, some of the non-metallic materials were fabricated into coupons by the suppliers. All coupons were coded weighed and visual inspected prior to testing. The coupons were installed in the unit by hanging using 316 CRES wire or Teflon coated wire. The coupons were situated in the west end of the hood and in the lower area under the baffles. The type of coupons date of installation, location and remarks are presented in Tables II and III.

Coatings were also applied to electrode headers, door panels and in the hood area. The surfaces to be coated were prepared by solvent wiping with MEK. It should be noted that it was very difficult to obtain clean surface due to access problems and the copious amounts of contaminating deposits and particulates in the atmospheres. Therefore, the adhesion of the coatings to the substrate is not expected to be as good as would be obtained under controlled conditions.

TABLE B-1. TABULATION OF MATERIALS AND COATINGS SELECTED FOR TESTING

A) Metals and Alloys

Designation	Composition	Supplier	Code
1010 Mild Steel	Fe - .01C - 0.45 Mn	———	S - ( )
304 CRES	Fe - 18 Cr - 8 Ni - 1.5 Mn	———	304 - ( )
316 CRES	Fe - 18 Cr - 8 Ni - 3 Mo - 1.5 Mn	———	316 - ( )
Al - 6X CRES	Fe - 20 Cr - 25 Ni - 6 Mo	Allegheney-Ludlum	Al - 6 - ( )
29 - 4 CRES	Fe - 29 Cr - 4 Mo	Allegheney-Ludlum	29 - 4 ( )
Ti 50 A	C. P. Ti	Timet	Ti - ( )
Ti - Code 12	Ti - 0.3 Mo - 0.8 Ni	Timet	Ti - 12 - ( )
Ti - 0.2 Pd	Ti - 0.2 Pd	Timet	Ti - Pd - ( )
Hastelloy C	Ni - 15.5 Cr - 16 Mo - 5 Fe - 2.5 Co	Huntington Alloys	Hast. C - ( )
Hastelloy C276	Ni - 15.5 Cr - 16 Mo - 5.5 Fe - 3.7 W - 2.5 Co	Huntington Alloys	Hast. C276 - ( )
Hastelloy B	Ni - 28 Mo - 2.5 Co - 1.0 Cr - 5 Fe	Huntington Alloys	Hast. B - ( )
Hastelloy X	Ni - 22 Cr - 18 Fe - 9 Mo - 1.5 Co - .6 W	Huntington Alloys	Hast. X - ( )
Incoloy 825	Ni - 30 Fe - 21.5 Cr - 3 Mo - .9 Ti	Huntington Alloys	1825 - ( )
Inconel 601	Ni - 23 Cr - 14 Fe - 1.35 Al - 0.5 Mn - 0.5 Cu	Huntington Alloys	1601 - ( )
Inconel 617	Ni - 22 Cr - 12.5 Co - 9.0 Mo - 1.0 Al - .07 C	Huntington Alloys	1617 - ( )
Nickel	Ni (pure)	Huntington Alloys	Ni - ( )
Chemical Lead	Pb - 0.05 Cu - 0.005 Ag	———	Pb - ( )

TABLE B-1 (continued)

B) Non-Metallic Structural Panels

Designation	Composition	Supplier	Code
Atalc 382/Flex Bend 4010A	Bisphenol Polyester FRP	ICI United States	AT382- ( )
Atlac 711-05A	Fire Resist. Polyester FRP	ICI United States	AT711 - ( )
Atlac 382-05A	Bisphenol Polyester FRP	ICI United States	AT382/05 - ( )
Atlac 580-05A	Bisphenol Vinylester FRP	ICI United States	AT580 - ( )
Derakane 470-45	Vinylester FRP	Dow Chemical	D470 - ( )
Derakane 510-A-40	Vinylester FRP	Dow Chemical	D510 - ( )
Polylite 33-402	Polyester FRP	Reichhold Chemical	P33 - ( )
Corralite 31-345	Polyester FRP	Reichhold Chemical	C31 - ( )
7241-6	IPA Polyester FRP	Ashland	ASH7241 - ( )
72L + 5b-1	Fire Retarded Polyester FRP	Ashland	ASH72L - ( )
7240-4	IPA Polyester FRP	Ashland	ASH7240 - ( )
197/3 + AT-8	Polyester FRP	Ashland	ASH197/3AT - ( )
800/801L-68	Furan FRP	Ashland	ASH800 - ( )
197/3-400	Poltester FRP	Ashland	ASH197/3 - ( )
800 FR-10	Flame Retarded Furan FRP	Ashland	ASH800FR - ( )
Neoprene Elastomer	Polychloroprene	Gacoflex Western	NB - ( )
Viton Elastomer	Fluorocarbon	Dupont	V - ( )

TABLE B-1 (continued)

B) Non-Metallic Structural Panels

Designation	Composition	Supplier	Code
Shrink Tubing - PVC	Polyvinylchloride		ST - ( )
6793 Hystl	Polybutadiene	TRW	HY - ( )

C) Non Metallic Coatings

Designation	Composition	Supplier	Code
850-321/855-255	Polytetrafluoroethylene	Dupont	T
EA 919	Bisphenol-polyamine cured epoxy	Hysol	E
Ryton	Polyphenylene sulfide	Phillips	PS
Compound W	Vinyl Plastisol	TRW	W
960/659	Alkyd Resin	Rust-Oleum Corp.	RO
Ceilcote 252	Glass Flake Filled Polyester	Ceilcote	C
Kynar	Polyvinllidene Fluoride	Pennwalt	K
N11R/N29 Neoprene	Polychloroprene	Gacoflex Western	N
Hypalon Elastomer	Polychlorosufonated Rubber	Gacoflex Western	H
4020	Filled Vinylester	Plasites	4020
4030	Filled Vinylester	Plasites	4030
4092	Filled Vinylester	Plasites	4092

TABLE B-2. LOCATION OF TEST COUPONS IN UPPER CASING (HOOD)

Row	Location	Sample No.	Date Installed	Remarks
1 (North)	1 (West)	304 - 2T	23 August 1977	
	2	304 - 13W		
	3	304 - 8 PS		
	4	304 - 11 RO		
	5	304 - 4E		
	6	Hastelloy C		
	7	I825 - 1		
1 (North)	8 (East)	I601 - 3	23 August 1977	
2 (Center)	1 (West)	Ti - Pd - 3	23 August 1977	
	2	Ti - 12 - 3		
	3	316 -19		
	4	304- 24		
	5	Ni - 2		
	6	I617 - 2		
	7	Ti - 12		
	8	316 - 2T		
	9	316 - 15W		
	10	316 - 9 PS		
2 (Center)	11 (East)	316 - 10 RO	23 August 1977	
3 (South)	1 (West)	316 - 21	23 August 1977	
	2	304 - 19		
	3	S - 4E		
	4	S - 12 RO		
	5	S - 9 PS		
	6	S - 5W		
	7	S - 2T		
3 (South)	8 (East)	316 - 5E	23 August 1977	

TABLE B-3. LOCATION OF TEST COUPONS IN LOWER CASING

NOTE: Rows are numbered with 1 being the furthest West and increasing numbers toward the East.

Locations of samples on a row are numbered with 1 being the furthest North and increasing numbers toward the South.

Row	Location	Sample No.	Date Installed	Remarks
1	1	S- ( ) C	10/6/77	
1	2	S- 23K	10/6/77	
2	1	304-18	8/23/77	
↑	2	S - 14W	↑	
	3	304 - 7PS		
	4	Ti - 12 - 1		
	5	Ti - Pd - 1		
	6	Ti - 1		
	7	304 - 17		
	8	Ni - 5		
	9	304 - 10 RO		
↓	10	S - 1T	↓	
2	11	304 - 16	8/23/77	
3	1	316 -18	8/23/77	
↑	2	S - 13 RO	↑	
	3	304 - 3T		
	4	I825 - 5		
	5	Ni - 1		
	6	316 - 17		
	7	I617 - 1		
	8	I601 - 2		
	9	316-13W		
↓	10	S - 8 PS	↓	
3	11	316 - 16	8/23/77	

TABLE B-3 (continued)

Row	Location	Sample No.	Date Installed	Remarks
4	1	316 - 4E	8/23/77	
	2	316 - 12 RO		
	3	AT 382/05		
	4	AT 711 -1		
	5	AT 382 - 1		
	6	AT 580 - 1		
	7	316 - 7 PS		
	8	316 - 14W		
4	9	316 - 1T	8/23/77	
5	1	ASH 7241 - 29	8/29/77	2"x5" Coupo
	2	ASH 72L - 22		"
	3	ASH 7240 - 39		"
	4	ASH 197/3 AT - 5		"
	5	ASH 800 - 25		"
	6	ASH 197/3 - 5		"
5	7	ASH 800 FR - 20	8/29/77	"
6	1	ASH 800 FR - 21	8/29/77	2"x5" Coupc
	2	ASH 197/3 -4		"
	3	ASH 800 - 24		"
	4	ASH 197/3 AT -6		"
	5	ASH 7240 - 40		"
	6	ASH 72L - 21		"
6	7	ASH 7241 - 30	8/29/77	"
7	1	HY - 180	8/29/77	
	2	HY - 132		
	3	P33-1		
7	4	C31-1	8/29/77	

TABLE B-3 (continued)

Row	Location	Sample No.	Date Installed	Remarks
8	1	Pb - 2	8/29/77	
8	2	Pb - 1	8/29/77	
9	1	316 - ( ) NB	8/29/77	
	2	316 - ( )) NB		
	3	S - ( ) NB		
	4	S - ( ) NB		
	5	316 - 26N		
	6	316 - 25N		
	7	S - 18N		
	8	S - 17N		
	9	316 - 29H		
	10	316 - 28H		
	11	S - ( )H		
9	12	S - ( )H	8/29/77	
10	1	316 - 22	8/23/77	
	2	304 - 9 PS		
	3	Ti - 2		
	4	Ti Pd - 2		
	5	Ti - 12 - 2		
	6	316 - 11 RO		
	7	304 - 1T		
10	8	304 - 12	8/23/77	

TABLE B-3 (continued)

Row	Location	Sample No.	Date Installed	Remarks
11	1	304 - 16 RO	8/23/77	
	2	S - 5E		
	3	I601 - 4		
	4	I617 - 3		
	5	316 - 23		
	6	304 - 21		
	7	316 - 8 PS		
	8	I825 - 2		
	9	304 - 5E		
11	10	S - 11 RO	8/23/77	
12	1	304 - 20	8/23/77	
	2	S - 3T		
	3	Ni - 3		
	4	304 - 14W		
	5	316 - 6E		
	6	316 - 3T		
	7	S - 16W		
	8	304 - 15W		
	9	S - 10 PS		
12	10	316 - 20	8/23/77	
13	1	304 - 28K	10/6/77	
	2	Hast B - 1		
	3	Hast C - 1		
13	4	S - ( ) C	10/6/77	
14	1	S - 24K	10/6/77	
14	2	304 - 29K	10/6/77	
15	1	4092 - 1	9/13/77	
16	1	4030 - 1	9/13/77	
17	1	4020 - 1	9/13/77	

The coatings applied were epoxy (Code E), vinyl (Code W) alkyd (Code RO), neoprene (Code N) and Hypalon (Code H). In addition, an Armalon fabric (TFE Teflon impregnated fiberglass) was applied to a door panel using epoxy EA919 as an adhesive.

Wash couplings, located in the upper casing (hood), were coated with epoxy, vinyl and alkyd and installed. Using the West to East numbering system for plates and the North to South numbering system for nozzles, the coated coupling locations are:

Plate No.	Nozzle No.	Coating Code
4	3	PS
4	8	PS
8	2	RO
8	4	RO
8	7	RO
12	1	W
12	4	W
12	7	W
18	1	E
18	3	E
18	7	E

The wash couplings were installed 8/23/77.

Header to electrode connectors were also coated and installed on the North side of the unit on 8/23/77. Again, numbering the electrodes from West to East, the location by stages (stage 1 at bottom, stage 4 at top) is:

Stage No.	Electrode No.	Coating Code
1	4	W
1	8	T
1	16	PS
2	4	PS
2	6	RO
2	8	E
2	16	W
2	20	RO

Stage No.	Electrode No.	Coating Code
3	4	E
3	8	PS
3	16	T
3	20	RO
4	4	T
4	8	W
4	16	E

The first major examination of the test coupons is tentatively scheduled for the week of 1 November 1977. Inspection of the door and header coatings have been made with the following observations. The lower temperature coatings, alkyd and vinyl, have blistered and discolored on the doors and some of the headers. The epoxy is also showing extensive blistering and peeling in the high temperature areas. The neoprene coating on the door has flaked off. The Hypalon appears to be holding up as is the armalon fabric. A detailed examination of the wash couplings and electrode to header connectors has not been made to date.

SUBTASK III

Thermo-chemical data has not been received by Materials Engineering as of this date. Correlations with corrosion data will be attempted upon receipt of the data.

Initial data on supply water and waste water chemistry has been received. The data shows a chloride content much higher than found during earlier tests (60 ppm vs 7 ppm). This has been attributed to a change in the domestic water source (Kaiser now using Colorado River water). The data also shows that approximately 35 ppm of chlorides are being lost in the system (not appearing in the waste water). If the chlorides are depositing in the scrubber, pitting attack of the 316 CRES can be expected to occur. The report showed the pH of the waste water to be approximately 2.5.

SUBTASK IV

Corrosion probe installation ports (3/4 NPT female ports) were installed on the north side of the unit as shown in Figure 1. Five 316 CRES Magna Corporation 21343/W40/8020 probes were installed in the ports on 13 September 1977. A sixth probe was found to be detective and was returned to Magna for replacement. The probes were located as follows:

Probe 1	-	Port A
Probe 2	-	Port C
Probe 3	-	Port D
Probe 4	-	Port L
Probe 5	-	Returned to Magna
Probe 6	-	Port K

Five readings have been taken to date (on an approximate weekly basis). Initial results indicate a very low general corrosion rate for the 316 CRES elements. Results will be tabulated and correlated with coupon results. Some problems with Probe 4 have been encountered during periods when the unit is running. Magna says that electrical interference or high vibration can produce the type of problems being encountered. Probe 4 is located near a junction box which has a fan cooling system.

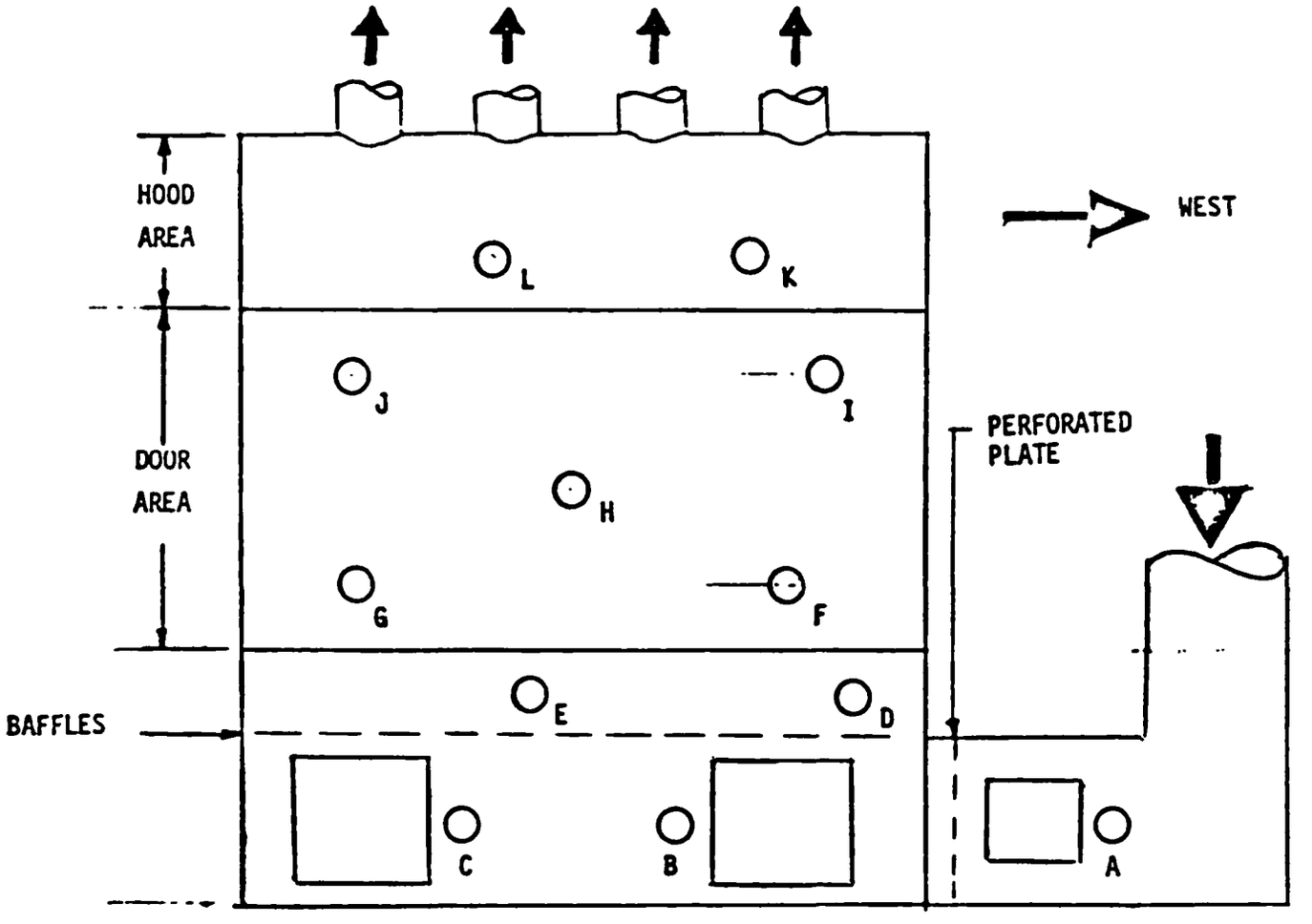

Figure B-1. Location of Corrosion Probe Ports Unit A

APPENDIX C

WASTEWATER CHEMISTRY

COKE OVEN WASTE HEAT FLUE GAS CORROSION STUDY

I. Statement of Objectives

The objective of the corrosion study is to identify materials of construction which are resistant to corrosive attack in the Kaiser Steel CDS environment. Metals and non-metals, including coatings and linings, will be evaluated with special emphasis on those materials which not only perform satisfactorily but are also practical from an economic and fabrication viewpoint.

II. Task Breakdown

The corrosion study is broken into 5 subtasks as follows:

Subtask I. Using data obtained by analysis of CDS components, literature, and TRW tests identify candidate materials for use in the scrubber. Consideration will be given to availability, fabricability, and cost as well as corrosion, stress corrosion, pitting and crevice corrosion resistance.

Subtask II. Prepare test coupons made of the candidate materials. Determine locations within the CDS and mount the coupons. Remove and metallurgically and chemically analyze coupons at appropriate time intervals. Determine type of corrosive attack and the rate.

Subtask III. Using thermal mapping and electrical system data, correlate corrosion data with the CDS operating modes. Special emphasis will be placed upon determining differences in performance due to differences in locations within the scrubber.

Subtask IV. Monitor instantaneous corrosion rate at selected locations within the scrubber by use of an electronic corrosion meter. Correlate meter data with test coupon data.

TASK SCHEDULE AND MAN LOADING

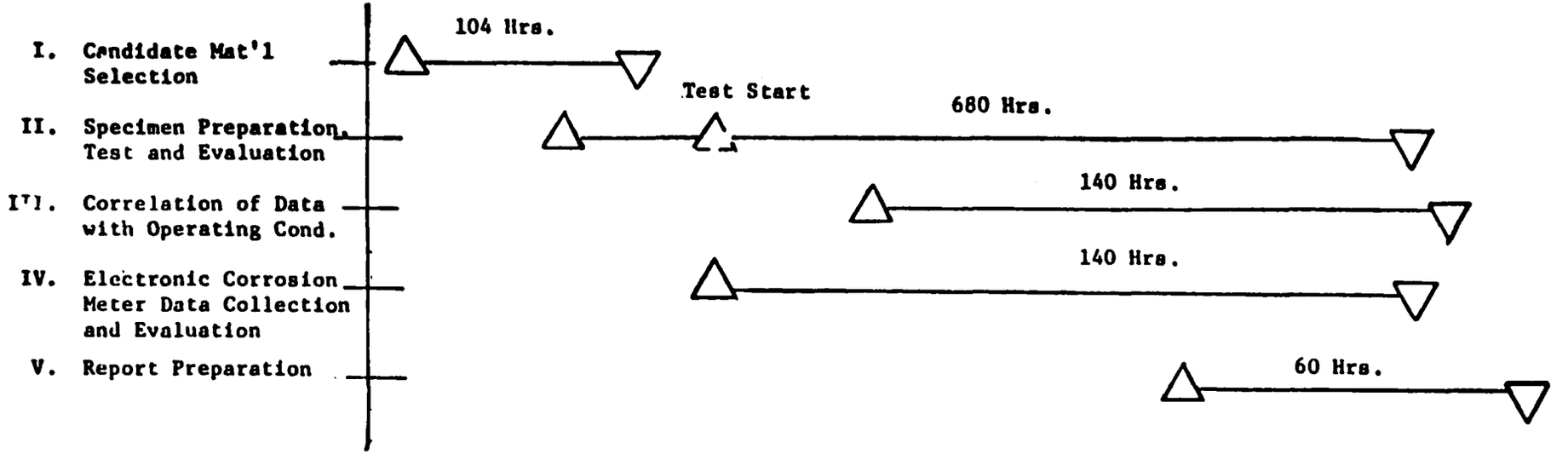

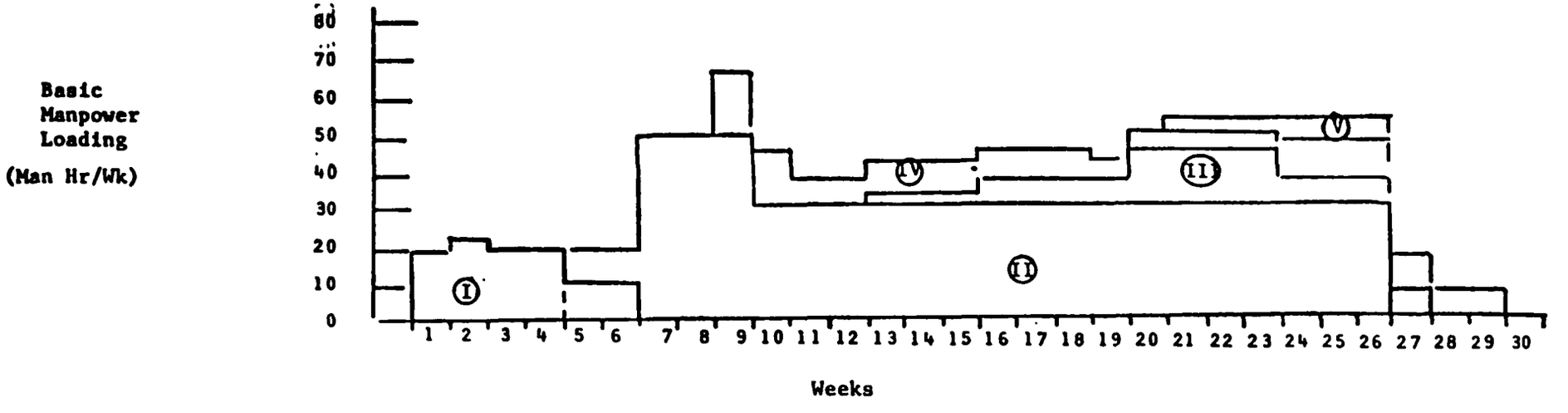

Subtask V. Prepare a final report which summarizes the corrosion study. The report will describe the coupon materials and configurations, test data, metallurgical and chemical analyses procedures and data, and conclusions and recommendations.

The manpower and time required for each subtask is:

Subtask I	104	Hours	6	Weeks
Subtask II	680	"	22	"
Subtask III	140	"	15	"
Subtask IV	140	"	18	"
Subtask V	60	"	9	"

III. Approach

The approach to the determination of the compatibility of material in the Kaiser CDS environment is to test in-situ and to evaluate by using weight change data, visual inspection, metallographic examination, electron microprobe analysis and the scanning electron microscope. All data will be correlated to specimen location within the scrubber and operating conditions. The electronic corrosion meter data will be used to determine transient corrosion rates due to changes in operating conditions and to determine corrosion trends in-situ.

LAR:dj
Distribution: L. Berman
F. Brewen
H. Burge
J. Hardgrove
R. Koppang
W. Krieve
D. Martin
R. Meeker
M. Moran
W. Rogers
D. Price
B. Spanier
J. Sweety
F. Whitson
R. Williams

certified testing laboratories, inc.
2905 EAST CENTURY BLVD. • SOUTH GATE, CALIF. 90280 • (213) 564-2641

LABORATORY NO. 62851 — REPORTED 10-7-77

CLIENT TRW
One Space Park
Redondo Beach, California 90278 — SAMPLED — RECEIVED 10-4-77

SAMPLE Wastewater (Kaiser)

MARKS See Below

BASED ON SAMPLE As Received

Results:

	#1	#2	#3	#4	#5	#6	#7
Nickel	<0.03	0.31	0.13	0.19	0.16	0.19	0.19
Chromium	<0.03	0.70	0.47	0.33	0.33	0.30	0.33
Copper	<0.02	<0.02	<0.02	<0.02	<0.02	<0.02	<0.02
Iron II	<0.04	1.64	2.53	1.67	2.30	1.68	1.86
Iron (Total)	<0.05	6.14	4.52	3.95	4.14	3.48	3.48
Chloride	60.1	25.5	25.0	26.8	26.5	25.8	25.5
Fluoride	0.19	0.75	0.75	0.75	0.75	0.75	0.75
Cyanide	0.02	0.04	0.06	0.07	0.06	0.04	0.12
Sulfite	<0.3	<0.3	<0.3	<0.3	<0.3	<0.3	<0.3
Sulfate	11.6	286	244	236	242	240	246
Sulfide	<0.10	<0.10	<0.10	<0.10	<0.10	<0.10	<0.10
pH (units)	7.96	2.43	2.50	2.51	2.51	2.52	2.50
Hardness (as $CaCO_3$)	82	91	91	91	91	91	91
Specific Conductivity @ 25° C micromhos/cm)	290	1310	1250	1210	1230	1230	1280

certified testing laboratories, inc.
2905 EAST CENTURY BLVD. • SOUTH GATE, CALIF. 90280 • (213) 564-2041

LABORATORY NO. -62851
CLIENT TRW
One Space Park
Redondo Beach, California 90278
SAMPLE Wastewater (Kaiser)

REPORTED 10-7-77
SAMPLED
RECEIVED 10-4-77

MARKS See Below
BASED ON SAMPLE As Received

Results (Cont.)

	#8	#9	#10	#11	#12	#13	#14
Nickel	0.22	0.19	0.25	0.22	0.25	<0.03	0.16
Chromium	0.38	0.34	0.47	0.53	0.56	<0.03	0.34
Copper	<0.02	<0.02	<0.02	<0.02	<0.02	<0.02	<0.02
Iron II	1.37	1.44	1.54	1.41	1.37	<0.04	0.99
Iron (Total)	3.81	4.05	4.29	4.05	4.76	<0.05	3.81
Chloride	28.0	28.3	29.0	27.5	26.8	59.8	26.8
Fluoride	0.75	0.75	0.75	0.75	0.75	0.19	0.75
Cyanide	0.13	0.15	0.05	0.12	0.06	0.03	0.05
Sulfite	<0.3	<0.3	<0.3	<0.3	<0.3	<0.3	<0.3
Sulfate	280	268	256	246	240	10.0	220
Sulfide	<0.10	<0.10	<0.10	<0.10	<0.10	<0.10	<0.10
pH (units)	2.48	2.46	2.45	2.47	2.50	7.96	2.53
Hardness (as $CaCO_3$)	91	91	91	91	91	82	91
Specific Conductivity @ 25° C (micromhos/cm)	1380	1440	1480	1420	1350	290	1210

certified testing laboratories, inc.

2905 EAST CENTURY BLVD. - SOUTH GATE, CALIF. 90280 • (213) 564-2641

LABORATORY NO.	62853	REPORTED	10-7-77
CLIENT	TRW One Space Park Redondo Beach, California 90278	SAMPLED	
		RECEIVED	10-4-77
SAMPLE	Wastewater (Kaiser)		
MARKS	See Below		
BASED ON SAMPLE	As Received		

Results (Cont)

	#15	#16	#17	#18	#19
Nickel	0.13	0.13	0.19	0.19	0.22
Chromium	0.25	0.28	0.30	0.34	0.41
Copper	<0.02	<0.02	<0.02	<0.02	<0.02
Iron II	1.86	2.17	0.67	0.61	0.72
Iron (Total)	3.10	3.95	3.62	4.76	4.71
Chloride	25.5	25.5	25.5	25.0	25.0
Fluoride	0.75	0.75	0.75	0.75	0.75
Cyanide	0.06	0.05	0.05	0.06	0.05
Sulfite	<0.3	<0.3	<0.3	<0.3	<0.3
Sulfate	216	232	250	260	265
Sulfide	<0.10	<0.10	<0.10	<0.10	<0.10
pH (units)	2.56	2.55	2.52	2.49	2.46
Hardness (as $CaCO_3$)	91	91	91	91	91
Specific Conductivity @ 25° C (micromhos/cm)	1180	1220	1290	1380	1480

*Expressed in mg/l except where noted.

Respectfully submitted,

CERTIFIED TESTING LABORATORIES, INC.

Stuart E. Solot, Ph.D.

certified testing laboratories, inc.
2905 EAST CENTURY BLVD. • SOUTH GATE, CALIF. 90280 • (213) 564-2041

LABORATORY NO. 62851 - Supplement REPORTED 10-12-77

CLIENT TRW
One Space Park
Redondo Beach, California 90278

Analytical Methods Used in Water Analysis:

All samples were filtered through 0.45 micron Millipore filters. Methods used were those described in Federal Register, 41, No. 232, 1976, when applicable.

Nickel	Atomic Absorption
Chromium	Atomic Absorption
Copper	Atomic Absorption
Iron (Total)	Atomic Absorption
Chlorides	Titration with Mercuric Nitrate
Fluoride	Ion Selective Electrode*
Cyanide	Pyridine - Barbituric Acid*
Sulfite	Titrimetric-Iodine
Sulfate	Turbidimetric
Sulfide	Photometric - Methylene Blue
pH	Electrometric
Hardness	Sum of Ca, Mg & Fe by AAS
Specific Conductivity	Wheatstone Bridge Conductimetry
Iron II	Photometric - 1,10 Phenanthroline

*Sample not distilled due to lack of sufficient sample.

Respectfully submitted,

CERTIFIED TESTING LABORATORIES, INC.

Stuart E. Salot, Ph.D.

KSC Water Samples
03 October 1977

NOTE: 30 Second time period to pull one sample with vacuum pump

Sample No.	Time	Location	Process Conditions
1	2:20	H_2O Input	Domestic Water
2	3:10	CDS Disch.	Battery in Steady State -- No Upset -- Before Pushing Begins
3	3:15	"	First Oven Pushed -- Started Sample at Ram Retraction plus one minute
4	3:20	"	Oven Pushed but not yet charged
5	3:23	"	Start of Charging Operation
6	3:25	"	Charging in process
7	3:27	"	Charging completed, slight stack emission - beginning of upset
8	3:29	"	Upset
9	3:31	"	Upset
10	3:33		Start of pushing operation on second oven
11	3:34		One minute after start of push
12	3:37		One minute after Ram retracted
13	3:57	Domestic Water	
14	3:40	CDS Disch.	Charging Vent Closed on Second Oven Pushed
15	3:43		Upset Continues -- 5 Minute Sample Time (3:43 Start, 3:48 Complete)
16	3:49		High Spark Rate in Unit - Heavy Upset
17	3:53		One Minute after Ram retracted on Third Oven Pushed
18	3:56		Upset Continues
19	4:00		End of Battery Activity -- Stack Looks Good - Slight Steam Plume

TECHNICAL REPORT DATA (Please read Instructions on the reverse before completing)		
1. REPORT NO. EPA-600/7-79-017	2.	3. RECIPIENT'S ACCESSION NO.
4. TITLE AND SUBTITLE TRW Charged Droplet Scrubber Corrosion Studies		5. REPORT DATE January 1979 6. PERFORMING ORGANIZATION CODE
7. AUTHOR(S) Frederick A. Whitson		8. PERFORMING ORGANIZATION REPORT NO.
9. PERFORMING ORGANIZATION NAME AND ADDRESS TRW, Energy Systems Group One Space Park Redondo Beach, California 90278		10. PROGRAM ELEMENT NO. EHE624 11. CONTRACT/GRANT NO. 68-02-2613, Task 7
12. SPONSORING AGENCY NAME AND ADDRESS EPA, Office of Research and Development Industrial Environmental Research Laboratory Research Triangle Park, NC 27711		13. TYPE OF REPORT AND PERIOD COVERED Task Final; 8/77 - 10/78 14. SPONSORING AGENCY CODE EPA/600/13

15. SUPPLEMENTARY NOTES IERL-RTP project officer is Dale L. Harmon, Mail Drop 61, 919/541-2925.

16. ABSTRACT The report gives results of corrosion studies to provide definitive data concerning the corrosive nature of coke-oven waste-heat flue gas and its effects on wet electrostatic precipitators, and specifically on TRW's Charged Droplet Scrubber (CDS). The study characterized the chemical composition of the waste heat flue gases; related these data to corrosion and to the effects on the electrostatic scrubbing mechanism; evaluated materials compatibility with the coking process waste heat environment; and identified candidate agents which may be introduced into the waste heat gas stream to minimize the corrosive effects. It was determined that, with several equipment and operating modifications, projected life of the CDS casing and internals is 5 to 10 years, and life expectancy of the electrode nozzles is 1 to 2 years.

17. KEY WORDS AND DOCUMENT ANALYSIS

a. DESCRIPTORS		b. IDENTIFIERS/OPEN ENDED TERMS	c. COSATI Field/Group
Air Pollution	Corrosion	Air Pollution Control	13B
Coking	Charged Particles	Stationary Sources	13H 20H
Flue Gases		Charged Droplet Scrubber	21B
Gas Scrubbing			07A
Drops		Waste Heat	07D
Electrostatic Precipitators		Wet Scrubbers	13I

18. DISTRIBUTION STATEMENT	19. SECURITY CLASS (This Report)	21. NO. OF PAGES
Unlimited	Unclassified	153
	20. SECURITY CLASS (This page) Unclassified	22. PRICE

EPA Form 2220-1 (9-73)